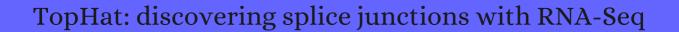
# CITATION REPORT List of articles citing



DOI: 10.1093/bioinformatics/btp120 Bioinformatics, 2009, 25, 1105-11.

Source: https://exaly.com/paper-pdf/46563111/citation-report.pdf

Version: 2024-04-24

This report has been generated based on the citations recorded by exaly.com for the above article. For the latest version of this publication list, visit the link given above.

The third column is the impact factor (IF) of the journal, and the fourth column is the number of citations of the article.

#	Paper	IF	Citations
2303	Multiscale Approach to Deciphering the Molecular Mechanisms Involved in the Direct and Intergenerational Effect of Ibuprofen on Mosquito Aedes aegypti.		
2302	Translation Termination Factor GSPT1 Is a Phenotypically Relevant Off-Target of Heterobifunctional Phthalimide Degraders.		
2301	Signal Transductions of BEAS-2B Cells in Response to Carcinogenic PM2.5 Exposure Based on a Microfluidic System.		
2300	Abstract.		
2299	Abstract.		O
2298	Abstract.		2
2297	Birthday Honours. <b>1899</b> , 1, 1421-1422		
2296	Changes in residual volume following oxygen breathing. <b>1983</b> , 55, 817-24		3
2295	The muon g-2 discrepancy: errors or new physics?. <b>2008</b> ,		4
2294	A report on the 2009 SIG on short read sequencing and algorithms (Short-SIG). <i>Bioinformatics</i> , <b>2009</b> , 25, 2863-4	7.2	
2293	How to map billions of short reads onto genomes. <b>2009</b> , 27, 455-7		216
2292	Computation for ChIP-seq and RNA-seq studies. <b>2009</b> , 6, S22-32		443
2291	Searching for SNPs with cloud computing. <b>2009</b> , 10, R134		333
2290	Cancer genome sequencing: a review. <b>2009</b> , 18, R163-8		154
2289	Identification of new pancreatic beta cell targets for in vivo imaging by a systems biology approach. <b>2010</b> , 16, 1609-18		10
2288	RNA-seq: from technology to biology. <b>2010</b> , 67, 569-79		356
2287	The utility of mass spectrometry-based proteomic data for validation of novel alternative splice forms reconstructed from RNA-Seq data: a preliminary assessment. <b>2010</b> , 11 Suppl 11, S14		49

# (2010-2010)

2286	Rnnotator: an automated de novo transcriptome assembly pipeline from stranded RNA-Seq reads. <b>2010</b> , 11, 663	168
2285	Massive parallel sequencing of mRNA in identification of unannotated salinity stress-inducible transcripts in rice (Oryza sativa L.). <b>2010</b> , 11, 683	64
2284	Comparison of transcriptomic landscapes of bovine embryos using RNA-Seq. <b>2010</b> , 11, 711	63
2283	SpliceIT: a hybrid method for splice signal identification based on probabilistic and biological inference. <b>2010</b> , 43, 208-17	6
2282	Transcriptome profiling in neurodegenerative disease. <b>2010</b> , 193, 189-202	50
2281	Systems analysis of alternative splicing and its regulation. <b>2010</b> , 2, 550-565	12
2280	Nuclear envelope alterations generate an aging-like epigenetic pattern in mice deficient in Zmpste24 metalloprotease. <b>2010</b> , 9, 947-57	44
2279	Genome-wide analysis of alternative splicing evolution among Mus subspecies. <b>2010</b> , 19 Suppl 1, 228-39	43
2278	Ab initio reconstruction of cell type-specific transcriptomes in mouse reveals the conserved multi-exonic structure of lincRNAs. <b>2010</b> , 28, 503-10	1030
2277	Advancing RNA-Seq analysis. <b>2010</b> , 28, 421-3	158
,,	Advancing RNA-Seq analysis. 2010, 28, 421-3  Haploidy with histones. 2010, 28, 423-4	158 9
,,		
,,	Haploidy with histones. <b>2010</b> , 28, 423-4  The developmental dynamics of the maize leaf transcriptome. <b>2010</b> , 42, 1060-7  Linking promoters to functional transcripts in small samples with panoCAGE and CAGEscap. <b>2010</b> .	9
2276 2275	Haploidy with histones. <b>2010</b> , 28, 423-4  The developmental dynamics of the maize leaf transcriptome. <b>2010</b> , 42, 1060-7  Linking promoters to functional transcripts in small samples with nanoCAGE and CAGEscan. <b>2010</b> ,	9
2276 2275 2274	Haploidy with histones. 2010, 28, 423-4  The developmental dynamics of the maize leaf transcriptome. 2010, 42, 1060-7  Linking promoters to functional transcripts in small samples with nanoCAGE and CAGEscan. 2010, 7, 528-34	9 550 123
2276 2275 2274 2273	Haploidy with histones. 2010, 28, 423-4  The developmental dynamics of the maize leaf transcriptome. 2010, 42, 1060-7  Linking promoters to functional transcripts in small samples with nanoCAGE and CAGEscan. 2010, 7, 528-34  Alternative expression analysis by RNA sequencing. 2010, 7, 843-7	9 550 123 227
2276 2275 2274 2273	Haploidy with histones. 2010, 28, 423-4  The developmental dynamics of the maize leaf transcriptome. 2010, 42, 1060-7  Linking promoters to functional transcripts in small samples with nanoCAGE and CAGEscan. 2010, 7, 528-34  Alternative expression analysis by RNA sequencing. 2010, 7, 843-7  De novo assembly and analysis of RNA-seq data. 2010, 7, 909-12	9 550 123 227 701

2268	Integrated genetic and epigenetic analysis identifies haplotype-specific methylation in the FTO type 2 diabetes and obesity susceptibility locus. <b>2010</b> , 5, e14040	193
2267	H-DBAS: human-transcriptome database for alternative splicing: update 2010. <b>2010</b> , 38, D86-90	33
2266	Cost-effective sequencing of full-length cDNA clones powered by a de novo-reference hybrid assembly. <b>2010</b> , 5, e10517	10
2265	Adaptive evolution of genes duplicated from the Drosophila pseudoobscura neo-X chromosome. <b>2010</b> , 27, 1963-78	11
2264	Deep mRNA sequencing for in vivo functional analysis of cardiac transcriptional regulators: application to Galphaq. <b>2010</b> , 106, 1459-67	66
2263	Transcriptome and targetome analysis in MIR155 expressing cells using RNA-seq. <b>2010</b> , 16, 1610-22	46
2262	A probabilistic framework for aligning paired-end RNA-seq data. <i>Bioinformatics</i> , <b>2010</b> , 26, 1950-7	19
2261	Changes in transcript abundance in Chlamydomonas reinhardtii following nitrogen deprivation predict diversion of metabolism. <b>2010</b> , 154, 1737-52	398
2260	MapSplice: accurate mapping of RNA-seq reads for splice junction discovery. <b>2010</b> , 38, e178	762
2259	Detection of splice junctions from paired-end RNA-seq data by SpliceMap. <b>2010</b> , 38, 4570-8	255
2258	Quantitative and qualitative RNA-Seq-based evaluation of Epstein-Barr virus transcription in type I latency Burkitt's lymphoma cells. <b>2010</b> , 84, 13053-8	42
2257	Constitutively active androgen receptor splice variants expressed in castration-resistant prostate cancer require full-length androgen receptor. <b>2010</b> , 107, 16759-65	485
2256	Sex-specific and lineage-specific alternative splicing in primates. <b>2010</b> , 20, 180-9	198
2255	Suppression of the vacuolar invertase gene prevents cold-induced sweetening in potato. <b>2010</b> , 154, 939-48	127
2254	Noisy splicing drives mRNA isoform diversity in human cells. <b>2010</b> , 6, e1001236	203
2253	Uncovering the complexity of transcriptomes with RNA-Seq. <b>2010</b> , 2010, 853916	248
2252	The transcriptome of the human pathogen Trypanosoma brucei at single-nucleotide resolution. <b>2010</b> , 6, e1001090	204
2251	Supersplatspliced RNA-seq alignment. <i>Bioinformatics</i> , <b>2010</b> , 26, 1500-5	36

# (2010-2010)

2	2250	mRNA-seq with agnostic splice site discovery for nervous system transcriptomics tested in chronic pain. <b>2010</b> , 20, 847-60	57
2	2249	RNA-Seq read alignments with PALMapper. <b>2010</b> , Chapter 11, Unit 11.6	39
2	2248	Statistical Issues in the Analysis of ChIP-Seq and RNA-Seq Data. <b>2010</b> , 1, 317-34	11
2	2247	Next-generation sequencing techniques for eukaryotic microorganisms: sequencing-based solutions to biological problems. <b>2010</b> , 9, 1300-10	106
2	2246	From RNA-seq reads to differential expression results. <b>2010</b> , 11, 220	471
2	2245	Unique signatures of long noncoding RNA expression in response to virus infection and altered innate immune signaling. <b>2010</b> , 1,	192
2	2244	Algorithms in Bioinformatics. <b>2010</b> ,	
2	2243	Exploring plant transcriptomes using ultra high-throughput sequencing. <b>2010</b> , 9, 118-28	91
2	2242	Transcript assembly and quantification by RNA-Seq reveals unannotated transcripts and isoform switching during cell differentiation. <b>2010</b> , 28, 511-5	10225
2	2241	A survey of sequence alignment algorithms for next-generation sequencing. <b>2010</b> , 11, 473-83	632
2	2240	Fast and SNP-tolerant detection of complex variants and splicing in short reads. <i>Bioinformatics</i> , <b>2010</b> , 26, 873-81	1457
2	2239	Bioinformatics approaches for genomics and post genomics applications of next-generation sequencing. <b>2010</b> , 11, 181-97	120
2	2238	Cloud-scale RNA-sequencing differential expression analysis with Myrna. <b>2010</b> , 11, R83	227
2	2237	Design and evaluation of genome-wide libraries for RNA interference screens. <b>2010</b> , 11, R61	59
2	2236	Screening the human exome: a comparison of whole genome and whole transcriptome sequencing. <b>2010</b> , 11, R57	106
2	2235	Global and unbiased detection of splice junctions from RNA-seq data. <b>2010</b> , 11, R34	65
2	2234	Comprehensive annotation of the transcriptome of the human fungal pathogen Candida albicans using RNA-seq. <b>2010</b> , 20, 1451-8	165
2	2233	Function annotation of the rice transcriptome at single-nucleotide resolution by RNA-seq. <b>2010</b> , 20, 1238-49	<b>2</b> 60

2232	PIntron: A fast method for gene structure prediction via maximal pairings of a pattern and a text. <b>2011</b> ,	
2231	Towards accurate detection and genotyping of expressed variants from whole transcriptome sequencing data. <b>2011</b> ,	
2230	A novel framework for chimeric transcript detection based on accurate gene fusion model. <b>2011</b> ,	
2229	Improved RNA-Seq Partitions in Linear Models for Isoform Quantification. 2011,	
2228	Comparative analysis of RNA-Seq alignment algorithms and the RNA-Seq unified mapper (RUM). <i>Bioinformatics</i> , <b>2011</b> , 27, 2518-28	261
2227	RNA-sequence analysis of human B-cells. <b>2011</b> , 21, 991-8	112
2226	Differential expression in RNA-seq: a matter of depth. <b>2011</b> , 21, 2213-23	1072
2225	. 2011,	1
2224	Rapid parallel genome indexing with MapReduce. 2011,	18
2223	IsoLasso: a LASSO regression approach to RNA-Seq based transcriptome assembly. <b>2011</b> , 18, 1693-707	100
2222	Genome sequence and analysis of the tuber crop potato. <b>2011</b> , 475, 189-95	1438
2221	Sequencing transcriptomes in toto. <b>2011</b> , 3, 522-8	16
2220	Exome sequencing identifies NBEAL2 as the causative gene for gray platelet syndrome. 2011, 43, 735-7	224
2219	Transcriptional activity regulates alternative cleavage and polyadenylation. 2011, 7, 534	87
2218	Application of high-throughput DNA sequencing in phytopathology. <b>2011</b> , 49, 87-105	53
2217	Deep proteome and transcriptome mapping of a human cancer cell line. <b>2011</b> , 7, 548	723
2216	SeqGene: a comprehensive software solution for mining exome- and transcriptome- sequencing data. <b>2011</b> , 12, 267	36
2215	RNA and DNA Editing. <b>2011</b> ,	1

2214	Transcriptome sequencing across a prostate cancer cohort identifies PCAT-1, an unannotated lincRNA implicated in disease progression. <b>2011</b> , 29, 742-9	824
2213	T-IDBA: A de novo Iterative de Bruijn Graph Assembler for Transcriptome. <b>2011</b> , 337-338	8
2212	Comparative genomics of the pathogenic ciliate Ichthyophthirius multifiliis, its free-living relatives and a host species provide insights into adoption of a parasitic lifestyle and prospects for disease control. <b>2011</b> , 12, R100	89
2211	TopHat-Fusion: an algorithm for discovery of novel fusion transcripts. <b>2011</b> , 12, R72	547
<b>22</b> 10	The head-regeneration transcriptome of the planarian Schmidtea mediterranea. <b>2011</b> , 12, R76	93
2209	Haplotype and isoform specific expression estimation using multi-mapping RNA-seq reads. <b>2011</b> , 12, R13	179
2208	Control of embryonic stem cell lineage commitment by core promoter factor, TAF3. <b>2011</b> , 146, 720-31	132
2207	The monarch butterfly genome yields insights into long-distance migration. <b>2011</b> , 147, 1171-85	410
2206	Combinatorial patterning of chromatin regulators uncovered by genome-wide location analysis in human cells. <b>2011</b> , 147, 1628-39	265
2205	Conserved function of lincRNAs in vertebrate embryonic development despite rapid sequence evolution. <b>2011</b> , 147, 1537-50	882
2204	Observations on novel splice junctions from RNA sequencing data. <b>2011</b> , 409, 299-303	16
2203	CTCF-promoted RNA polymerase II pausing links DNA methylation to splicing. <b>2011</b> , 479, 74-9	700
2202	Functional analysis of the microtubule-interacting transcriptome. <b>2011</b> , 22, 4312-23	49
2201	Identification of novel transcripts in annotated genomes using RNA-Seq. <i>Bioinformatics</i> , <b>2011</b> , 27, 2325-9.2	716
2200	Synthetic spike-in standards for RNA-seq experiments. <b>2011</b> , 21, 1543-51	437
2199	Genome-wide regulation of 5hmC, 5mC, and gene expression by Tet1 hydroxylase in mouse embryonic stem cells. <b>2011</b> , 42, 451-64	493
2198	Transcriptome-wide analysis of regulatory interactions of the RNA-binding protein HuR. <b>2011</b> , 43, 340-52	513
2197	The little elongation complex regulates small nuclear RNA transcription. <b>2011</b> , 44, 954-65	64

2196	A Dictyostelium SH2 adaptor protein required for correct DIF-1 signaling and pattern formation. <b>2011</b> , 353, 290-301	3
2195	A whole-genome analysis of premature termination codons. <b>2011</b> , 98, 337-42	10
2194	A transcriptomic atlas of mouse neocortical layers. <b>2011</b> , 71, 605-16	224
2193	Omics, Bioinformatics, and Infectious Disease Research. <b>2011</b> , 523-539	
2192	Unraveling the genetics of cancer: genome sequencing and beyond. <b>2011</b> , 12, 407-30	73
2191	Improving RNA-Seq expression estimates by correcting for fragment bias. <b>2011</b> , 12, R22	804
2190	ExpressionPlot: a web-based framework for analysis of RNA-Seq and microarray gene expression data. <b>2011</b> , 12, R69	31
2189	An introduction to the informatics of "next-generation" sequencing. <b>2011</b> , Chapter 11, Unit 11.1.	11
2188	Gene Expression Analysis Using RNA-Seq from Organisms Lacking Substantial Genomic Resources. <b>2011</b> ,	
2187	Utility of RNA Sequencing for Analysis of Maize Reproductive Transcriptomes. <b>2011</b> , 4, 191-203	100
2186	Asymmetric distribution of gene expression in the centromeric region of rice chromosome 5. <b>2011</b> , 2, 16	12
2185	Next generation quantitative genetics in plants. <b>2011</b> , 2, 77	10
2184	SOAPsplice: Genome-Wide ab initio Detection of Splice Junctions from RNA-Seq Data. <b>2011</b> , 2, 46	82
2183	Thousands of Novel Transcripts Identified in Mouse Cerebrum, Testis, and ES Cells Based on ribo-minus RNA Sequencing. <b>2011</b> , 2, 93	12
2182	Noncanonical compensation of zygotic X transcription in early Drosophila melanogaster development revealed through single-embryo RNA-seq. <b>2011</b> , 9, e1000590	141
2181	PoPoolation: a toolbox for population genetic analysis of next generation sequencing data from pooled individuals. <b>2011</b> , 6, e15925	372
2180	Mayday SeaSight: combined analysis of deep sequencing and microarray data. 2011, 6, e16345	16
2179	Massive-scale RNA-Seq analysis of non ribosomal transcriptome in human trisomy 21. <b>2011</b> , 6, e18493	53

# (2011-2011)

2178	RNA-Seq of human neurons derived from iPS cells reveals candidate long non-coding RNAs involved in neurogenesis and neuropsychiatric disorders. <b>2011</b> , 6, e23356	195
2177	Genomic analysis of parent-of-origin allelic expression in Arabidopsis thaliana seeds. <b>2011</b> , 6, e23687	148
2176	Transcriptional profiling of endocrine cerebro-osteodysplasia using microarray and next-generation sequencing. <b>2011</b> , 6, e25400	8
2175	RNA-Seq analyses generate comprehensive transcriptomic landscape and reveal complex transcript patterns in hepatocellular carcinoma. <b>2011</b> , 6, e26168	77
2174	Statistical Modeling of RNA-Seq Data. <b>2011</b> , 26,	53
2173	Identification of Common Carp Innate Immune Genes with Whole-Genome Sequencing and RNA-Seq Data. <b>2011</b> , 8, 165-175	18
2172	Transcriptomic Technologies and Statistical Data Analysis. <b>2011</b> , 133-162	
2171	Quantification of gene transcripts with deep sequencing analysis of gene expression (DSAGE) using 1 to 2 µg total RNA. <b>2011</b> , Chapter 25, Unit25B.9	7
2170	Transcription factor genes of Schizophyllum commune involved in regulation of mushroom formation. <b>2011</b> , 81, 1433-45	96
2169	Understanding the pathogenesis of Alzheimer's disease: will RNA-Seq realize the promise of transcriptomics?. <b>2011</b> , 116, 937-46	49
2168	Regulatory mechanisms underlying C4 photosynthesis. <b>2011</b> , 190, 9-20	35
2167	Computational methods for transcriptome annotation and quantification using RNA-seq. <b>2011</b> , 8, 469-77	711
2166	RNA sequencing: advances, challenges and opportunities. <b>2011</b> , 12, 87-98	1432
2165	Next-generation transcriptome assembly. <b>2011</b> , 12, 671-82	878
2164	Transcriptome-wide sequencing reveals numerous APOBEC1 mRNA-editing targets in transcript 3' UTRs. <b>2011</b> , 18, 230-6	172
2163	Hotspots of aberrant epigenomic reprogramming in human induced pluripotent stem cells. <b>2011</b> , 471, 68-73	1241
2162	Dynamic regulation of 5-hydroxymethylcytosine in mouse ES cells and during differentiation. <b>2011</b> , 473, 398-402	911
2161	Full-length transcriptome assembly from RNA-Seq data without a reference genome. <b>2011</b> , 29, 644-52	11785

2160	The study of eQTL variations by RNA-seq: from SNPs to phenotypes. <b>2011</b> , 27, 72-9	176
2159	Characterization of the abomasal transcriptome for mechanisms of resistance to gastrointestinal nematodes in cattle. <b>2011</b> , 42, 114	36
2158	MAKER2: an annotation pipeline and genome-database management tool for second-generation genome projects. <b>2011</b> , 12, 491	1008
2157	Revealing the missing expressed genes beyond the human reference genome by RNA-Seq. <b>2011</b> , 12, 590	23
2156	Using RNA-seq to determine the transcriptional landscape and the hypoxic response of the pathogenic yeast Candida parapsilosis. <b>2011</b> , 12, 628	59
2155	Deep RNA sequencing analysis of readthrough gene fusions in human prostate adenocarcinoma and reference samples. <b>2011</b> , 4, 11	120
2154	Metabolic labeling of RNA uncovers principles of RNA production and degradation dynamics in mammalian cells. <b>2011</b> , 29, 436-42	406
2153	The integration of 'omic' disciplines and systems biology in cattle breeding. <b>2011</b> , 5, 493-505	15
2152	The evolution of gene expression levels in mammalian organs. <b>2011</b> , 478, 343-8	787
2151	IsoLasso: A LASSO Regression Approach to RNA-Seq Based Transcriptome Assembly. <b>2011</b> , 168-188	14
	IsoLasso: A LASSO Regression Approach to RNA-Seq Based Transcriptome Assembly. <b>2011</b> , 168-188  Ascaris suum draft genome. <b>2011</b> , 479, 529-33	217
2150		
2150	Ascaris suum draft genome. <b>2011</b> , 479, 529-33	217
2150 2149	Ascaris suum draft genome. <b>2011</b> , 479, 529-33  Next-generation sequencing and its applications in molecular diagnostics. <b>2011</b> , 11, 333-43	217
2150 2149 2148	Ascaris suum draft genome. <b>2011</b> , 479, 529-33  Next-generation sequencing and its applications in molecular diagnostics. <b>2011</b> , 11, 333-43  In vivo and transcriptome-wide identification of RNA binding protein target sites. <b>2011</b> , 44, 828-40  RNA-Seq of the xylose-fermenting yeast Scheffersomyces stipitis cultivated in glucose or xylose.	217 125 124
2150 2149 2148 2147	Ascaris suum draft genome. 2011, 479, 529-33  Next-generation sequencing and its applications in molecular diagnostics. 2011, 11, 333-43  In vivo and transcriptome-wide identification of RNA binding protein target sites. 2011, 44, 828-40  RNA-Seq of the xylose-fermenting yeast Scheffersomyces stipitis cultivated in glucose or xylose. 2011, 92, 1237-49  mRNA-Seq Reveals a Comprehensive Transcriptome Profile of Rice under Phosphate Stress. 2011, 4, 50-65	217 125 124 25
2150 2149 2148 2147 2146	Ascaris suum draft genome. 2011, 479, 529-33  Next-generation sequencing and its applications in molecular diagnostics. 2011, 11, 333-43  In vivo and transcriptome-wide identification of RNA binding protein target sites. 2011, 44, 828-40  RNA-Seq of the xylose-fermenting yeast Scheffersomyces stipitis cultivated in glucose or xylose. 2011, 92, 1237-49  mRNA-Seq Reveals a Comprehensive Transcriptome Profile of Rice under Phosphate Stress. 2011, 4, 50-65	217 125 124 25 36

2142	Estimation of alternative splicing isoform frequencies from RNA-Seq data. <b>2011</b> , 6, 9	125
2141	SAMMate: a GUI tool for processing short read alignments in SAM/BAM format. <b>2011</b> , 6, 2	50
2140	An integrative analysis of DNA methylation and RNA-Seq data for human heart, kidney and liver. <b>2011</b> , 5 Suppl 3, S4	30
2139	An integrated database of Eucalyptusspp. genome project. <b>2011</b> , 5,	2
2138	NSMAP: a method for spliced isoforms identification and quantification from RNA-Seq. <b>2011</b> , 12, 162	26
2137	rnaSeqMap: a Bioconductor package for RNA sequencing data exploration. <b>2011</b> , 12, 200	10
2136	Bias detection and correction in RNA-Sequencing data. <b>2011</b> , 12, 290	110
2135	IsoformEx: isoform level gene expression estimation using weighted non-negative least squares from mRNA-Seq data. <b>2011</b> , 12, 305	21
2134	RSEM: accurate transcript quantification from RNA-Seq data with or without a reference genome. <b>2011</b> , 12, 323	9564
2133	eXframe: reusable framework for storage, analysis and visualization of genomics experiments. <b>2011</b> , 12, 452	5
2132	UMARS: Un-MAppable Reads Solution. <b>2011</b> , 12 Suppl 1, S9	7
2131	Analysis of cancer metabolism with high-throughput technologies. <b>2011</b> , 12 Suppl 10, S8	9
2130	Oqtans: a Galaxy-integrated workflow for quantitative transcriptome analysis from NGS Data. <b>2011</b> , 12,	2
2129	Optimizing de novo transcriptome assembly from short-read RNA-Seq data: a comparative study. <b>2011</b> , 12 Suppl 14, S2	325
2128	Detection of splicing events and multiread locations from RNA-seq data based on a geometric-tail (GT) distribution of intron length. <b>2011</b> , 12 Suppl 5, S2	
2127	Rice-Map: a new-generation rice genome browser. <b>2011</b> , 12, 165	9
2126	RNA-seq: technical variability and sampling. <b>2011</b> , 12, 293	195
2125	Somatic sex-specific transcriptome differences in Drosophila revealed by whole transcriptome sequencing. <b>2011</b> , 12, 364	66

2124	Addressing challenges in the production and analysis of illumina sequencing data. <b>2011</b> , 12, 382	99
2123	A global view of porcine transcriptome in three tissues from a full-sib pair with extreme phenotypes in growth and fat deposition by paired-end RNA sequencing. <b>2011</b> , 12, 448	80
2122	Comparative analysis of neural transcriptomes and functional implication of unannotated intronic expression. <b>2011</b> , 12, 494	3
2121	False negative rates in Drosophila cell-based RNAi screens: a case study. <b>2011</b> , 12, 50	36
2120	De novo sequence assembly of Albugo candida reveals a small genome relative to other biotrophic oomycetes. <b>2011</b> , 12, 503	94
2119	The classification of mRNA expression levels by the phosphorylation state of RNAPII CTD based on a combined genome-wide approach. <b>2011</b> , 12, 516	29
2118	RNA-Seq improves annotation of protein-coding genes in the cucumber genome. <b>2011</b> , 12, 540	134
2117	Exploring the gonad transcriptome of two extreme male pigs with RNA-seq. <b>2011</b> , 12, 552	72
2116	Directional gene expression and antisense transcripts in sexual and asexual stages of Plasmodium falciparum. <b>2011</b> , 12, 587	221
2115	Comprehensive identification and quantification of microbial transcriptomes by genome-wide unbiased methods. <b>2011</b> , 22, 32-41	54
2114	Applications of second generation sequencing technologies in complex disorders. <b>2012</b> , 12, 321-43	3
2113	Optimizing bioinformatics workflows for data analysis using cloud management techniques. <b>2011</b> ,	11
2112	A conceptual data model for transcriptome project pipeline. 2011,	1
2111	A comparison of analog and Next-Generation transcriptomic tools for mammalian studies. <b>2011</b> , 10, 135-50	48
2110	SPATA: A seeding and patching algorithm for de novo transcriptome assembly. <b>2011</b> ,	1
2109	Multimodal RNA-seq using single-strand, double-strand, and CircLigase-based capture yields a refined and extended description of the C. elegans transcriptome. <b>2011</b> , 21, 265-75	34
2108	RNA-Seq based discovery and reconstruction of unannotated transcripts in partially annotated genomes. <b>2011</b> ,	1
2107	Whole-transcriptome RNAseq analysis from minute amount of total RNA. <b>2011</b> , 39, e120	115

2106	SpliceTrap: a method to quantify alternative splicing under single cellular conditions. <i>Bioinformatics</i> , <b>2011</b> , 27, 3010-6	73
2105	FDM: a graph-based statistical method to detect differential transcription using RNA-seq data.  Bioinformatics, <b>2011</b> , 27, 2633-40  7.2	42
2104	Nonrandom gene loss from the Drosophila miranda neo-Y chromosome. <b>2011</b> , 3, 1329-37	41
2103	RNA-Seq analysis of splicing in Plasmodium falciparum uncovers new splice junctions, alternative splicing and splicing of antisense transcripts. <b>2011</b> , 39, 3820-35	97
2102	Ab initio identification of transcription start sites in the Rhesus macaque genome by histone modification and RNA-Seq. <b>2011</b> , 39, 1408-18	16
<b>2</b> 101	Genome-wide in silico identification of new conserved and functional retinoic acid receptor response elements (direct repeats separated by 5 bp). <b>2011</b> , 286, 33322-34	63
2100	Characterizing the impact of smoking and lung cancer on the airway transcriptome using RNA-Seq. <b>2011</b> , 4, 803-17	117
2099	Comparative analysis of proteome and transcriptome variation in mouse. <b>2011</b> , 7, e1001393	417
2098	Isoform-level microRNA-155 target prediction using RNA-seq. <b>2011</b> , 39, e61	26
2097	Nascent-seq indicates widespread cotranscriptional pre-mRNA splicing in Drosophila. <b>2011</b> , 25, 2502-12	185
2096	The genome of the leaf-cutting ant Acromyrmex echinatior suggests key adaptations to advanced social life and fungus farming. <b>2011</b> , 21, 1339-48	183
2095	Inference of isoforms from short sequence reads. <b>2011</b> , 18, 305-21	41
2094	ExpEdit: a webserver to explore human RNA editing in RNA-Seq experiments. <i>Bioinformatics</i> , <b>2011</b> , 27, 1311-2	24
2093	RNA-Seq analysis of a soybean near-isogenic line carrying bacterial leaf pustule-resistant and -susceptible alleles. <b>2011</b> , 18, 483-97	75
2092	Euchromatic subdomains in rice centromeres are associated with genes and transcription. <b>2011</b> , 23, 4054-64	42
2091	Accurate quantification of transcriptome from RNA-Seq data by effective length normalization. <b>2011</b> , 39, e9	91
2090	Single-stranded noncoding RNAs mediate local epigenetic alterations at gene promoters in rat cell lines. <b>2011</b> , 286, 34788-99	31
2089	A pipeline for RNA-seq data processing and quality assessment. <i>Bioinformatics</i> , <b>2011</b> , 27, 867-9 7.2	48

2088	Using non-uniform read distribution models to improve isoform expression inference in RNA-Seq. <i>Bioinformatics</i> , <b>2011</b> , 27, 502-8	7.2	72
2087	RISC RNA sequencing for context-specific identification of in vivo microRNA targets. <b>2011</b> , 108, 18-26		87
2086	Whole transcriptome sequencing reveals gene expression and splicing differences in brain regions affected by Alzheimer's disease. <b>2011</b> , 6, e16266		213
2085	Next-generation sequencing reveals HIV-1-mediated suppression of T cell activation and RNA processing and regulation of noncoding RNA expression in a CD4+ T cell line. <b>2011</b> , 2,		54
2084	ABMapper: a suffix array-based tool for multi-location searching and splice-junction mapping. <i>Bioinformatics</i> , <b>2011</b> , 27, 421-2	7.2	14
2083	Efficiently identifying genome-wide changes with next-generation sequencing data. <b>2011</b> , 39, e130		27
2082	Cryptococcal titan cell formation is regulated by G-protein signaling in response to multiple stimuli. <b>2011</b> , 10, 1306-16		80
2081	Nuclear effects of G-protein receptor kinase 5 on histone deacetylase 5-regulated gene transcription in heart failure. <b>2011</b> , 4, 659-68		37
2080	Mouse Rankl expression is regulated in T cells by c-Fos through a cluster of distal regulatory enhancers designated the T cell control region. <b>2011</b> , 286, 20880-91		39
2079	FusionMap: detecting fusion genes from next-generation sequencing data at base-pair resolution. <i>Bioinformatics</i> , <b>2011</b> , 27, 1922-8	7.2	192
2078	Evidence for compensatory upregulation of expressed X-linked genes in mammals, Caenorhabditis elegans and Drosophila melanogaster. <b>2011</b> , 43, 1179-85		206
2077	Sensitive gene fusion detection using ambiguously mapping RNA-Seq read pairs. <i>Bioinformatics</i> , <b>2011</b> , 27, 1068-75	7.2	48
2076	The reality of pervasive transcription. <b>2011</b> , 9, e1000625; discussion e1001102		325
2075	Sex chromosome-specific regulation in the Drosophila male germline but little evidence for chromosomal dosage compensation or meiotic inactivation. <b>2011</b> , 9, e1001126		98
2074	Structural and functional differences in the long non-coding RNA hotair in mouse and human. <b>2011</b> , 7, e1002071		191
2073	A deep sequencing approach to comparatively analyze the transcriptome of lifecycle stages of the filarial worm, Brugia malayi. <b>2011</b> , 5, e1409		69
2072	Over-expression of DSCAM and COL6A2 cooperatively generates congenital heart defects. <b>2011</b> , 7, e10	02344	53
2071	Characterization and improvement of RNA-Seq precision in quantitative transcript expression profiling. <i>Bioinformatics</i> , <b>2011</b> , 27, i383-91	7.2	108

	Sort: all pairs similarity search for short reads. <i>Bioinformatics</i> , <b>2011</b> , 27, 464-70	7.2	18
2069 <b>Gen</b> c	me-wide analysis of promoter architecture in Drosophila melanogaster. <b>2011</b> , 21, 182-92		178
	gen detection using short-RNA deep sequencing subtraction and assembly. <i>Bioinformatics</i> , 27, 2027-30	7.2	50
2067 <b>Tow</b> a	rd an integrated model of capsule regulation in Cryptococcus neoformans. <b>2011</b> , 7, e1002411		71
2066 <b>Nex</b> t	generation sequencing technologies for insect virus discovery. <b>2011</b> , 3, 1849-69		81
	criptome analysis of rice mature root tissue and root tips in early development by massive el sequencing. <b>2012</b> , 63, 2141-57		37
	lation in giant viruses: a unique mixture of bacterial and eukaryotic termination schemes. 8, e1003122		22
2063 <b>Rapi</b> o	turnover of long noncoding RNAs and the evolution of gene expression. <b>2012</b> , 8, e1002841		238
	genetic and transcriptomic analysis of chemosensory receptors in a pair of divergent ant es reveals sex-specific signatures of odor coding. <b>2012</b> , 8, e1002930		150
2061 <b>Cot</b> ra	nscriptional splicing efficiency differs dramatically between Drosophila and mouse. <b>2012</b> , 18, 217	4-86	72
2060 <b>Wo</b> rr	Base: Annotating many nematode genomes. <b>2012</b> , 1, 15-21		
			11
	ST: a functional annotation tool for putative proteins encoded by alternatively spliced cripts. <i>Bioinformatics</i> , <b>2012</b> , 28, 2076-7	7.2	2
<sup>2059</sup> trans		7.2	
2059 trans 2058 A cor	cripts. <i>Bioinformatics</i> , <b>2012</b> , 28, 2076-7	7.2	2
2059 trans 2058 A cor Calpa 2057 dege	ripts. <i>Bioinformatics</i> , <b>2012</b> , 28, 2076-7  aparison of brain gene expression levels in domesticated and wild animals. <b>2012</b> , 8, e1002962  in-5 mutations cause autoimmune uveitis, retinal neovascularization, and photoreceptor	7.2	91
2059 trans 2058 A cor Calpa 2057 dege 2056 Polya prote	ripts. <i>Bioinformatics</i> , <b>2012</b> , 28, 2076-7  aparison of brain gene expression levels in domesticated and wild animals. <b>2012</b> , 8, e1002962  in-5 mutations cause autoimmune uveitis, retinal neovascularization, and photoreceptor neration. <b>2012</b> , 8, e1003001  denylation-dependent control of long noncoding RNA expression by the poly(A)-binding	7.2	2 91 58
2059 trans 2058 A cor  2057 Calpa dege  2056 Polya prote  2055 A his morp	ripts. <i>Bioinformatics</i> , <b>2012</b> , 28, 2076-7  Inparison of brain gene expression levels in domesticated and wild animals. <b>2012</b> , 8, e1002962  In-5 mutations cause autoimmune uveitis, retinal neovascularization, and photoreceptor neration. <b>2012</b> , 8, e1003001  Idenylation-dependent control of long noncoding RNA expression by the poly(A)-binding in nuclear 1. <b>2012</b> , 8, e1003078  In one deacetylase adjusts transcription kinetics at coding sequences during Candida albicans	7.2	2 91 58 110

2052	A systematically improved high quality genome and transcriptome of the human blood fluke Schistosoma mansoni. <b>2012</b> , 6, e1455		306
2051	Genome-wide transcriptional profiling of appressorium development by the rice blast fungus Magnaporthe oryzae. <b>2012</b> , 8, e1002514		132
2050	BatMis: a fast algorithm for k-mismatch mapping. <i>Bioinformatics</i> , <b>2012</b> , 28, 2122-8	7.2	25
2049	Systematic identification of rhythmic genes reveals camk1gb as a new element in the circadian clockwork. <b>2012</b> , 8, e1003116		32
2048	Evidence for widespread positive and purifying selection across the European rabbit (Oryctolagus cuniculus) genome. <b>2012</b> , 29, 1837-49		57
2047	Transcription factor Amr1 induces melanin biosynthesis and suppresses virulence in Alternaria brassicicola. <b>2012</b> , 8, e1002974		57
2046	PASSion: a pattern growth algorithm-based pipeline for splice junction detection in paired-end RNA-Seq data. <i>Bioinformatics</i> , <b>2012</b> , 28, 479-86	7.2	20
2045	Positional correlation analysis improves reconstruction of full-length transcripts and alternative isoforms from noisy array signals or short reads. <i>Bioinformatics</i> , <b>2012</b> , 28, 929-37	7.2	6
2044	Bellerophontes: an RNA-Seq data analysis framework for chimeric transcripts discovery based on accurate fusion model. <i>Bioinformatics</i> , <b>2012</b> , 28, 2114-21	7.2	33
2043	Dynamic deposition of histone variant H3.3 accompanies developmental remodeling of the Arabidopsis transcriptome. <b>2012</b> , 8, e1002658		93
2042	Persistent androgen receptor-mediated transcription in castration-resistant prostate cancer under androgen-deprived conditions. <b>2012</b> , 40, 10765-79		80
2041	Genome-wide analysis reveals distinct patterns of epigenetic features in long non-coding RNA loci. <b>2012</b> , 40, 10018-31		110
2040	Tools for mapping high-throughput sequencing data. <i>Bioinformatics</i> , <b>2012</b> , 28, 3169-77	7.2	211
2039	5-hydroxymethyl-cytosine enrichment of non-committed cells is not a universal feature of vertebrate development. <b>2012</b> , 7, 383-9		44
2038	The genome of Prunus mume. <b>2012</b> , 3, 1318		295
2037	A proteogenomic survey of the Medicago truncatula genome. <b>2012</b> , 11, 933-44		24
2036	Computational inference of mRNA stability from histone modification and transcriptome profiles. <b>2012</b> , 40, 6414-23		16
2035	Age-related changes of gene expression in the neocortex: preliminary data on RNA-Seq of the transcriptome in three functionally distinct cortical areas. <b>2012</b> , 24, 1427-42		18

2034	Qualimap: evaluating next-generation sequencing alignment data. <i>Bioinformatics</i> , <b>2012</b> , 28, 2678-9	7.2	457
2033	High-resolution mapping of open chromatin in the rice genome. <b>2012</b> , 22, 151-62		168
2032	Detection of murine leukemia virus in the Epstein-Barr virus-positive human B-cell line JY, using a computational RNA-Seq-based exogenous agent detection pipeline, PARSES. <b>2012</b> , 86, 2970-7		26
2031	Gene expression changes governing extreme dehydration tolerance in an Antarctic insect. <b>2012</b> , 109, 20744-9		85
2030	Surveillance of 3' Noncoding Transcripts Requires FIERY1 and XRN3 in Arabidopsis. <b>2012</b> , 2, 487-98		33
2029	Whole genome expression differences in human left and right atria ascertained by RNA sequencing. <b>2012</b> , 5, 327-35		43
2028	Transcriptomes of mouse olfactory epithelium reveal sexual differences in odorant detection. <b>2012</b> , 4, 703-12		34
2027	Identification and functional characterization of Rca1, a transcription factor involved in both antifungal susceptibility and host response in Candida albicans. <b>2012</b> , 11, 916-31		38
2026	Pinstripe: a suite of programs for integrating transcriptomic and proteomic datasets identifies novel proteins and improves differentiation of protein-coding and non-coding genes. <i>Bioinformatics</i> , <b>2012</b> , 28, 3042-50	7.2	59
2025	Reverse engineering biomolecular systems using -omic data: challenges, progress and opportunities. <b>2012</b> , 13, 430-45		17
2024	The central role of the host cell in symbiotic nitrogen metabolism. <b>2012</b> , 279, 2965-73		57
2023	VectorBase: improvements to a bioinformatics resource for invertebrate vector genomics. <b>2012</b> , 40, D729-34		134
2022	Transcriptome survey reveals increased complexity of the alternative splicing landscape in Arabidopsis. <b>2012</b> , 22, 1184-95		520
2021	Cell type-specific genomics of Drosophila neurons. <b>2012</b> , 40, 9691-704		114
2020	Benchmarking spliced alignment programs including Spaln2, an extended version of Spaln that incorporates additional species-specific features. <b>2012</b> , 40, e161		65
2019	deepBlockAlign: a tool for aligning RNA-seq profiles of read block patterns. <i>Bioinformatics</i> , <b>2012</b> , 28, 17-24	7.2	16
2018	RNA-Seq mapping and detection of gene fusions with a suffix array algorithm. <b>2012</b> , 8, e1002464		40
2017	H2B monoubiquitylation is a 5'-enriched active transcription mark and correlates with exon-intron structure in human cells. <b>2012</b> , 22, 1026-35		50

2016	Identification of allele-specific alternative mRNA processing via transcriptome sequencing. <b>2012</b> , 40, e104	53
2015	Direct and indirect involvement of microRNA-499 in clinical and experimental cardiomyopathy. <b>2012</b> , 111, 521-31	105
2014	Genome update of Botrytis cinerea strains B05.10 and T4. <b>2012</b> , 11, 1413-4	99
2013	Tissue-specific alternative polyadenylation at the imprinted gene Mest regulates allelic usage at Copg2. <b>2012</b> , 40, 1523-35	20
2012	Accurate identification of A-to-I RNA editing in human by transcriptome sequencing. <b>2012</b> , 22, 142-50	246
2011	The grapevine expression atlas reveals a deep transcriptome shift driving the entire plant into a maturation program. <b>2012</b> , 24, 3489-505	252
2010	The transcriptome of Verticillium dahliae-infected Nicotiana benthamiana determined by deep RNA sequencing. <b>2012</b> , 7, 1065-9	33
2009	Extensive alternative polyadenylation during zebrafish development. <b>2012</b> , 22, 2054-66	220
2008	fus/TLS orchestrates splicing of developmental regulators during gastrulation. 2012, 26, 1351-63	35
2007	An integer programming approach to novel transcript reconstruction from paired-end RNA-Seq reads. <b>2012</b> ,	12
2006	shutdown is a component of the Drosophila piRNA biogenesis machinery. <b>2012</b> , 18, 1446-57	66
2005	Unexpected diversity and expression of avian endogenous retroviruses. <b>2012</b> , 3, e00344-12	42
2004	RNA sequencing: platform selection, experimental design, and data interpretation. 2012, 22, 271-4	140
2003	Long noncoding RNAs in C. elegans. <b>2012</b> , 22, 2529-40	157
2002	Analysis of C. elegans intestinal gene expression and polyadenylation by fluorescence-activated nuclei sorting and 3'-end-seq. <b>2012</b> , 40, 6304-18	54
2001	Novel roles for KLF1 in erythropoiesis revealed by mRNA-seq. <b>2012</b> , 22, 2385-98	65
<b>2</b> 000	Loss of miR-29 in myoblasts contributes to dystrophic muscle pathogenesis. <b>2012</b> , 20, 1222-33	90
1999	SPLOOCE: a new portal for the analysis of human splicing variants. <b>2012</b> , 9, 1339-43	7

1998	Revealing stable processing products from ribosome-associated small RNAs by deep-sequencing data analysis. <b>2012</b> , 40, 4013-24	45
1997	Algorithm to identify frequent coupled modules from two-layered network series: application to study transcription and splicing coupling. <b>2012</b> , 19, 710-30	14
1996	Mining Arabidopsis thaliana RNA-seq data with Integrated Genome Browser reveals stress-induced alternative splicing of the putative splicing regulator SR45a. <b>2012</b> , 99, 219-31	34
1995	Genome-wide identification of regulatory DNA elements and protein-binding footprints using signatures of open chromatin in Arabidopsis. <b>2012</b> , 24, 2719-31	164
1994	Effects of drought on gene expression in maize reproductive and leaf meristem tissue revealed by RNA-Seq. <b>2012</b> , 160, 846-67	228
1993	Workshop: Gene fusion detection with short and medium length next generation sequencing. 2012,	
1992	Transcriptome assembly and isoform expression level estimation from biased RNA-Seq reads. <i>Bioinformatics</i> , <b>2012</b> , 28, 2914-21	68
1991	A new strategy to reduce allelic bias in RNA-Seq readmapping. <b>2012</b> , 40, e127	74
1990	Combining RT-PCR-seq and RNA-seq to catalog all genic elements encoded in the human genome. <b>2012</b> , 22, 1698-710	44
1989	Cold-inducible RNA-binding protein modulates circadian gene expression posttranscriptionally. <b>2012</b> , 338, 379-83	188
1988	Essential role of EBF1 in the generation and function of distinct mature B cell types. <b>2012</b> , 209, 775-92	88
1987	Detecting differential usage of exons from RNA-seq data. <b>2012</b> , 22, 2008-17	882
1986	X-chromosome hyperactivation in mammals via nonlinear relationships between chromatin states and transcription. <b>2011</b> , 19, 56-61	67
1985	Cutaneous retinoic acid levels determine hair follicle development and downgrowth. <b>2012</b> , 287, 39304-15	17
1984	Reduced DICER1 elicits an interferon response in endometrial cancer cells. <b>2012</b> , 10, 316-25	12
1983	Genome sequence of the oleaginous red yeast Rhodosporidium toruloides MTCC 457. <b>2012</b> , 11, 1083-4	51
1982	W chromosome expression responds to female-specific selection. <b>2012</b> , 109, 8207-11	76
1981	Identification and properties of 1,119 candidate lincRNA loci in the Drosophila melanogaster genome. <b>2012</b> , 4, 427-42	165

1980	A genome-wide regulatory framework identifies maize pericarp color1 controlled genes. <b>2012</b> , 24, 2745-64	120
1979	Whole-exome sequencing of human pancreatic cancers and characterization of genomic instability caused by MLH1 haploinsufficiency and complete deficiency. <b>2012</b> , 22, 208-19	95
1978	Digging in the RNA-seq Garbage: Evaluating the Characteristics of Unmapped RNA-seq Reads in Normal Tissues. <b>2012</b> ,	1
1977	MiRGator v3.0: a microRNA portal for deep sequencing, expression profiling and mRNA targeting. <b>2013</b> , 41, D252-7	118
1976	A novel computational strategy to identify A-to-I RNA editing sites by RNA-Seq data: de novo detection in human spinal cord tissue. <b>2012</b> , 7, e44184	15
1975	Activation of the carbon concentrating mechanism by CO2 deprivation coincides with massive transcriptional restructuring in Chlamydomonas reinhardtii. <b>2012</b> , 24, 1860-75	90
1974	Rapid phosphoproteomic and transcriptomic changes in the rhizobia-legume symbiosis. <b>2012</b> , 11, 724-44	91
1973	Alternative splicing and trans-splicing events revealed by analysis of the Bombyx mori transcriptome. <b>2012</b> , 18, 1395-407	31
1972	Genome-wide determination of a broad ESRP-regulated posttranscriptional network by high-throughput sequencing. <b>2012</b> , 32, 1468-82	102
1971	Determinants of exon-level evolutionary rates in Arabidopsis species. <b>2012</b> , 8, 389-415	3
1970	Quantification of Transcriptome Responses of the Rumen Epithelium to Butyrate Infusion using RNA-seq Technology. <b>2012</b> , 6, 67-80	37
1969	Alkbh1 and Tzfp repress a non-repeat piRNA cluster in pachytene spermatocytes. <b>2012</b> , 40, 10950-63	13
1968	Retinoic acid receptors recognize the mouse genome through binding elements with diverse spacing and topology. <b>2012</b> , 287, 26328-41	100
1967	Characterization of novel genomic alterations and therapeutic approaches using acute megakaryoblastic leukemia xenograft models. <b>2012</b> , 209, 2017-31	63
1966	Xenomea tool for classifying reads from xenograft samples. <i>Bioinformatics</i> , <b>2012</b> , 28, i172-8 7.2	149
1965	Identification of new viral genes and transcript isoforms during Epstein-Barr virus reactivation using RNA-Seq. <b>2012</b> , 86, 1458-67	52
1964	Identification of candidate genes underlying an iron efficiency quantitative trait locus in soybean. <b>2012</b> , 158, 1745-54	49
1963	AutismKB: an evidence-based knowledgebase of autism genetics. <b>2012</b> , 40, D1016-22	129

1962	RNASEQRa streamlined and accurate RNA-seq sequence analysis program. <b>2012</b> , 40, e42	25
1961	The super elongation complex family of RNA polymerase II elongation factors: gene target specificity and transcriptional output. <b>2012</b> , 32, 2608-17	126
1960	Transcriptomic landscape of breast cancers through mRNA sequencing. <b>2012</b> , 2, 264	67
1959	Comparative transcriptome analyses of deltamethrin-resistant and -susceptible Anopheles gambiae mosquitoes from Kenya by RNA-Seq. <b>2012</b> , 7, e44607	69
1958	Characterizing regulatory and functional differentiation between maize mesophyll and bundle sheath cells by transcriptomic analysis. <b>2012</b> , 160, 165-77	111
1957	Characteristics and significance of intergenic polyadenylated RNA transcription in Arabidopsis. <b>2013</b> , 161, 210-24	18
1956	sizzled function and secreted factor network dynamics. <b>2012</b> , 1, 286-94	
1955	GenomicTools: an open source platform for developing high-throughput analytics in genomics. <b>2012</b> , 189-220	
1954	Gene expression profiling of liver cancer stem cells by RNA-sequencing. <b>2012</b> , 7, e37159	62
1953	A Method for Isoform Prediction from RNA-Seq Data by Iterative Mapping. <b>2012</b> , 5, 27-33	
1952	MKL1 and MKL2 play redundant and crucial roles in megakaryocyte maturation and platelet formation. <b>2012</b> , 120, 2317-29	46
1951	The biology of nematode- and IL4REdependent murine macrophage polarization in vivo as defined by RNA-Seq and targeted lipidomics. <b>2012</b> , 120, e93-e104	44
1950	A zinc-finger-family transcription factor, AbVf19, is required for the induction of a gene subset important for virulence in Alternaria brassicicola. <b>2012</b> , 25, 443-52	24
1949	Chromatin modification by SUMO-1 stimulates the promoters of translation machinery genes. <b>2012</b> , 40, 10172-86	52
1948	Promoter-specific transcription inhibition in Staphylococcus aureus by a phage protein. <b>2012</b> , 151, 1005-16	19
1947	From specific to global analysis of posttranscriptional regulation in eukaryotes: posttranscriptional regulatory networks. <b>2012</b> , 11, 505-21	12
1946	Tomato immune receptor Ve1 recognizes effector of multiple fungal pathogens uncovered by genome and RNA sequencing. <b>2012</b> , 109, 5110-5	360
1945	Suppression of progenitor differentiation requires the long noncoding RNA ANCR. <b>2012</b> , 26, 338-43	321

1944	Somatic copy number mosaicism in human skin revealed by induced pluripotent stem cells. <b>2012</b> , 492, 438-42	299
1943	Codependency of H2B monoubiquitination and nucleosome reassembly on Chd1. <b>2012</b> , 26, 914-9	58
1942	Transcriptional reprogramming by root knot and migratory nematode infection in rice. <b>2012</b> , 196, 887-900	117
1941	Cardiovascular genomics: a biomarker identification pipeline. <b>2012</b> , 16, 809-22	8
1940	Genome-wide analysis uncovers regulation of long intergenic noncoding RNAs in Arabidopsis. <b>2012</b> , 24, 4333-45	471
1939	Dicer partner proteins tune the length of mature miRNAs in flies and mammals. <b>2012</b> , 151, 533-46	134
1938	Artemis: an integrated platform for visualization and analysis of high-throughput sequence-based experimental data. <i>Bioinformatics</i> , <b>2012</b> , 28, 464-9	665
1937	The evolutionary landscape of alternative splicing in vertebrate species. <b>2012</b> , 338, 1587-93	657
1936	Evolutionary dynamics of gene and isoform regulation in Mammalian tissues. <b>2012</b> , 338, 1593-9	587
1935	Identification of gene expression changes associated with long-term memory of courtship rejection in Drosophila males. <b>2012</b> , 2, 1437-45	22
1934	Activating transcription factor 3 regulates immune and metabolic homeostasis. <b>2012</b> , 32, 3949-62	54
1933	Human RNA methyltransferase BCDIN3D regulates microRNA processing. <b>2012</b> , 151, 278-88	111
1932	Bioinformatics tools and databases for analysis of next-generation sequence data. <b>2012</b> , 11, 12-24	59
1931	Morphine epigenomically regulates behavior through alterations in histone H3 lysine 9 dimethylation in the nucleus accumbens. <b>2012</b> , 32, 17454-64	101
1930	The histone deacetylase SIRT6 is a tumor suppressor that controls cancer metabolism. <b>2012</b> , 151, 1185-99	476
1929	How to analyze gene expression using RNA-sequencing data. <b>2012</b> , 802, 259-74	22
1928	Stable intronic sequence RNA (sisRNA), a new class of noncoding RNA from the oocyte nucleus of Xenopus tropicalis. <b>2012</b> , 26, 2550-9	98
1927	Adiponectin regulates expression of hepatic genes critical for glucose and lipid metabolism. <b>2012</b> , 109, 14568-73	95

1926	Retrograde signaling and photoprotection in a gun4 mutant of Chlamydomonas reinhardtii. <b>2012</b> , 5, 1242-62	42
1925	Towards accurate detection and genotyping of expressed variants from whole transcriptome sequencing data. <b>2012</b> , 13 Suppl 2, S6	31
1924	SpliceGrapher: detecting patterns of alternative splicing from RNA-Seq data in the context of gene models and EST data. <b>2012</b> , 13, R4	101
1923	The birth of the Epitranscriptome: deciphering the function of RNA modifications. <b>2012</b> , 13, 175	275
1922	Chromatin accessibility reveals insights into androgen receptor activation and transcriptional specificity. <b>2012</b> , 13, R88	53
1921	Evidence for conserved post-transcriptional roles of unitary pseudogenes and for frequent bifunctionality of mRNAs. <b>2012</b> , 13, R102	51
1920	Mammalian tissues defective in nonsense-mediated mRNA decay display highly aberrant splicing patterns. <b>2012</b> , 13, R35	90
1919	The genomic landscape shaped by selection on transposable elements across 18 mouse strains. <b>2012</b> , 13, R45	124
1918	Genome-wide survey of recurrent HBV integration in hepatocellular carcinoma. <b>2012</b> , 44, 765-9	627
1917	Human histone H3K79 methyltransferase DOT1L protein [corrected] binds actively transcribing RNA polymerase II to regulate gene expression. <b>2012</b> , 287, 39698-709	62
1916	Lin28b reprograms adult bone marrow hematopoietic progenitors to mediate fetal-like lymphopoiesis. <b>2012</b> , 335, 1195-200	229
1915	Introns in UTRs: why we should stop ignoring them. <b>2012</b> , 34, 1025-34	89
1914	Development of a molecular test to determine the vitality status of Norway spruce (Picea abies) seedlings during frozen storage. <b>2012</b> , 43, 665-678	21
1913	A validated regulatory network for Th17 cell specification. <b>2012</b> , 151, 289-303	794
1912	Mono-uridylation of pre-microRNA as a key step in the biogenesis of group II let-7 microRNAs. <b>2012</b> , 151, 521-32	224
1911	MED12 controls the response to multiple cancer drugs through regulation of TGF-🛮 receptor signaling. <b>2012</b> , 151, 937-50	310
1910	First exon length controls active chromatin signatures and transcription. <b>2012</b> , 2, 62-8	119
1909	FACS purification and transcriptome analysis of drosophila neural stem cells reveals a role for Klumpfuss in self-renewal. <b>2012</b> , 2, 407-18	98

1908	The microtubule plus-end tracking protein CLASP2 is required for hematopoiesis and hematopoietic stem cell maintenance. <b>2012</b> , 2, 781-8	12
1907	A Plasmodium calcium-dependent protein kinase controls zygote development and transmission by translationally activating repressed mRNAs. <b>2012</b> , 12, 9-19	127
1906	Early storage lesions in apheresis platelets are induced by the activation of the integrin ∄b⊞and focal adhesion signaling pathways. <b>2012</b> , 76 Spec No., 297-315	30
1905	Exploring the host transcriptome for mechanisms underlying protective immunity and resistance to nematode infections in ruminants. <b>2012</b> , 190, 1-11	10
1904	Transcriptome analysis of Drosophila CNS midline cells reveals diverse peptidergic properties and a role for castor in neuronal differentiation. <b>2012</b> , 372, 131-42	18
1903	RNA-seq transcriptome analysis of male and female zebra finch cell lines. <b>2012</b> , 100, 363-9	20
1902	Genome-wide identification of miRNA targets by PAR-CLIP. <b>2012</b> , 58, 94-105	79
1901	Poised RNA polymerase II changes over developmental time and prepares genes for future expression. <b>2012</b> , 2, 1670-83	74
1900	WikiCell: a unified resource platform for human transcriptomics research. <b>2012</b> , 16, 357-62	11
1899	A Cloud Infrastructure for Optimization of a Massive Parallel Sequencing Workflow. 2012,	1
1898	Perturbation of FliL interferes with Proteus mirabilis swarmer cell gene expression and differentiation. <b>2012</b> , 194, 437-47	39
1897	A multi-omic map of the lipid-producing yeast Rhodosporidium toruloides. <b>2012</b> , 3, 1112	244
1896	R-SAP: a multi-threading computational pipeline for the characterization of high-throughput RNA-sequencing data. <b>2012</b> , 40, e67	6
1895	BAsplice: Bi-direction alignment for detecting splice junctions. <b>2012</b> ,	
1894	Application of next-generation sequencing technologies in virology. <b>2012</b> , 93, 1853-1868	189
1893	Next-generation sequencing technologies for gene expression profiling in plants. <b>2012</b> , 11, 63-70	100
1892	Systematic identification of long noncoding RNAs expressed during zebrafish embryogenesis. <b>2012</b> , 22, 577-91	590
1891	Characterization of a highly conserved histone related protein, Ydl156w, and its functional associations using quantitative proteomic analyses. <b>2012</b> , 11, M111.011544	24

1890	Comparative analysis of protein-coding genes and long non-coding RNAs of prostate cancer between Caucasian and Chinese populations. <b>2012</b> ,	1
1889	Pepitome: evaluating improved spectral library search for identification complementarity and quality assessment. <b>2012</b> , 11, 1686-95	52
1888	Retinal transcriptome profiling by directional next-generation sequencing using 100 ng of total RNA. <b>2012</b> , 884, 319-34	22
1887	Alternative splicing of mRNA in the molecular pathology of neurodegenerative diseases. <b>2012</b> , 33, 1012.e11-	<b>24</b> 76
1886	Basic leucine zipper transcription factor OsbZIP16 positively regulates drought resistance in rice. <b>2012</b> , 193-194, 8-17	75
1885	Genome-wide transcriptome analysis in murine neural retina using high-throughput RNA sequencing. <b>2012</b> , 99, 44-51	35
1884	Detection, annotation and visualization of alternative splicing from RNA-Seq data with SplicingViewer. <b>2012</b> , 99, 178-82	29
1883	Identification of long non-protein coding RNAs in chicken skeletal muscle using next generation sequencing. <b>2012</b> , 99, 292-8	119
1882	Transcriptome analysis of rosette and folding leaves in Chinese cabbage using high-throughput RNA sequencing. <b>2012</b> , 99, 299-307	35
1881	Splice variant of the SND1 transcription factor is a dominant negative of SND1 members and their regulation in Populus trichocarpa. <b>2012</b> , 109, 14699-704	101
1880	Methods and software in NGS for TE analysis. <b>2012</b> , 859, 105-14	6
1879	Binding profiles of chromatin-modifying proteins are predictive for transcriptional activity and promoter-proximal pausing. <b>2012</b> , 19, 126-38	8
1878	A high-throughput chromatin immunoprecipitation approach reveals principles of dynamic gene regulation in mammals. <b>2012</b> , 47, 810-22	299
1877	mRNA-Seq reveals complex patterns of gene regulation and expression in the mouse skeletal muscle transcriptome associated with calorie restriction. <b>2012</b> , 44, 331-44	12
1876	Genome-wide in silico prediction of gene expression. <i>Bioinformatics</i> , <b>2012</b> , 28, 2789-96 7.2	42
1875	Genomic landscape of non-small cell lung cancer in smokers and never-smokers. <b>2012</b> , 150, 1121-34	860
1874	Polycomb associates genome-wide with a specific RNA polymerase II variant, and regulates metabolic genes in ESCs. <b>2012</b> , 10, 157-70	221
1873	Lifestyle transitions in plant pathogenic Colletotrichum fungi deciphered by genome and transcriptome analyses. <b>2012</b> , 44, 1060-5	564

1872	Comparing DNA Sequence Collections by Direct Comparison of Compressed Text Indexes. <b>2012</b> , 214-224	11
1871	OSA: a fast and accurate alignment tool for RNA-Seq. <i>Bioinformatics</i> , <b>2012</b> , 28, 1933-4 7.2	87
1870	Age-associated inflammation inhibits epidermal stem cell function. <b>2012</b> , 26, 2144-53	101
1869	Detection and quantification of alternative splicing variants using RNA-seq. <b>2012</b> , 883, 97-110	17
1868	Self-Adaptive and Resource-Efficient SLA Enactment for Cloud Computing Infrastructures. 2012,	24
1867	Strategies for transcriptome analysis in nonmodel plants. <b>2012</b> , 99, 267-76	103
1866	Massively parallel sequencing technology in pathogenic microbes. <b>2012</b> , 835, 271-94	5
1865	Polycomb protein Ezh1 promotes RNA polymerase II elongation. <b>2012</b> , 45, 255-62	138
1864	Intragenic enhancers act as alternative promoters. <b>2012</b> , 45, 447-58	193
1863	Differential impact of nutrition on developmental and metabolic gene expression during fruiting body development in Neurospora crassa. <b>2012</b> , 49, 405-13	19
1862	Transcriptome analyses during fruiting body formation in Fusarium graminearum and Fusarium verticillioides reflect species life history and ecology. <b>2012</b> , 49, 663-73	56
1861	Personal omics profiling reveals dynamic molecular and medical phenotypes. <b>2012</b> , 148, 1293-307	921
1860	The pan-ErbB negative regulator Lrig1 is an intestinal stem cell marker that functions as a tumor suppressor. <b>2012</b> , 149, 146-58	486
1859	Cell-free formation of RNA granules: bound RNAs identify features and components of cellular assemblies. <b>2012</b> , 149, 768-79	564
1858	Comprehensive analysis of mRNA methylation reveals enrichment in 3' UTRs and near stop codons. <b>2012</b> , 149, 1635-46	2100
1857	Noncanonical Wnt signaling maintains hematopoietic stem cells in the niche. <b>2012</b> , 150, 351-65	218
1856	Efficient direct reprogramming of mature amniotic cells into endothelial cells by ETS factors and TGFI suppression. <b>2012</b> , 151, 559-75	170
1855	Regulation of pluripotency and self- renewal of ESCs through epigenetic-threshold modulation and mRNA pruning. <b>2012</b> , 151, 576-89	53

1854	Poly-gene fusion transcripts and chromothripsis in prostate cancer. <b>2012</b> , 51, 1144-53	39
1853	Regulation and expression of the ATP-binding cassette transporter ABCG2 in human embryonic stem cells. <b>2012</b> , 30, 2175-87	33
1852	Computational analysis of noncoding RNAs. <b>2012</b> , 3, 759-78	44
1851	A genome resource to address mechanisms of developmental programming: determination of the fetal sheep heart transcriptome. <b>2012</b> , 590, 2873-84	13
1850	Oculus: faster sequence alignment by streaming read compression. <b>2012</b> , 13, 297	3
1849	Global gene expression of the inner cell mass and trophectoderm of the bovine blastocyst. <b>2012</b> , 12, 33	61
1848	Genetic dissection of growth, wood basic density and gene expression in interspecific backcrosses of Eucalyptus grandis and E. urophylla. <b>2012</b> , 13, 60	24
1847	RNA-Seq analysis uncovers transcriptomic variations between morphologically similar in vivo- and in vitro-derived bovine blastocysts. <b>2012</b> , 13, 118	82
1846	Characterization and gene expression analysis of the cir multi-gene family of Plasmodium chabaudi chabaudi (AS). <b>2012</b> , 13, 125	19
1845	Single-base resolution maps of cultivated and wild rice methylomes and regulatory roles of DNA methylation in plant gene expression. <b>2012</b> , 13, 300	202
1844	Transcriptome sequencing of Eucalyptus camaldulensis seedlings subjected to water stress reveals functional single nucleotide polymorphisms and genes under selection. <b>2012</b> , 13, 364	47
1843	Detecting transcription of ribosomal protein pseudogenes in diverse human tissues from RNA-seq data. <b>2012</b> , 13, 412	25
1842	NG6: Integrated next generation sequencing storage and processing environment. 2012, 13, 462	48
1841	A draft of the genome and four transcriptomes of a medicinal and pesticidal angiosperm Azadirachta indica. <b>2012</b> , 13, 464	62
1840	Whole transcriptome analyses of six thoroughbred horses before and after exercise using RNA-Seq. <b>2012</b> , 13, 473	56
1839	Genome-wide association between DNA methylation and alternative splicing in an invertebrate. <b>2012</b> , 13, 480	115
1838	Global endometrial transcriptomic profiling: transient immune activation precedes tissue proliferation and repair in healthy beef cows. <b>2012</b> , 13, 489	22
1837	Comparison of transcriptome technologies in the pathogenic fungus Aspergillus fumigatus reveals novel insights into the genome and MpkA dependent gene expression. <b>2012</b> , 13, 519	30

1836	Analysis of a native whitefly transcriptome and its sequence divergence with two invasive whitefly species. <b>2012</b> , 13, 529	47
1835	Liver transcriptome profile in pigs with extreme phenotypes of intramuscular fatty acid composition. <b>2012</b> , 13, 547	89
1834	Comparison of total and cytoplasmic mRNA reveals global regulation by nuclear retention and miRNAs. <b>2012</b> , 13, 574	30
1833	Resolving candidate genes of mouse skeletal muscle QTL via RNA-Seq and expression network analyses. <b>2012</b> , 13, 592	17
1832	Downy mildew resistance induced by Trichoderma harzianum T39 in susceptible grapevines partially mimics transcriptional changes of resistant genotypes. <b>2012</b> , 13, 660	108
1831	Transcriptome analysis at four developmental stages of grape berry (Vitis vinifera cv. Shiraz) provides insights into regulated and coordinated gene expression. <b>2012</b> , 13, 691	108
1830	De novo reconstruction of the Toxoplasma gondii transcriptome improves on the current genome annotation and reveals alternatively spliced transcripts and putative long non-coding RNAs. <b>2012</b> , 13, 696	36
1829	Strand-specific RNA-seq reveals widespread occurrence of novel cis-natural antisense transcripts in rice. <b>2012</b> , 13, 721	62
1828	Global transcriptome analysis reveals distinct expression among duplicated genes during sorghum-interaction. <b>2012</b> , 12, 121	37
1827	Scheffersomyces stipitis: a comparative systems biology study with the Crabtree positive yeast Saccharomyces cerevisiae. <b>2012</b> , 11, 136	48
1826	Potential role of multiple carbon fixation pathways during lipid accumulation in Phaeodactylum tricornutum. <b>2012</b> , 5, 40	147
1825	Transcriptomic analysis of the oleaginous microalga Neochloris oleoabundans reveals metabolic insights into triacylglyceride accumulation. <b>2012</b> , 5, 74	155
1824	A systematic comparison and evaluation of high density exon arrays and RNA-seq technology used to unravel the peripheral blood transcriptome of sickle cell disease. <b>2012</b> , 5, 28	65
1823	Adipose co-expression networks across Finns and Mexicans identify novel triglyceride-associated genes. <b>2012</b> , 5, 61	24
1822	Strand-specific libraries for high throughput RNA sequencing (RNA-Seq) prepared without poly(A) selection. <b>2012</b> , 3, 9	92
1821	Strategies to identify long noncoding RNAs involved in gene regulation. <b>2012</b> , 2, 37	63
1820	Metalloproteinases and their associated genes contribute to the functional integrity and noise-induced damage in the cochlear sensory epithelium. <b>2012</b> , 32, 14927-41	34
1819	Reversible switching between epigenetic states in honeybee behavioral subcastes. <b>2012</b> , 15, 1371-3	237

1818	Clonal evolution of preleukemic hematopoietic stem cells precedes human acute myeloid leukemia. <b>2012</b> , 4, 149ra118	517
1817	The diverse applications of RNA-seq for functional genomic studies in Aspergillus fumigatus. <b>2012</b> , 1273, 25-34	14
1816	Expression of lec-1, a mycobiont gene encoding a galectin-like protein in the lichen Peltigera membranacea. <b>2012</b> , 57, 23-31	25
1815	Transcriptome sequencing in Sezary syndrome identifies Sezary cell and mycosis fungoides-associated lncRNAs and novel transcripts. <b>2012</b> , 120, 3288-97	71
1814	Gene structure in the sea urchin Strongylocentrotus purpuratus based on transcriptome analysis. <b>2012</b> , 22, 2079-87	113
1813	Deciphering the plant splicing code: experimental and computational approaches for predicting alternative splicing and splicing regulatory elements. <b>2012</b> , 3, 18	61
1812	De novo derivation of proteomes from transcriptomes for transcript and protein identification. <b>2012</b> , 9, 1207-11	131
1811	Protein identification using customized protein sequence databases derived from RNA-Seq data. <b>2012</b> , 11, 1009-17	128
1810	Single-neuron RNA-Seq: technical feasibility and reproducibility. <b>2012</b> , 3, 124	52
1809	Stranded RNA-Seq: Strand-Specific Shotgun Sequencing of RNA. <b>2012</b> , 91-108	
1808	Clinical integration of next-generation sequencing technology. <b>2012</b> , 32, 585-99	49
1807	MicroRNA signature in patients with eosinophilic esophagitis, reversibility with glucocorticoids, and assessment as disease biomarkers. <b>2012</b> , 129, 1064-75.e9	122
1806	Genome-wide and caste-specific DNA methylomes of the ants Camponotus floridanus and Harpegnathos saltator. <b>2012</b> , 22, 1755-64	266
1805	Simplification and desexualization of gene expression in self-fertile nematodes. <b>2012</b> , 22, 2167-72	53
1804	AGO4 regulates entry into meiosis and influences silencing of sex chromosomes in the male mouse germline. <b>2012</b> , 23, 251-64	70
1803	A global view of gene activity at the flowering transition phase in precocious trifoliate orange and its wild-type [Poncirus trifoliata (L.) Raf.] by transcriptome and proteome analysis. <b>2012</b> , 510, 47-58	11
1802	The physiology of sterol nutrition in the pea aphid Acyrthosiphon pisum. <b>2012</b> , 58, 1383-9	22
1801	Beyond the Pipelines: Cloud Computing Facilitates Management, Distribution, Security, and Analysis of High-Speed Sequencer Data. <b>2012</b> , 449-468	3

1800	Interaction between BZR1 and PIF4 integrates brassinosteroid and environmental responses. <b>2012</b> , 14, 802-9	541
1799	Next-generation sequencing technologies and fragment assembly algorithms. 2012, 855, 155-74	19
1798	Using genomic tools to study regulatory evolution. <b>2012</b> , 856, 335-61	5
1797	Next generation sequencing in clinical medicine: Challenges and lessons for pathology and biomedical informatics. <b>2012</b> , 3, 40	106
1796	Experimental Design and Quality Control of Next-Generation Sequencing Experiments. 2012, 417-433	
1795	Library preparation and data analysis packages for rapid genome sequencing. <b>2012</b> , 944, 1-22	16
1794	Brassinosteroid, gibberellin and phytochrome impinge on a common transcription module in Arabidopsis. <b>2012</b> , 14, 810-7	431
1793	Application of a systems approach to study developmental gene regulation. <b>2012</b> , 4, 245-253	1
1792	The Arabidopsis Information Resource (TAIR): improved gene annotation and new tools. <b>2012</b> , 40, D1202-10	1348
1791	Allelic imbalance in Drosophila hybrid heads: exons, isoforms, and evolution. <b>2012</b> , 29, 1521-32	51
1790	Transdifferentiation of MALME-3M and MCF-7 Cells toward Adipocyte-like Cells is Dependent on Clathrin-mediated Endocytosis. <b>2012</b> , 1, 44	3
1789	Current status and future perspectives for sequencing livestock genomes. <b>2012</b> , 3, 8	30
1788	A comprehensive comparison of RNA-Seq-based transcriptome analysis from reads to differential gene expression and cross-comparison with microarrays: a case study in Saccharomyces cerevisiae. <b>2012</b> , 40, 10084-97	222
1787	Genomic approaches for interrogating the biochemistry of medicinal plant species. <b>2012</b> , 517, 139-59	41
1786	Omics Era in Stem Cell Research: Data Integration of Multi-regulatory Layers. <b>2012</b> , 119-137	
1785	Identification of Splicing Factor Target Genes by High-Throughput Sequencing. <b>2012</b> , 556-564	
1784	Improving the Flexibility of RNA-Seq Data Analysis Pipelines. <b>2012</b> , 2012, 70-73	1
1783	Reverse Engineering of TopHat: Splice Junction Mapper for Improving Computational Aspect. 2012,	

1782	RBM20, a gene for hereditary cardiomyopathy, regulates titin splicing. <b>2012</b> , 18, 766-73	337
1781	Transcriptional architecture and chromatin landscape of the core circadian clock in mammals. <b>2012</b> , 338, 349-54	931
1780	RNA Abundance Analysis. <b>2012</b> ,	2
1779	Utilizing RNA-Seq data for cancer network inference. <b>2012</b> ,	4
1778	RNA-seq analysis of synovial fibroblasts brings new insights into rheumatoid arthritis. <b>2012</b> , 2, 43	34
1777	Accuracy of RNA-Seq and its dependence on sequencing depth. <b>2012</b> , 13 Suppl 13, S5	20
1776	Prediction of novel long non-coding RNAs based on RNA-Seq data of mouse Klf1 knockout study. <b>2012</b> , 13, 331	93
1775	Alt Event Finder: a tool for extracting alternative splicing events from RNA-seq data. <b>2012</b> , 13 Suppl 8, S10	19
1774	DFI: gene feature discovery in RNA-seq experiments from multiple sources. <b>2012</b> , 13 Suppl 8, S11	3
1773	RNA-Seq analysis implicates dysregulation of the immune system in schizophrenia. <b>2012</b> , 13 Suppl 8, S2	48
1772	Retinal Development. <b>2012</b> ,	3
1771	Transposable elements reveal a stem cell-specific class of long noncoding RNAs. <b>2012</b> , 13, R107	361
1770	Genome-wide Profiling of RNA splicing in prostate tumor from RNA-seq data using virtual microarrays. <b>2012</b> , 2, 21	2
1769	Maize (Zea mays L.) genome diversity as revealed by RNA-sequencing. <b>2012</b> , 7, e33071	123
1768	A powerful method for transcriptional profiling of specific cell types in eukaryotes: laser-assisted microdissection and RNA sequencing. <b>2012</b> , 7, e29685	88
1767	Characterization and comparison of the leukocyte transcriptomes of three cattle breeds. <b>2012</b> , 7, e30244	25
1766	Inhibition of miR-29 by TGF-beta-Smad3 signaling through dual mechanisms promotes transdifferentiation of mouse myoblasts into myofibroblasts. <b>2012</b> , 7, e33766	102
1765	Population differences in transcript-regulator expression quantitative trait loci. <b>2012</b> , 7, e34286	6

1764	Transcriptome analysis reveals strain-specific and conserved stemness genes in Schmidtea mediterranea. <b>2012</b> , 7, e34447	44
1763	Transcriptome responses of insect fat body cells to tissue culture environment. <b>2012</b> , 7, e34940	10
1762	Expression profiling of Cucumis sativus in response to infection by Pseudoperonospora cubensis. <b>2012</b> , 7, e34954	43
1761	Transcriptome characterization by RNA-seq unravels the mechanisms of butyrate-induced epigenomic regulation in bovine cells. <b>2012</b> , 7, e36940	39
1760	Effector CD4+ T cell expression signatures and immune-mediated disease associated genes. <b>2012</b> , 7, e38510	13
1759	Comparative transcriptomics of the saprobic and parasitic growth phases in Coccidioides spp. <b>2012</b> , 7, e41034	54
1758	High-resolution transcriptome of human macrophages. <b>2012</b> , 7, e45466	168
1757	Gene expression profiles in paired gingival biopsies from periodontitis-affected and healthy tissues revealed by massively parallel sequencing. <b>2012</b> , 7, e46440	40
1756	The transcriptome profile of the mosquito Culex quinquefasciatus following permethrin selection. <b>2012</b> , 7, e47163	47
1755	Complex modulation of the Aedes aegypti transcriptome in response to dengue virus infection. <b>2012</b> , 7, e50512	96
1754	Development of transcriptomic resources for interrogating the biosynthesis of monoterpene indole alkaloids in medicinal plant species. <b>2012</b> , 7, e52506	121
1753	Chromatin is an ancient innovation conserved between Archaea and Eukarya. <b>2012</b> , 1, e00078	60
1752	Alternative splicing regulated by butyrate in bovine epithelial cells. <b>2012</b> , 7, e39182	10
1751	The human transcriptome: an unfinished story. <b>2012</b> , 3, 344-60	80
1750	Improving RNA-Seq Precision with MapAl. <b>2012</b> , 3, 28	2
1749	Whole-exome sequencing and an iPSC-derived cardiomyocyte model provides a powerful platform for gene discovery in left ventricular hypertrophy. <b>2012</b> , 3, 92	18
1748	Global Approaches to the Role of miRNAs in Drug-Induced Changes in Gene Expression. <b>2012</b> , 3, 109	20
1747	Big (sequencing) future of non-coding RNA research for the understanding of cocaine. <b>2012</b> , 3, 158	1

1746	Invading Innate Immune Cells. <b>2012</b> , 3, 85	103
1745	Detecting differential usage of exons from RNA-Seq data. <b>2012</b> ,	11
1744	HELLP babies link a novel lincRNA to the trophoblast cell cycle. <b>2012</b> , 122, 4003-11	53
1743	Identification of artifactual microarray probe signals constantly present in multiple sample types. <b>2012</b> , 53, 91-8	5
1742	The Tissue Specific Role of Estrogen and Progesterone in Human Endometrium and Mammary Gland. <b>2012</b> ,	1
1741	cDNA normalization by hydroxyapatite chromatography to enrich transcriptome diversity in RNA-seq applications. <b>2012</b> , 53, 373-80	23
1740	Differential gene and transcript expression analysis of RNA-seq experiments with TopHat and Cufflinks. <b>2012</b> , 7, 562-78	8342
1739	Global DNA hypomethylation coupled to repressive chromatin domain formation and gene silencing in breast cancer. <b>2012</b> , 22, 246-58	385
1738	Exome sequencing identifies recurrent mutations of the splicing factor SF3B1 gene in chronic lymphocytic leukemia. <b>2011</b> , 44, 47-52	752
1737	A beginner's guide to eukaryotic genome annotation. <b>2012</b> , 13, 329-42	416
1736	RBE controls microRNA164 expression to effect floral organogenesis. <b>2012</b> , 139, 2161-9	60
1735	Topology of the human and mouse m6A RNA methylomes revealed by m6A-seq. <b>2012</b> , 485, 201-6	2387
1734	Nprl3 is required for normal development of the cardiovascular system. <b>2012</b> , 23, 404-15	25
1733	Transcriptome and methylome interactions in rice hybrids. <b>2012</b> , 109, 12040-5	153
1732	Global assembly of expressed sequence tags. <b>2012</b> , 883, 193-9	
1731	Sex-specific adaptation drives early sex chromosome evolution in Drosophila. <b>2012</b> , 337, 341-5	135
1730	The origin and evolution of mutations in acute myeloid leukemia. <b>2012</b> , 150, 264-78	1143
1729	RNA editing of protein sequences: a rare event in human transcriptomes. <b>2012</b> , 18, 1586-96	35

1728	Histone variant H2A.Bbd is associated with active transcription and mRNA processing in human cells. <b>2012</b> , 47, 596-607	77
1727	Transcriptome variance in single oocytes within, and between, genotypes. <b>2012</b> , 79, 502-3	6
1726	Nascent-seq indicates widespread cotranscriptional RNA editing in Drosophila. 2012, 47, 27-37	97
1725	"Calling cards" for DNA-binding proteins in mammalian cells. <b>2012</b> , 190, 941-9	41
1724	High-Throughput Sequencing Data Analysis Software: Current State and Future Developments. <b>2012</b> , 231-248	4
1723	Applications of High-Throughput Sequencing. <b>2012</b> , 27-53	1
1722	Differential Expression for RNA Sequencing (RNA-Seq) Data: Mapping, Summarization, Statistical Analysis, and Experimental Design. <b>2012</b> , 169-190	2
1721	Designing a transcriptome next-generation sequencing project for a nonmodel plant species. <b>2012</b> , 99, 257-66	166
1720	Next generation RNA-sequencing in prognostic subsets of chronic lymphocytic leukemia. <b>2012</b> , 87, 737-40	21
1719	Genome sequence of foxtail millet (Setaria italica) provides insights into grass evolution and biofuel potential. <b>2012</b> , 30, 549-54	447
		573
1718	biofuel potential. <b>2012</b> , 30, 549-54	
1718 1717	biofuel potential. 2012, 30, 549-54  Reference genome sequence of the model plant Setaria. 2012, 30, 555-61	573
1718 1717	biofuel potential. 2012, 30, 549-54  Reference genome sequence of the model plant Setaria. 2012, 30, 555-61  Genome regulation by long noncoding RNAs. 2012, 81, 145-66	573 2939
1718 1717 1716	Reference genome sequence of the model plant Setaria. 2012, 30, 555-61  Genome regulation by long noncoding RNAs. 2012, 81, 145-66  The yak genome and adaptation to life at high altitude. 2012, 44, 946-9	573 2939 472
1718 1717 1716 1715	Reference genome sequence of the model plant Setaria. 2012, 30, 555-61  Genome regulation by long noncoding RNAs. 2012, 81, 145-66  The yak genome and adaptation to life at high altitude. 2012, 44, 946-9  Reorganization of the host epigenome by a viral oncogene. 2012, 22, 1212-21	573 2939 472 51
1718 1717 1716 1715 1714	Reference genome sequence of the model plant Setaria. 2012, 30, 555-61  Genome regulation by long noncoding RNAs. 2012, 81, 145-66  The yak genome and adaptation to life at high altitude. 2012, 44, 946-9  Reorganization of the host epigenome by a viral oncogene. 2012, 22, 1212-21  Macro lncRNAs: a new layer of cis-regulatory information in the mammalian genome. 2012, 9, 731-41	573 2939 472 51 56

1710 Widespread dynamic DNA methylation in response to biotic stress. <b>2012</b> , 109, E2183-91	640
1709 Targeted RNA sequencing reveals the deep complexity of the human transcriptome. <b>2011</b> , 30, 99-104	356
1708 The atm-1 gene is required for genome stability in Caenorhabditis elegans. <b>2012</b> , 287, 325-35	19
1707 Repetitive DNA and next-generation sequencing: computational challenges and solutions. <b>2011</b> , 13, 36-	46 1053
1706 Protein-RNA interactions: new genomic technologies and perspectives. <b>2012</b> , 13, 77-83	408
1705 Duel of the fates: the role of transcriptional circuits and noise in CD4+ cells. <b>2012</b> , 24, 350-8	11
A de novo transcriptome assembly of Lucilia sericata (Diptera: Calliphoridae) with predicted alternative splices, single nucleotide polymorphisms and transcript expression estimates. <b>2012</b> , 21, 205	-21 <sup>43</sup>
Confirmation of an epilepsy modifier locus on mouse chromosome 11 and candidate gene analysis by RNA-Seq. <b>2012</b> , 11, 452-60	20
Cestode genomics - progress and prospects for advancing basic and applied aspects of flatworm biology. <b>2012</b> , 34, 130-50	71
Alternative mRNA processing increases the complexity of microRNA-based gene regulation in Arabidopsis. <b>2012</b> , 70, 421-31	50
1700 Advances in plant genome sequencing. <b>2012</b> , 70, 177-90	128
1699 Parental genome imbalance in Brassica oleracea causes asymmetric triploid block. <b>2012</b> , 71, 503-16	32
1698 Isoform diversity and its importance for axon regeneration. <b>2012</b> , 32, 420-31	3
PIntron: a fast method for detecting the gene structure due to alternative splicing via maximal pairings of a pattern and a text. <b>2012</b> , 13 Suppl 5, S2	8
Challenges in estimating percent inclusion of alternatively spliced junctions from RNA-seq data. <b>2012</b> , 13 Suppl 6, S11	36
A context-based approach to identify the most likely mapping for RNA-seq experiments. <b>2012,</b> 13 Suppl 6, S9	11
1694 Integrating many co-splicing networks to reconstruct splicing regulatory modules. <b>2012</b> , 6 Suppl 1, S17	14
1693 Next generation sequencing and a new era of medicine. <b>2013</b> , 62, 920-32	19

1692	eQTL Mapping Using RNA-seq Data. <b>2013</b> , 5, 198-219	51
1691	Transcriptomic alterations in human prostate cancer cell LNCaP tumor xenograft modulated by dietary phenethyl isothiocyanate. <b>2013</b> , 52, 426-37	12
1690	High throughput investigative Dermatology in 2012 and beyond: A new era beckons. <b>2013</b> , 54, 1-8	2
1689	Changes in the transcriptome of morula-stage bovine embryos caused by heat shock: relationship to developmental acquisition of thermotolerance. <b>2013</b> , 11, 3	32
1688	Peripheral nerve injury is accompanied by chronic transcriptome-wide changes in the mouse prefrontal cortex. <b>2013</b> , 9, 21	62
1687	Reference genomes and transcriptomes of Nicotiana sylvestris and Nicotiana tomentosiformis. <b>2013</b> , 14, R60	139
1686	Hyperosmotic priming of Arabidopsis seedlings establishes a long-term somatic memory accompanied by specific changes of the epigenome. <b>2013</b> , 14, R59	200
1685	TopHat2: accurate alignment of transcriptomes in the presence of insertions, deletions and gene fusions. <b>2013</b> , 14, R36	8607
1684	Quartz-Seq: a highly reproducible and sensitive single-cell RNA sequencing method, reveals non-genetic gene-expression heterogeneity. <b>2013</b> , 14, R31	289
1683	RNA sequencing reveals sexually dimorphic gene expression before gonadal differentiation in chicken and allows comprehensive annotation of the W-chromosome. <b>2013</b> , 14, R26	72
1682	The western painted turtle genome, a model for the evolution of extreme physiological adaptations in a slowly evolving lineage. <b>2013</b> , 14, R28	227
1681	The BET protein FSH functionally interacts with ASH1 to orchestrate global gene activity in Drosophila. <b>2013</b> , 14, R18	22
1680	RNaseIII and T4 polynucleotide Kinase sequence biases and solutions during RNA-seq library construction. <b>2013</b> , 8, 16	9
1679	Characteristics of cross-hybridization and cross-alignment of expression in pseudo-xenograft samples by RNA-Seq and microarrays. <b>2013</b> , 3, 8	3
1678	Significance of expression of ITGA5 and its splice variants in acute myeloid leukemia: a report from the Children's Oncology Group. <b>2013</b> , 88, 694-702	6
1677	Lessons learned from implementing a national infrastructure in Sweden for storage and analysis of next-generation sequencing data. <b>2013</b> , 2, 9	59
1676	Molecular mechanisms of desiccation tolerance in the resurrection glacial relic Haberlea rhodopensis. <b>2013</b> , 70, 689-709	130
1675	Diversity in the complexity of phosphate starvation transcriptomes among rice cultivars based on RNA-Seq profiles. <b>2013</b> , 83, 523-37	42

1674	Independent specialization of the human and mouse X chromosomes for the male germ line. <b>2013</b> , 45, 1083-7	111
1673	High-throughput RNA sequencing of a formalin-fixed, paraffin-embedded autopsy lung tissue sample from the 1918 influenza pandemic. <b>2013</b> , 229, 535-45	48
1672	Deep Sequencing Data Analysis. <b>2013</b> ,	4
1671	Decoding the Ascaris suum Genome using Massively Parallel Sequencing and Advanced Bioinformatic Methods [Inprecedented Prospects for Fundamental and Applied Research. <b>2013</b> , 287-314	
1670	Prioritization of retinal disease genes: an integrative approach. <b>2013</b> , 34, 853-9	6
1669	Bioinformatics Research and Applications. 2013,	
1668	Global aspects of pacC regulation of pathogenicity genes in Colletotrichum gloeosporioides as revealed by transcriptome analysis. <b>2013</b> , 26, 1345-58	70
1667	Competition between pre-mRNAs for the splicing machinery drives global regulation of splicing. <b>2013</b> , 51, 338-48	80
1666	Pairwise comparisons of ten porcine tissues identify differential transcriptional regulation at the gene, isoform, promoter and transcription start site level. <b>2013</b> , 438, 346-52	11
1665	Genomic landscapes of Chinese hamster ovary cell lines as revealed by the Cricetulus griseus draft genome. <b>2013</b> , 31, 759-65	289
1664	Whole transcriptome sequencing of the aging rat brain reveals dynamic RNA changes in the dark matter of the genome. <b>2013</b> , 35, 763-76	82
1663	Transcriptomic profiling of Aspergillus flavus in response to 5-azacytidine. <b>2013</b> , 56, 78-86	58
1662	Maternal imprinting at the H19-Igf2 locus maintains adult haematopoietic stem cell quiescence. <b>2013</b> , 500, 345-9	201
1661	The evolution and pathogenic mechanisms of the rice sheath blight pathogen. <b>2013</b> , 4, 1424	177
1660	The haplotype-resolved genome and epigenome of the aneuploid HeLa cancer cell line. 2013, 500, 207-11	236
1659	Messenger RNA is a functional component of a chromatin insulator complex. <b>2013</b> , 14, 916-22	16
1658	Single Nucleotide Polymorphism (SNP) Detection and Genotype Calling from Massively Parallel Sequencing (MPS) Data. <b>2013</b> , 5, 3-25	14
1657	Statistical and Computational Methods for High-Throughput Sequencing Data Analysis of Alternative Splicing. <b>2013</b> , 5, 138-155	10

1656	Next generation sequencing in cancer research and clinical application. 2013, 15, 4	76
1655	Parallel comparison of Illumina RNA-Seq and Affymetrix microarray platforms on transcriptomic profiles generated from 5-aza-deoxy-cytidine treated HT-29 colon cancer cells and simulated datasets. <b>2013</b> , 14 Suppl 9, S1	69
1654	NGS-Trex: Next Generation Sequencing Transcriptome profile explorer. <b>2013</b> , 14 Suppl 7, S10	14
1653	State of art fusion-finder algorithms are suitable to detect transcription-induced chimeras in normal tissues?. <b>2013</b> , 14 Suppl 7, S2	54
1652	Examples of sequence conservation analyses capture a subset of mouse long non-coding RNAs sharing homology with fish conserved genomic elements. <b>2013</b> , 14 Suppl 7, S14	14
1651	CLASS: constrained transcript assembly of RNA-seq reads. <b>2013</b> , 14 Suppl 5, S14	20
1650	A novel min-cost flow method for estimating transcript expression with RNA-Seq. <b>2013</b> , 14 Suppl 5, S15	48
1649	NURD: an implementation of a new method to estimate isoform expression from non-uniform RNA-seq data. <b>2013</b> , 14, 220	12
1648	PASTA: splice junction identification from RNA-sequencing data. <b>2013</b> , 14, 116	16
1647	Differential expression analysis for paired RNA-Seq data. <b>2013</b> , 14, 110	18
.,	Differential expression analysis for paired RNA-Seq data. <b>2013</b> , 14, 110  Estimation of data-specific constitutive exons with RNA-Seq data. <b>2013</b> , 14, 31	18
.,	Estimation of data-specific constitutive exons with RNA-Seq data. <b>2013</b> , 14, 31	
1646	Estimation of data-specific constitutive exons with RNA-Seq data. 2013, 14, 31  Mef2A, a homologue of animal Mef2 transcription factors, regulates cell differentiation in Dictyostelium discoideum. 2013, 13, 12  Comparative transcriptome analysis of obligately asexual and cyclically sexual rotifers reveals	4
1646 1645	Estimation of data-specific constitutive exons with RNA-Seq data. 2013, 14, 31  Mef2A, a homologue of animal Mef2 transcription factors, regulates cell differentiation in Dictyostelium discoideum. 2013, 13, 12  Comparative transcriptome analysis of obligately asexual and cyclically sexual rotifers reveals genes with putative functions in sexual reproduction, dormancy, and asexual egg production. 2013,	5
1646 1645 1644	Estimation of data-specific constitutive exons with RNA-Seq data. 2013, 14, 31  Mef2A, a homologue of animal Mef2 transcription factors, regulates cell differentiation in Dictyostelium discoideum. 2013, 13, 12  Comparative transcriptome analysis of obligately asexual and cyclically sexual rotifers reveals genes with putative functions in sexual reproduction, dormancy, and asexual egg production. 2013, 14, 412  The characteristics and expression profiles of the mitochondrial genome for the Mediterranean	<ul><li>4</li><li>5</li><li>19</li></ul>
1646 1645 1644	Estimation of data-specific constitutive exons with RNA-Seq data. 2013, 14, 31  Mef2A, a homologue of animal Mef2 transcription factors, regulates cell differentiation in Dictyostelium discoideum. 2013, 13, 12  Comparative transcriptome analysis of obligately asexual and cyclically sexual rotifers reveals genes with putative functions in sexual reproduction, dormancy, and asexual egg production. 2013, 14, 412  The characteristics and expression profiles of the mitochondrial genome for the Mediterranean species of the Bemisia tabaci complex. 2013, 14, 401	4 5 19 36
1646 1645 1644 1643	Estimation of data-specific constitutive exons with RNA-Seq data. 2013, 14, 31  Mef2A, a homologue of animal Mef2 transcription factors, regulates cell differentiation in Dictyostelium discoideum. 2013, 13, 12  Comparative transcriptome analysis of obligately asexual and cyclically sexual rotifers reveals genes with putative functions in sexual reproduction, dormancy, and asexual egg production. 2013, 14, 412  The characteristics and expression profiles of the mitochondrial genome for the Mediterranean species of the Bemisia tabaci complex. 2013, 14, 401  Alternative splicing tends to avoid partial removals of protein-protein interaction sites. 2013, 14, 379  Insights into organ-specific pathogen defense responses in plants: RNA-seq analysis of potato	4 5 19 36 3

1638	Functional transcriptomic analysis of the role of MAB-5/Hox in Q neuroblast migration in Caenorhabditis elegans. <b>2013</b> , 14, 304	8
1637	Unscrambling butterfly oogenesis. <b>2013</b> , 14, 283	32
1636	Prediction of constitutive A-to-I editing sites from human transcriptomes in the absence of genomic sequences. <b>2013</b> , 14, 206	27
1635	RNAseq versus genome-predicted transcriptomes: a large population of novel transcripts identified in an Illumina-454 Hydra transcriptome. <b>2013</b> , 14, 204	53
1634	Xylem transcription profiles indicate potential metabolic responses for economically relevant characteristics of Eucalyptus species. <b>2013</b> , 14, 201	25
1633	Dynamic regulation of epigenomic landscapes during hematopoiesis. <b>2013</b> , 14, 193	38
1632	Determination of dosage compensation of the mammalian X chromosome by RNA-seq is dependent on analytical approach. <b>2013</b> , 14, 150	25
1631	Systematic analysis of palatal transcriptome to identify cleft palate genes within TGFB-knockout mice alleles: RNA-Seq analysis of TGFB Mice. <b>2013</b> , 14, 113	26
1630	Draft genome sequence of the rubber tree Hevea brasiliensis. <b>2013</b> , 14, 75	181
1629	Genome-wide identification, characterization, and expression analysis of lineage-specific genes within zebrafish. <b>2013</b> , 14, 65	34
1628	Genome reannotation of the lizard Anolis carolinensis based on 14 adult and embryonic deep transcriptomes. <b>2013</b> , 14, 49	45
1627	Transcriptional profiling of the Arabidopsis abscission mutant hae hsl2 by RNA-Seq. <b>2013</b> , 14, 37	61
1626	RNA-Seq analysis reveals new gene models and alternative splicing in the fungal pathogen Fusarium graminearum. <b>2013</b> , 14, 21	64
1625	Potential roles of microRNAs in regulating long intergenic noncoding RNAs. 2013, 6 Suppl 1, S7	63
1624	Personal genomes, quantitative dynamic omics and personalized medicine. <b>2013</b> , 1, 71-90	26
1623	Pathway analysis of the human brain transcriptome in disease. <b>2013</b> , 51, 28-36	11
1622	Comprehensively identifying and characterizing the missing gene sequences in human reference genome with integrated analytic approaches. <b>2013</b> , 132, 899-911	10
1621	Genomic inversion caused by gamma irradiation contributes to downregulation of a WBC11 homolog in bloomless sorghum. <b>2013</b> , 126, 1513-20	10

1620	Directional RNA-seq reveals highly complex condition-dependent transcriptomes in E. coli K12 through accurate full-length transcripts assembling. <b>2013</b> , 14, 520	29
1619	A long noncoding RNA mediates both activation and repression of immune response genes. <b>2013</b> , 341, 789-92	698
1618	Next Generation Sequencing in Cancer Research. 2013,	4
1617	Comprehensive analyses of microRNA gene evolution in paleopolyploid soybean genome. <b>2013</b> , 76, 332-44	16
1616	The sacred lotus genome provides insights into the evolution of flowering plants. 2013, 76, 557-67	55
1615	A glimpse into past, present, and future DNA sequencing. <b>2013</b> , 110, 3-24	106
1614	Genome-wide identification of cancer-related polyadenylated and non-polyadenylated RNAs in human breast and lung cell lines. <b>2013</b> , 56, 503-12	1
1613	Critical role of bioinformatics in translating huge amounts of next-generation sequencing data into personalized medicine. <b>2013</b> , 56, 110-8	23
1612	Comparative study of de novo assembly and genome-guided assembly strategies for transcriptome reconstruction based on RNA-Seq. <b>2013</b> , 56, 143-55	40
1611	Selection of bone metastasis seeds by mesenchymal signals in the primary tumor stroma. <b>2013</b> , 154, 1060-1073	296
1610	Count-based differential expression analysis of RNA sequencing data using R and Bioconductor. <b>2013</b> , 8, 1765-86	788
1609	Mechanism for full-length RNA processing of Arabidopsis genes containing intragenic heterochromatin. <b>2013</b> , 4, 2301	63
1608	Mutations in KARS, encoding lysyl-tRNA synthetase, cause autosomal-recessive nonsyndromic hearing impairment DFNB89. <b>2013</b> , 93, 132-40	80
1607	Selective suppression of endothelial cytokine production by progesterone receptor. <b>2013</b> , 59, 36-43	19
1606	A common set of DNA regulatory elements shapes Drosophila appendages. <b>2013</b> , 27, 306-18	93
1605	Targeted disruption of Hotair leads to homeotic transformation and gene derepression. <b>2013</b> , 5, 3-12	247
1604	Cellular source and mechanisms of high transcriptome complexity in the mammalian testis. <b>2013</b> , 3, 2179-90	334
1603	The histone H3 methyltransferase G9A epigenetically activates the serine-glycine synthesis pathway to sustain cancer cell survival and proliferation. <b>2013</b> , 18, 896-907	151

1602	Methylmercury exposure increases lipocalin related (lpr) and decreases activated in blocked unfolded protein response (abu) genes and specific miRNAs in Caenorhabditis elegans. <b>2013</b> , 222, 189-96	18
1601	Genetic control of primary microRNA insight into cis- and trans-regulatory variations by RNA-seq. <b>2013</b> , 517, 224-9	1
1600	Infection structure-specific expression of \$\mathbb{D}\$1,3-glucan synthase is essential for pathogenicity of Colletotrichum graminicola and evasion of \$\mathbb{D}\$glucan-triggered immunity in maize. <b>2013</b> , 25, 2356-78	64
1599	Nuclear Wave1 is required for reprogramming transcription in oocytes and for normal development. <b>2013</b> , 341, 1002-5	69
1598	Next-Generation Sequencing (NGS): A Revolutionary Technology in Pharmacogenomics and Personalized Medicine. <b>2013</b> , 39-61	2
1597	BRANCH: boosting RNA-Seq assemblies with partial or related genomic sequences. <i>Bioinformatics</i> , <b>2013</b> , 29, 1250-9	24
1596	Benchmarking RNA-Seq quantification tools. <b>2013</b> , 2013, 647-50	23
1595	The long noncoding RNA SChLAP1 promotes aggressive prostate cancer and antagonizes the SWI/SNF complex. <b>2013</b> , 45, 1392-8	515
1594	Image-based transcriptomics in thousands of single human cells at single-molecule resolution. <b>2013</b> , 10, 1127-33	194
1593	Expression and regulation of intergenic long noncoding RNAs during T cell development and differentiation. <b>2013</b> , 14, 1190-8	315
1592	DNMT1-interacting RNAs block gene-specific DNA methylation. <b>2013</b> , 503, 371-6	379
1591	Genome analysis reveals insights into physiology and longevity of the Brandt's bat Myotis brandtii. <b>2013</b> , 4, 2212	160
1590	SON connects the splicing-regulatory network with pluripotency in human embryonic stem cells. <b>2013</b> , 15, 1141-1152	62
1589	Hierarchical mechanisms for direct reprogramming of fibroblasts to neurons. <b>2013</b> , 155, 621-35	403
1588	Neuronal ROS signaling rather than AMPK/sirtuin-mediated energy sensing links dietary restriction to lifespan extension. <b>2013</b> , 2, 92-102	113
1587	Assessment of transcript reconstruction methods for RNA-seq. <b>2013</b> , 10, 1177-84	477
1586	Systematic evaluation of spliced alignment programs for RNA-seq data. <b>2013</b> , 10, 1185-91	371
1585	Sequencing and automated whole-genome optical mapping of the genome of a domestic goat (Capra hircus). <b>2013</b> , 31, 135-41	355

1584	Extensive variation in chromatin states across humans. 2013, 342, 750-2	276
1583	Identification of the C3a receptor (C3AR1) as the target of the VGF-derived peptide TLQP-21 in rodent cells. <b>2013</b> , 288, 27434-27443	71
1582	Super-enhancers in the control of cell identity and disease. <b>2013</b> , 155, 934-47	2053
1581	Genes involved in cell adhesion and signaling: a new repertoire of retinoic acid receptor target genes in mouse embryonic fibroblasts. <b>2014</b> , 127, 521-33	24
1580	Clinical application of amplicon-based next-generation sequencing in cancer. <b>2013</b> , 206, 413-9	85
1579	The high polyphenol content of grapevine cultivar tannat berries is conferred primarily by genes that are not shared with the reference genome. <b>2013</b> , 25, 4777-88	88
1578	Whole-transcriptome analysis of hepatocellular carcinoma. <b>2013</b> , 30, 736	4
1577	RNA-methylation-dependent RNA processing controls the speed of the circadian clock. <b>2013</b> , 155, 793-806	607
1576	Coexpression networks implicate human midfetal deep cortical projection neurons in the pathogenesis of autism. <b>2013</b> , 155, 997-1007	591
1575	Genomic insights into salt adaptation in a desert poplar. <b>2013</b> , 4, 2797	183
1574	Analysis of the canine brain transcriptome with an emphasis on the hypothalamus and cerebral cortex. <b>2013</b> , 24, 484-99	16
1573	SplicingCompass: differential splicing detection using RNA-seq data. <i>Bioinformatics</i> , <b>2013</b> , 29, 1141-8 7.2	48
1572	RNA sequencing of cancer reveals novel splicing alterations. <b>2013</b> , 3, 1689	134
1571	Dynamic expression of 3' UTRs revealed by Poisson hidden Markov modeling of RNA-Seq: implications in gene expression profiling. <b>2013</b> , 527, 616-23	18
1570	Genome-wide binding analysis of the transcription activator ideal plant architecture1 reveals a complex network regulating rice plant architecture. <b>2013</b> , 25, 3743-59	417
1569	Mammalian 5'-capped microRNA precursors that generate a single microRNA. <b>2013</b> , 155, 1568-80	141
1568	A heterozygous moth genome provides insights into herbivory and detoxification. <b>2013</b> , 45, 220-5	366
1567	Jasmonate Signaling. <b>2013</b> ,	3

1566	Transcriptome analysis of mouse brain infected with Toxoplasma gondii. 2013, 81, 3609-19		63
1565	RNA-Seq analysis of Citrus reticulata in the early stages of Xylella fastidiosa infection reveals auxin-related genes as a defense response. <b>2013</b> , 14, 676		49
1564	Male-specific Fruitless isoforms have different regulatory roles conferred by distinct zinc finger DNA binding domains. <b>2013</b> , 14, 659		48
1563	RNA-seq analyses of gene expression in the microsclerotia of Verticillium dahliae. <b>2013</b> , 14, 607		55
1562	Accurate identification of polyadenylation sites from 3' end deep sequencing using a naive Bayes classifier. <i>Bioinformatics</i> , <b>2013</b> , 29, 2564-71	7.2	17
1561	Integrated detection of natural antisense transcripts using strand-specific RNA sequencing data. <b>2013</b> , 23, 1730-9		45
1560	Transcriptome-wide identification of RNA binding sites by CLIP-seq. <b>2013</b> , 63, 32-40		25
1559	Global analyses of UPF1 binding and function reveal expanded scope of nonsense-mediated mRNA decay. <b>2013</b> , 23, 1636-50		167
1558	Investigating the physiological response of Pichia (Komagataella) pastoris GS115 to the heterologous expression of misfolded proteins using chemostat cultures. <b>2013</b> , 97, 9747-9762		39
1557	Whole transcriptome sequencing reveals genes involved in plastid/chloroplast division and development are regulated by the HP1/DDB1 at an early stage of tomato fruit development. <b>2013</b> , 238, 923-36		13
1556	Comprehensive analysis of RNA-seq data reveals the complexity of the transcriptome in Brassica rapa. <b>2013</b> , 14, 689		125
1555	Histoplasma yeast and mycelial transcriptomes reveal pathogenic-phase and lineage-specific gene expression profiles. <b>2013</b> , 14, 695		43
1554	Web Apollo: a web-based genomic annotation editing platform. <b>2013</b> , 14, R93		237
1553	The genome and transcriptome of Haemonchus contortus, a key model parasite for drug and vaccine discovery. <b>2013</b> , 14, R88		225
1552	Systematically profiling and annotating long intergenic non-coding RNAs in human embryonic stem cell. <b>2013</b> , 14 Suppl 5, S3		8
1551	Expression of non-protein-coding antisense RNAs in genomic regions related to autism spectrum disorders. <b>2013</b> , 4, 32		39
1550	Transcriptome analysis of human tissues and cell lines reveals one dominant transcript per gene. <b>2013</b> , 14, R70		175
1549	The genome and transcriptome of the enteric parasite Entamoeba invadens, a model for encystation. <b>2013</b> , 14, R77		68

1548	GLiMMPS: robust statistical model for regulatory variation of alternative splicing using RNA-seq data. <b>2013</b> , 14, R74	60
1547	Transcriptomics: advances and approaches. <b>2013</b> , 56, 960-7	44
1546	Genome and transcriptome sequencing of the halophilic fungus Wallemia ichthyophaga: haloadaptations present and absent. <b>2013</b> , 14, 617	83
1545	Expansion of ruminant-specific microRNAs shapes target gene expression divergence between ruminant and non-ruminant species. <b>2013</b> , 14, 609	18
1544	Transcriptomic characterization of cold acclimation in larval zebrafish. <b>2013</b> , 14, 612	102
1543	The importance of tissue specificity for RNA-seq: highlighting the errors of composite structure extractions. <b>2013</b> , 14, 586	39
1542	Inferring the expression variability of human transposable element-derived exons by linear model analysis of deep RNA sequencing data. <b>2013</b> , 14, 584	5
1541	Limited evidence for evolutionarily conserved targeting of long non-coding RNAs by microRNAs. <b>2013</b> , 4, 4	4
1540	CRAC: an integrated approach to the analysis of RNA-seq reads. <b>2013</b> , 14, R30	54
1539	RNA-Seq optimization with eQTL gold standards. <b>2013</b> , 14, 892	15
1539 1538	RNA-Seq optimization with eQTL gold standards. 2013, 14, 892  Transcriptomics-based screen for genes induced by flagellin and repressed by pathogen effectors identifies a cell wall-associated kinase involved in plant immunity. 2013, 14, R139	15 92
	Transcriptomics-based screen for genes induced by flagellin and repressed by pathogen effectors	
1538	Transcriptomics-based screen for genes induced by flagellin and repressed by pathogen effectors identifies a cell wall-associated kinase involved in plant immunity. <b>2013</b> , 14, R139  Ups and downs of a transcriptional landscape shape iron deficiency associated chlorosis of the	92
1538 1537	Transcriptomics-based screen for genes induced by flagellin and repressed by pathogen effectors identifies a cell wall-associated kinase involved in plant immunity. <b>2013</b> , 14, R139  Ups and downs of a transcriptional landscape shape iron deficiency associated chlorosis of the maize inbreds B73 and Mo17. <b>2013</b> , 13, 213	92
1538 1537 1536	Transcriptomics-based screen for genes induced by flagellin and repressed by pathogen effectors identifies a cell wall-associated kinase involved in plant immunity. <b>2013</b> , 14, R139  Ups and downs of a transcriptional landscape shape iron deficiency associated chlorosis of the maize inbreds B73 and Mo17. <b>2013</b> , 13, 213  The nucleosome regulates the usage of polyadenylation sites in the human genome. <b>2013</b> , 14, 912  Uncovering the genetic basis for early isogamete differentiation: a case study of Ectocarpus	92 9 16
1538 1537 1536 1535	Transcriptomics-based screen for genes induced by flagellin and repressed by pathogen effectors identifies a cell wall-associated kinase involved in plant immunity. <b>2013</b> , 14, R139  Ups and downs of a transcriptional landscape shape iron deficiency associated chlorosis of the maize inbreds B73 and Mo17. <b>2013</b> , 13, 213  The nucleosome regulates the usage of polyadenylation sites in the human genome. <b>2013</b> , 14, 912  Uncovering the genetic basis for early isogamete differentiation: a case study of Ectocarpus siliculosus. <b>2013</b> , 14, 909	92 9 16 21
1538 1537 1536 1535	Transcriptomics-based screen for genes induced by flagellin and repressed by pathogen effectors identifies a cell wall-associated kinase involved in plant immunity. 2013, 14, R139  Ups and downs of a transcriptional landscape shape iron deficiency associated chlorosis of the maize inbreds B73 and Mo17. 2013, 13, 213  The nucleosome regulates the usage of polyadenylation sites in the human genome. 2013, 14, 912  Uncovering the genetic basis for early isogamete differentiation: a case study of Ectocarpus siliculosus. 2013, 14, 909  Fungal gene expression levels do not display a common mode of distribution. 2013, 6, 559  Chromatin signatures at transcriptional start sites separate two equally populated yet distinct	92 9 16 21 4

1530	Analysis of porcine adipose tissue transcriptome reveals differences in de novo fatty acid synthesis in pigs with divergent muscle fatty acid composition. <b>2013</b> , 14, 843	58
1529	The Clostridium small RNome that responds to stress: the paradigm and importance of toxic metabolite stress in C. acetobutylicum. <b>2013</b> , 14, 849	43
1528	HSA: a heuristic splice alignment tool. <b>2013</b> , 7 Suppl 2, S10	5
1527	Analysis of banana transcriptome and global gene expression profiles in banana roots in response to infection by race 1 and tropical race 4 of Fusarium oxysporum f. sp. cubense. <b>2013</b> , 14, 851	84
1526	Polysome profiling reveals translational control of gene expression in the human malaria parasite Plasmodium falciparum. <b>2013</b> , 14, R128	105
1525	Transcriptional profiling of adult Drosophila antennae by high-throughput sequencing. <b>2013</b> , 52, 42	19
1524	Transcriptome analysis of the filamentous fungus Aspergillus nidulans directed to the global identification of promoters. <b>2013</b> , 14, 847	43
1523	Sequencing the transcriptome of milk production: milk trumps mammary tissue. <b>2013</b> , 14, 872	35
1522	Clustering of transcriptional profiles identifies changes to insulin signaling as an early event in a mouse model of Alzheimer's disease. <b>2013</b> , 14, 831	24
1521	Comparative transcriptome analysis of tomato (Solanum lycopersicum) in response to exogenous abscisic acid. <b>2013</b> , 14, 841	67
1520	DNA from dead cancer cells induces TLR9-mediated invasion and inflammation in living cancer cells. <b>2013</b> , 142, 477-87	28
1519	Finding the active genes in deep RNA-seq gene expression studies. <b>2013</b> , 14, 778	125
1518	Expression analysis and in silico characterization of intronic long noncoding RNAs in renal cell carcinoma: emerging functional associations. <b>2013</b> , 12, 140	48
1517	Comparative genomics reveals candidate carotenoid pathway regulators of ripening watermelon fruit. <b>2013</b> , 14, 781	77
1516	Identification of novel transcripts and noncoding RNAs in bovine skin by deep next generation sequencing. <b>2013</b> , 14, 789	96
1515	Efficient cellular fractionation improves RNA sequencing analysis of mature and nascent transcripts from human tissues. <b>2013</b> , 13, 99	33
1514	Design of RNA splicing analysis null models for post hoc filtering of Drosophila head RNA-Seq data with the splicing analysis kit (Spanki). <b>2013</b> , 14, 320	35
1513	Aging is associated with highly defined epigenetic changes in the human epidermis. <b>2013</b> , 6, 36	62

1512	Assessing the impact of human genome annotation choice on RNA-seq expression estimates. <b>2013</b> , 14 Suppl 11, S8	30
1511	eRNAs promote transcription by establishing chromatin accessibility at defined genomic loci. <b>2013</b> , 51, 606-17	342
1510	A patient tumor transplant model of squamous cell cancer identifies PI3K inhibitors as candidate therapeutics in defined molecular bins. <b>2013</b> , 7, 776-90	116
1509	SILAC-based proteome analysis of Starmerella bombicola sophorolipid production. <b>2013</b> , 12, 4376-92	20
1508	A fresh look at the male-specific region of the human Y chromosome. <b>2013</b> , 12, 6-22	39
1507	Selective regulation of lymphopoiesis and leukemogenesis by individual zinc fingers of Ikaros. <b>2013</b> , 14, 1073-83	79
1506	Sequencing of mRNA identifies re-expression of fetal splice variants in cardiac hypertrophy. <b>2013</b> , 62, 99-107	28
1505	Nanog, Pou5f1 and SoxB1 activate zygotic gene expression during the maternal-to-zygotic transition. <b>2013</b> , 503, 360-4	281
1504	Hira-dependent histone H3.3 deposition facilitates PRC2 recruitment at developmental loci in ES cells. <b>2013</b> , 155, 107-20	185
1503	Gene regulation and priming by topoisomerase II⊞n embryonic stem cells. <b>2013</b> , 4, 2478	59
1502	Role of sirtuins in lifespan regulation is linked to methylation of nicotinamide. <b>2013</b> , 9, 693-700	159
1501	Reliable identification of genomic variants from RNA-seq data. <b>2013</b> , 93, 641-51	247
1500	Gene expression in bovine rumen epithelium during weaning identifies molecular regulators of rumen development and growth. <b>2013</b> , 13, 133-42	54
1499	Genetically engineered transvestites reveal novel mating genes in budding yeast. <b>2013</b> , 195, 1277-90	8
1498	Maize LAZY1 mediates shoot gravitropism and inflorescence development through regulating auxin transport, auxin signaling, and light response. <b>2013</b> , 163, 1306-22	88
1497	QLZCClust: Quaternary lempel-Ziv complexity based clustering of the RNA-seq read block segments. <b>2013</b> ,	
1496	Genome of the Chinese tree shrew. <b>2013</b> , 4, 1426	230

1494	evolution. <b>2013</b> , 5, 723-33		30
1493	Complexity of the alternative splicing landscape in plants. <b>2013</b> , 25, 3657-83		453
1492	Genome-wide analysis of transcriptional regulators in human HSPCs reveals a densely interconnected network of coding and noncoding genes. <b>2013</b> , 122, e12-22		96
1491	IDBA-tran: a more robust de novo de Bruijn graph assembler for transcriptomes with uneven expression levels. <i>Bioinformatics</i> , <b>2013</b> , 29, i326-34	2	139
1490	customProDB: an R package to generate customized protein databases from RNA-Seq data for proteomics search. <i>Bioinformatics</i> , <b>2013</b> , 29, 3235-7	2	109
1489	Genome-wide analysis of the rat colon reveals proximal-distal differences in histone modifications and proto-oncogene expression. <b>2013</b> , 45, 1229-43		19
1488	An Approach for Assessing RNA-seq Quantification Algorithms in Replication Studies. <b>2013</b> , 2013, 15-18		2
1487	SpliceGrapherXT. <b>2013</b> ,		O
1486	Histone acetylation regulates intracellular pH. <b>2013</b> , 49, 310-21		171
1485	Whole-genome sequencing of the Akata and Mutu Epstein-Barr virus strains. 2013, 87, 1172-82		84
1484	A triple helix-loop-helix/basic helix-loop-helix cascade controls cell elongation downstream of multiple hormonal and environmental signaling pathways in Arabidopsis. <b>2012</b> , 24, 4917-29		147
1483	Use of Metabolomics and Transcriptomics to Gain Insights into the Regulation and Biosynthesis of Medicinal Compounds: Hypericum as a Model. <b>2013</b> , 395-411		3
1482	Recurrent SETBP1 mutations in atypical chronic myeloid leukemia. 2013, 45, 18-24		272
1481	Using Tablet for visual exploration of second-generation sequencing data. <b>2013</b> , 14, 193-202		590
1480	Functional genomics identifies type I interferon pathway as central for host defense against Candida albicans. <b>2013</b> , 4, 1342		119
1479	Trimethylamine-N-oxide, a metabolite associated with atherosclerosis, exhibits complex genetic and dietary regulation. <b>2013</b> , 17, 49-60		602
1478	Latent enhancers activated by stimulation in differentiated cells. 2013, 152, 157-71		552
1477	Comparative analysis of bat genomes provides insight into the evolution of flight and immunity. <b>2013</b> , 339, 456-60		377

1476	Control of somatic tissue differentiation by the long non-coding RNA TINCR. 2013, 493, 231-5	665
1475	The blue light receptor complex WC-1/2 of Schizophyllum commune is involved in mushroom formation and protection against phototoxicity. <b>2013</b> , 15, 943-55	44
1474	Peptidomic discovery of short open reading frame-encoded peptides in human cells. <b>2013</b> , 9, 59-64	407
1473	Next-generation sequencing in the clinic: promises and challenges. <b>2013</b> , 340, 284-95	206
1472	ALKBH5 is a mammalian RNA demethylase that impacts RNA metabolism and mouse fertility. <b>2013</b> , 49, 18-29	1627
1471	RNA sequencing reveals a diverse and dynamic repertoire of the Xenopus tropicalis transcriptome over development. <b>2013</b> , 23, 201-16	107
1470	iReckon: simultaneous isoform discovery and abundance estimation from RNA-seq data. <b>2013</b> , 23, 519-29	92
1469	The draft genome of watermelon (Citrullus lanatus) and resequencing of 20 diverse accessions. <b>2013</b> , 45, 51-8	503
1468	Identification of early replicating fragile sites that contribute to genome instability. <b>2013</b> , 152, 620-32	280
1467	Transcriptome-wide identification of A > I RNA editing sites by inosine specific cleavage. <b>2013</b> , 19, 257-70	47
1466	General olfactory sensitivity database (GOSdb): candidate genes and their genomic variations. <b>2013</b> , 34, 32-41	37
1465	Long noncoding RNAs regulate adipogenesis. <b>2013</b> , 110, 3387-92	315
1464	Whole-genome methylation sequencing reveals distinct impact of differential methylations on gene transcription in prostate cancer. <b>2013</b> , 183, 1960-1970	33
1463	Endothelial cells provide a niche for placental hematopoietic stem/progenitor cell expansion through broad transcriptomic modification. <b>2013</b> , 11, 1074-90	24
1462	Genome-wide, whole mount in situ analysis of transcriptional regulators in zebrafish embryos. <b>2013</b> , 380, 351-62	43
1461	Solution NMR studies of the plant peptide hormone CEP inform function. <b>2013</b> , 587, 3979-85	33
1460	Role of antisense RNAs in evolution of yeast regulatory complexity. <b>2013</b> , 102, 484-90	9
1459	Cell-cycle control of developmentally regulated transcription factors accounts for heterogeneity in human pluripotent cells. <b>2013</b> , 1, 532-44	98

1458	Gustatory receptor expression in the labella and tarsi of Aedes aegypti. <b>2013</b> , 43, 1161-71	41
1457	Fine mapping of the 1p36 deletion syndrome identifies mutation of PRDM16 as a cause of cardiomyopathy. <b>2013</b> , 93, 67-77	127
1456	Evaluation of higher plant virus resistance genes in the green alga, Chlorella variabilis NC64A, during the early phase of infection with Paramecium bursaria chlorella virus-1. <b>2013</b> , 442, 101-13	10
1455	A recurrent PDGFRB mutation causes familial infantile myofibromatosis. <b>2013</b> , 92, 996-1000	108
1454	Directed migration of cortical interneurons depends on the cell-autonomous action of Sip1. <b>2013</b> , 77, 70-82	92
1453	Spt6 regulates intragenic and antisense transcription, nucleosome positioning, and histone modifications genome-wide in fission yeast. <b>2013</b> , 33, 4779-92	71
1452	Gene networks and chromatin and transcriptional regulation of the phaseolin promoter in Arabidopsis. <b>2013</b> , 25, 2601-17	17
1451	Discovery and mass spectrometric analysis of novel splice-junction peptides using RNA-Seq. <b>2013</b> , 12, 2341-53	96
1450	Novel insights into breast cancer genetic variance through RNA sequencing. <b>2013</b> , 3, 2256	46
1449	Assessing gene-level translational control from ribosome profiling. <i>Bioinformatics</i> , <b>2013</b> , 29, 2995-3002 $_{7.2}$	64
1448	Assessment of gene expression in peripheral blood using RNAseq before and after weight restoration in anorexia nervosa. <b>2013</b> , 210, 287-93	9
1447	Signal transduction involved in GnRH2-stimulation of identified LH-producing gonadotropes from lhb-GFP transgenic medaka (Oryzias latipes). <b>2013</b> , 372, 128-39	24
1446	Spatial transcriptional profile of the chick and mouse endocardial cushions identify novel regulators of endocardial EMT in vitro. <b>2013</b> , 59, 196-204	31
1445	Interpretation, stratification and evidence for sequence variants affecting mRNA splicing in complete human genome sequences. <b>2013</b> , 11, 77-85	23
1444	Zinc-mediated RNA fragmentation allows robust transcript reassembly upon whole transcriptome RNA-Seq. <b>2013</b> , 63, 25-31	18
1443	Transcriptome characterization by RNA-Seq reveals the involvement of the complement components in noise-traumatized rat cochleae. <b>2013</b> , 248, 1-16	27
1442	NSun2-mediated cytosine-5 methylation of vault noncoding RNA determines its processing into regulatory small RNAs. <b>2013</b> , 4, 255-61	344
1441	Recoding RNA editing of AZIN1 predisposes to hepatocellular carcinoma. <b>2013</b> , 19, 209-16	313

1440	Direct competition between hnRNP C and U2AF65 protects the transcriptome from the exonization of Alu elements. <b>2013</b> , 152, 453-66		285
1439	Divergent transcription of long noncoding RNA/mRNA gene pairs in embryonic stem cells. <b>2013</b> , 110, 2876-81		345
1438	RNA-seq-based mapping and candidate identification of mutations from forward genetic screens. <b>2013</b> , 23, 679-86		68
1437	Two new and distinct roles for Drosophila Argonaute-2 in the nucleus: alternative pre-mRNA splicing and transcriptional repression. <b>2013</b> , 27, 378-89		81
1436	Computational analysis of associations between alternative splicing and histone modifications. <b>2013</b> , 587, 516-21		22
1435	Bacterial nitric oxide extends the lifespan of C. elegans. <b>2013</b> , 152, 818-30		126
1434	Single-base resolution methylomes of tomato fruit development reveal epigenome modifications associated with ripening. <b>2013</b> , 31, 154-9		493
1433	NOT2 proteins promote polymerase II-dependent transcription and interact with multiple MicroRNA biogenesis factors in Arabidopsis. <b>2013</b> , 25, 715-27		113
1432	A role for the RNA-binding protein MOS2 in microRNA maturation in Arabidopsis. 2013, 23, 645-57		75
1431	Comparative study of RNA-seq- and microarray-derived coexpression networks in Arabidopsis thaliana. <i>Bioinformatics</i> , <b>2013</b> , 29, 717-24	7.2	76
1430	High-throughput sequencing of the melanoma genome. <b>2013</b> , 22, 10-7		31
1429	Genes, behavior and next-generation RNA sequencing. <b>2013</b> , 12, 1-12		65
1428	Sigma factor-mediated plastid retrograde signals control nuclear gene expression. <b>2013</b> , 73, 1-13		117
1427	Incomplete transfer of accessory loci influencing SbMATE expression underlies genetic background effects for aluminum tolerance in sorghum. <b>2013</b> , 73, 276-88		27
1426	De novo transcriptome characterization of Vitis vinifera cv. Corvina unveils varietal diversity. <b>2013</b> , 14, 41		82
			2
1425	ASAP: an environment for automated preprocessing of sequencing data. <b>2013</b> , 6, 5		3
1425	ASAP: an environment for automated preprocessing of sequencing data. <b>2013</b> , 6, 5  The RNA Pol II elongation factor Ell3 marks enhancers in ES cells and primes future gene activation. <b>2013</b> , 152, 144-56		73

NFIB is a governor of epithelial-melanocyte stem cell behaviour in a shared niche. <b>2013</b> , 495, 98-102	116
Identifying differentially spliced genes from two groups of RNA-seq samples. <b>2013</b> , 518, 164-70	39
Untangling the transcriptome from fungus-infected plant tissues. <b>2013</b> , 519, 238-44	6
LBR and lamin A/C sequentially tether peripheral heterochromatin and inversely regulate differentiation. <b>2013</b> , 152, 584-98	541
Removal of retained introns regulates translation in the rapidly developing gametophyte of Marsilea vestita. <b>2013</b> , 24, 517-29	84
Bioinformatics challenges in de novo transcriptome assembly using short read sequences in the absence of a reference genome sequence. <b>2013</b> , 30, 490-500	54
Braveheart, a long noncoding RNA required for cardiovascular lineage commitment. <b>2013</b> , 152, 570-83	701
Transcriptome analysis of Inbred Long Sleep and Inbred Short Sleep mice. <b>2013</b> , 12, 263-74	12
COPI transport complexes bind to specific RNAs in neuronal cells. <b>2013</b> , 22, 729-36	34
Genomic diversity and evolution of the head crest in the rock pigeon. <b>2013</b> , 339, 1063-7	169
Genome-wide localization of exosome components to active promoters and chromatin insulators in Drosophila. <b>2013</b> , 41, 2963-80	31
Nascent-Seq analysis of Drosophila cycling gene expression. <b>2013</b> , 110, E275-84	71
Genomic distribution of maize facultative heterochromatin marked by trimethylation of H3K27. <b>2013</b> , 25, 780-93	77
The livid modistry contration D4 inhibits influence views configuration and improve course influence	
The lipid mediator protectin D1 inhibits influenza virus replication and improves severe influenza. <b>2013</b> , 153, 112-25	315
	315 630
<b>2013</b> , 153, 112-25	
<b>2013</b> , 153, 112-25  The draft genome of sweet orange (Citrus sinensis). <b>2013</b> , 45, 59-66	630
	Untangling the transcriptome from fungus-infected plant tissues. 2013, 519, 238-44  LBR and lamin A/C sequentially tether peripheral heterochromatin and inversely regulate differentiation. 2013, 152, 584-98  Removal of retained introns regulates translation in the rapidly developing gametophyte of Marsilea vestita. 2013, 24, 517-29  Bioinformatics challenges in de novo transcriptome assembly using short read sequences in the absence of a reference genome sequence. 2013, 30, 490-500  Braveheart, a long noncoding RNA required for cardiovascular lineage commitment. 2013, 152, 570-83  Transcriptome analysis of Inbred Long Sleep and Inbred Short Sleep mice. 2013, 12, 263-74  COPI transport complexes bind to specific RNAs in neuronal cells. 2013, 22, 729-36  Genomic diversity and evolution of the head crest in the rock pigeon. 2013, 339, 1063-7  Genome-wide localization of exosome components to active promoters and chromatin insulators in Drosophila. 2013, 41, 2963-80  Nascent-Seq analysis of Drosophila cycling gene expression. 2013, 110, E275-84  Genomic distribution of maize facultative heterochromatin marked by trimethylation of H3K27. 2013, 25, 780-93

1404	An ancient transcription factor initiates the burst of piRNA production during early meiosis in mouse testes. <b>2013</b> , 50, 67-81	243
1403	Whole transcriptome analysis using next-generation sequencing of model species Setaria viridis to support C4 photosynthesis research. <b>2013</b> , 83, 77-87	49
1402	Limited RNA editing in exons of mouse liver and adipose. <b>2013</b> , 193, 1107-15	22
1401	Genome-wide mapping of RNA structure using nuclease digestion and high-throughput sequencing. <b>2013</b> , 8, 849-69	71
1400	Whole-transcriptome, high-throughput RNA sequence analysis of the bovine macrophage response to Mycobacterium bovis infection in vitro. <b>2013</b> , 14, 230	34
1399	Integration of genome-wide approaches identifies lncRNAs of adult neural stem cells and their progeny in vivo. <b>2013</b> , 12, 616-28	193
1398	Computational solutions for omics data. <b>2013</b> , 14, 333-46	218
1397	Genome-wide profiling of 5-formylcytosine reveals its roles in epigenetic priming. <b>2013</b> , 153, 678-91	453
1396	Detecting and visualizing gene fusions. <b>2013</b> , 59, S24-8	11
1395	Predicting long non-coding RNAs using RNA sequencing. <b>2013</b> , 63, 50-9	82
1395 1394	Predicting long non-coding RNAs using RNA sequencing. <b>2013</b> , 63, 50-9  Integrated systems approach identifies genetic nodes and networks in late-onset Alzheimer's disease. <b>2013</b> , 153, 707-20	1058
	Integrated systems approach identifies genetic nodes and networks in late-onset Alzheimer's	
1394	Integrated systems approach identifies genetic nodes and networks in late-onset Alzheimer's disease. 2013, 153, 707-20  DAF-16 employs the chromatin remodeller SWI/SNF to promote stress resistance and longevity.	1058
1394 1393	Integrated systems approach identifies genetic nodes and networks in late-onset Alzheimer's disease. 2013, 153, 707-20  DAF-16 employs the chromatin remodeller SWI/SNF to promote stress resistance and longevity. 2013, 15, 491-501  Correlates of relative resistance against low-dose rectal simian immunodeficiency virus challenges	1058
1394 1393 1392	Integrated systems approach identifies genetic nodes and networks in late-onset Alzheimer's disease. 2013, 153, 707-20  DAF-16 employs the chromatin remodeller SWI/SNF to promote stress resistance and longevity. 2013, 15, 491-501  Correlates of relative resistance against low-dose rectal simian immunodeficiency virus challenges in peripheral blood mononuclear cells of vaccinated rhesus macaques. 2013, 93, 437-48  Comparative study of transcriptome profiles of mechanical- and skin-transformed Schistosoma	<ul><li>1058</li><li>145</li><li>6</li></ul>
1394 1393 1392 1391	Integrated systems approach identifies genetic nodes and networks in late-onset Alzheimer's disease. 2013, 153, 707-20  DAF-16 employs the chromatin remodeller SWI/SNF to promote stress resistance and longevity. 2013, 15, 491-501  Correlates of relative resistance against low-dose rectal simian immunodeficiency virus challenges in peripheral blood mononuclear cells of vaccinated rhesus macaques. 2013, 93, 437-48  Comparative study of transcriptome profiles of mechanical- and skin-transformed Schistosoma mansoni schistosomula. 2013, 7, e2091  Principles of transcriptome analysis and gene expression quantification: an RNA-seq tutorial. 2013,	<ul><li>1058</li><li>145</li><li>6</li><li>50</li></ul>
1394 1393 1392 1391 1390	Integrated systems approach identifies genetic nodes and networks in late-onset Alzheimer's disease. 2013, 153, 707-20  DAF-16 employs the chromatin remodeller SWI/SNF to promote stress resistance and longevity. 2013, 15, 491-501  Correlates of relative resistance against low-dose rectal simian immunodeficiency virus challenges in peripheral blood mononuclear cells of vaccinated rhesus macaques. 2013, 93, 437-48  Comparative study of transcriptome profiles of mechanical- and skin-transformed Schistosoma mansoni schistosomula. 2013, 7, e2091  Principles of transcriptome analysis and gene expression quantification: an RNA-seq tutorial. 2013, 13, 559-72  Guard cell purification and RNA isolation suitable for high-throughput transcriptional analysis of	<ul><li>1058</li><li>145</li><li>6</li><li>50</li><li>123</li></ul>

1386	Exonuclease hDIS3L2 specifies an exosome-independent 3'-5' degradation pathway of human cytoplasmic mRNA. <b>2013</b> , 32, 1855-68	113
1385	Dynamics of 5-hydroxymethylcytosine during mouse spermatogenesis. <b>2013</b> , 4, 1995	139
1384	Single-cell transcriptomics reveals bimodality in expression and splicing in immune cells. <b>2013</b> , 498, 236-40	867
1383	Comparative analysis of RNA sequencing methods for degraded or low-input samples. <b>2013</b> , 10, 623-9	320
1382	Global regulation of promoter melting in naive lymphocytes. <b>2013</b> , 153, 988-99	111
1381	Vector transmission regulates immune control of Plasmodium virulence. <b>2013</b> , 498, 228-31	113
1380	Malt1-induced cleavage of regnase-1 in CD4(+) helper T cells regulates immune activation. <b>2013</b> , 153, 1036-49	230
1379	The microRNA miR-181 is a critical cellular metabolic rheostat essential for NKT cell ontogenesis and lymphocyte development and homeostasis. <b>2013</b> , 38, 984-97	195
1378	A comprehensive analysis of the effects of the deaminase AID on the transcriptome and methylome of activated B cells. <b>2013</b> , 14, 749-55	46
1377	Comparative analysis of de novo transcriptome assembly. <b>2013</b> , 56, 156-62	33
1376	Ribosome profiling reveals resemblance between long non-coding RNAs and 5' leaders of coding RNAs. <b>2013</b> , 140, 2828-34	196
1375	New insight into transcription of human endogenous retroviral elements. <b>2013</b> , 30, 314-8	14
1374	Transcriptome analysis of the parasite Encephalitozoon cuniculi: an in-depth examination of pre-mRNA splicing in a reduced eukaryote. <b>2013</b> , 14, 207	30
1373	Differential gene expression in Acromyrmex leaf-cutting ants after challenges with two fungal pathogens. <b>2013</b> , 22, 2173-87	22
1372	Sequencing of the sea lamprey (Petromyzon marinus) genome provides insights into vertebrate evolution. <b>2013</b> , 45, 415-21, 421e1-2	465
1371	Deep RNA-Seq uncovers the peach transcriptome landscape. <b>2013</b> , 83, 365-77	72
1370	Identification of recurrent FGFR3 fusion genes in lung cancer through kinome-centred RNA sequencing. <b>2013</b> , 230, 270-6	94
1369	Ground tit genome reveals avian adaptation to living at high altitudes in the Tibetan plateau. <b>2013</b> , 4, 2071	154

1368	Analysis of RNA-Seq data with TopHat and Cufflinks for genome-wide expression analysis of jasmonate-treated plants and plant cultures. <b>2013</b> , 1011, 305-15	54
1367	Transcriptome-wide mapping of N(6)-methyladenosine by m(6)A-seq based on immunocapturing and massively parallel sequencing. <b>2013</b> , 8, 176-89	358
1366	Transcriptional and epigenetic dynamics during specification of human embryonic stem cells. <b>2013</b> , 153, 1149-63	332
1365	EZH2 is required for germinal center formation and somatic EZH2 mutations promote lymphoid transformation. <b>2013</b> , 23, 677-92	547
1364	Mapping the Functional Genome. <b>2013</b> , 28-40	1
1363	Npas4 is activated by melatonin, and drives the clock gene Cry1 in the ovine pars tuberalis. <b>2013</b> , 27, 979-89	23
1362	Using the iPlant collaborative discovery environment. <b>2013</b> , Chapter 1, Unit1.22	20
1361	Genome-wide characterization and expression analysis of genetic variants in sweet orange. <b>2013</b> , 75, 954-64	20
1360	Adaptive resource configuration for Cloud infrastructure management. <b>2013</b> , 29, 472-487	62
1359	Targeting the endothelial progenitor cell surface proteome to identify novel mechanisms that mediate angiogenic efficacy in a rodent model of vascular disease. <b>2013</b> , 45, 999-1011	17
1358	Transcriptome analysis of the sulfate deficiency response in the marine microalga Emiliania huxleyi. <b>2013</b> , 199, 650-62	53
1357	Managing and Optimizing Bioinformatics Workflows for Data Analysis in Clouds. <b>2013</b> , 11, 407-428	16
1356	The genome of the platyfish, Xiphophorus maculatus, provides insights into evolutionary adaptation and several complex traits. <b>2013</b> , 45, 567-72	201
1355	High occurrence of functional new chimeric genes in survey of rice chromosome 3 short arm genome sequences. <b>2013</b> , 5, 1038-48	8
1354	CathaCyc, a metabolic pathway database built from Catharanthus roseus RNA-Seq data. <b>2013</b> , 54, 673-85	95
1353	Evolutionary and ontogenetic changes in RNA editing in human, chimpanzee, and macaque brains. <b>2013</b> , 19, 1693-702	25
1352	Induction of a human pluripotent state with distinct regulatory circuitry that resembles preimplantation epiblast. <b>2013</b> , 13, 663-75	284
1351	Comprehensive genomic profiling in diabetic nephropathy reveals the predominance of proinflammatory pathways. <b>2013</b> , 45, 710-9	18

1350	Common fusion transcripts identified in colorectal cancer cell lines by high-throughput RNA sequencing. <b>2013</b> , 6, 546-53	22
1349	Ribosome profiling reveals features of normal and disease-associated mitochondrial translation. <b>2013</b> , 4, 2886	63
1348	Whole-genome DNA/RNA sequencing identifies truncating mutations in RBCK1 in a novel Mendelian disease with neuromuscular and cardiac involvement. <b>2013</b> , 5, 67	66
1347	Transcriptional analysis through RNA sequencing of giant cells induced by Meloidogyne graminicola in rice roots. <b>2013</b> , 64, 3885-98	98
1346	Exome RNA sequencing reveals rare and novel alternative transcripts. <b>2013</b> , 41, e6	38
1345	Intrauterine calorie restriction affects placental DNA methylation and gene expression. 2013, 45, 565-76	72
1344	The CTRB1/2 locus affects diabetes susceptibility and treatment via the incretin pathway. <b>2013</b> , 62, 3275-81	63
1343	Genome-guided transcriptome assembly in the age of next-generation sequencing. <b>2013</b> , 10, 1234-40	12
1342	The challenges of delivering bioinformatics training in the analysis of high-throughput data. <b>2013</b> , 14, 538-47	9
1341	RNA deep sequencing as a tool for selection of cell lines for systematic subcellular localization of all human proteins. <b>2013</b> , 12, 299-307	14
1340	Functional identification of valerena-1,10-diene synthase, a terpene synthase catalyzing a unique chemical cascade in the biosynthesis of biologically active sesquiterpenes in Valeriana officinalis. <b>2013</b> , 288, 3163-73	34
1339	Catabolism of L-methionine in the formation of sulfur and other volatiles in melon (Cucumis melo L.) fruit. <b>2013</b> , 74, 458-72	63
1338	When less is more: the forbidden fruits of gene repression in the adult □cell. <b>2013</b> , 15, 503-12	71
1337	STAR: ultrafast universal RNA-seq aligner. <i>Bioinformatics</i> , <b>2013</b> , 29, 15-21	18121
1336	Algal swimming velocities signal fatty acid accumulation. <b>2013</b> , 110, 143-52	7
1335	Simultaneous isoform discovery and quantification from RNA-seq. <b>2013</b> , 5, 100-118	16
1334	Genome sequences of six wheat-infecting fusarium species isolates. <b>2013</b> , 1,	23
1333	c-Src modulates estrogen-induced stress and apoptosis in estrogen-deprived breast cancer cells. <b>2013</b> , 73, 4510-20	65

1332	Genome of Drosophila suzukii, the spotted wing drosophila. <b>2013</b> , 3, 2257-71	83
1331	Rat retinal transcriptome: effects of aging and AMD-like retinopathy. <b>2013</b> , 12, 1745-61	51
1330	Genes that escape X-inactivation in humans have high intraspecific variability in expression, are associated with mental impairment but are not slow evolving. <b>2013</b> , 30, 2588-601	81
1329	Cryptococcus neoformans Rim101 is associated with cell wall remodeling and evasion of the host immune responses. <b>2013</b> , 4,	76
1328	Regulatory role of glycerol in Candida albicans biofilm formation. <b>2013</b> , 4, e00637-12	55
1327	Female-specific induction of rat pituitary dentin matrix protein-1 by GnRH. <b>2013</b> , 27, 1840-55	14
1326	Epithelial splicing regulator protein 1 and alternative splicing in somatotroph adenomas. <b>2013</b> , 154, 3331-43	7
1325	Inference of alternative splicing from RNA-Seq data with probabilistic splice graphs. <i>Bioinformatics</i> , <b>2013</b> , 29, 2300-10	18
1324	Splicing kinetics and transcript release from the chromatin compartment limit the rate of Lipid A-induced gene expression. <b>2013</b> , 19, 811-27	71
1323	The transition from a phytopathogenic smut ancestor to an anamorphic biocontrol agent deciphered by comparative whole-genome analysis. <b>2013</b> , 25, 1946-59	39
1322	Ontology-aware classification of tissue and cell-type signals in gene expression profiles across platforms and technologies. <i>Bioinformatics</i> , <b>2013</b> , 29, 3036-44	21
1321	A probabilistic approach to learn chromatin architecture and accurate inference of the NF- <b>B</b> /RelA regulatory network using ChIP-Seq. <b>2013</b> , 41, 7240-59	34
1320	Multiplatform single-sample estimates of transcriptional activation. <b>2013</b> , 110, 17778-83	68
1319	Tissue-specific splicing of a ubiquitously expressed transcription factor is essential for muscle differentiation. <b>2013</b> , 27, 1247-59	73
1318	The genomic landscape of cohesin-associated chromatin interactions. <b>2013</b> , 23, 1224-34	85
1317	Comparative genomics in Chlamydomonas and Plasmodium identifies an ancient nuclear envelope protein family essential for sexual reproduction in protists, fungi, plants, and vertebrates. <b>2013</b> , 27, 1198-215	62
1316	Characterization of the rat developmental liver transcriptome. <b>2013</b> , 45, 301-11	15
1315	Novel association of early onset hepatocellular carcinoma with transaldolase deficiency. <b>2014</b> , 12, 121-7	23

1314	Suppression of artifacts and barcode bias in high-throughput transcriptome analyses utilizing template switching. <b>2013</b> , 41, e44	46
1313	Quantification of stochastic noise of splicing and polyadenylation in Entamoeba histolytica. <b>2013</b> , 41, 1936-52	51
1312	A large-scale in vivo analysis reveals that TALENs are significantly more mutagenic than ZFNs generated using context-dependent assembly. <b>2013</b> , 41, 2769-78	110
1311	Read Annotation Pipeline for High-Throughput Sequencing Data. 2013,	4
1310	Systematic Assessment of RNA-Seq Quantification Tools Using Simulated Sequence Data. <b>2013</b> , 2013,	2
1309	Transforming Genomes Using MOD Files with Applications. 2013,	7
1308	BamView: visualizing and interpretation of next-generation sequencing read alignments. 2013, 14, 203-12	50
1307	DBATE: database of alternative transcripts expression. <b>2013</b> , 2013, bat050	10
1306	The splicing landscape is globally reprogrammed during male meiosis. 2013, 41, 10170-84	50
1305	DUX4 binding to retroelements creates promoters that are active in FSHD muscle and testis. <b>2013</b> , 9, e1003947	102
1304	Host cell transcriptome profile during wild-type and attenuated dengue virus infection. <b>2013</b> , 7, e2107	50
1303	Dynamics of the Saccharomyces cerevisiae transcriptome during bread dough fermentation. <b>2013</b> , 79, 7325-33	23
1302	Function and evolution of DNA methylation in Nasonia vitripennis. 2013, 9, e1003872	133
1301	A contribution to the study of plant development evolution based on gene co-expression networks. <b>2013</b> , 4, 291	18
1300	Identification of genes critical for resistance to infection by West Nile virus using RNA-Seq analysis. <b>2013</b> , 5, 1664-81	18
1299	DDBJ read annotation pipeline: a cloud computing-based pipeline for high-throughput analysis of next-generation sequencing data. <b>2013</b> , 20, 383-90	63
1298	Discovery of anthelmintic drug targets and drugs using chokepoints in nematode metabolic pathways. <b>2013</b> , 9, e1003505	57
1297	Transcription of the major neurospora crassa microRNA-like small RNAs relies on RNA polymerase III. <b>2013</b> , 9, e1003227	25

1296	An essential role for zygotic expression in the pre-cellular Drosophila embryo. <b>2013</b> , 9, e1003428	44
1295	Xbp1 directs global repression of budding yeast transcription during the transition to quiescence and is important for the longevity and reversibility of the quiescent state. <b>2013</b> , 9, e1003854	51
1294	The Fusarium graminearum histone H3 K27 methyltransferase KMT6 regulates development and expression of secondary metabolite gene clusters. <b>2013</b> , 9, e1003916	170
1293	Ras-induced changes in H3K27me3 occur after those in transcriptional activity. <b>2013</b> , 9, e1003698	35
1292	Extensive chromosomal reshuffling drives evolution of virulence in an asexual pathogen. <b>2013</b> , 23, 1271-82	221
1291	The Tarenaya hassleriana genome provides insight into reproductive trait and genome evolution of crucifers. <b>2013</b> , 25, 2813-30	67
1290	Functional Development of the Octenol Response in Aedes aegypti. <b>2013</b> , 4, 39	35
1289	Evolutionarily conserved long intergenic non-coding RNAs in the eye. <b>2013</b> , 22, 2992-3002	35
1288	The non-obese diabetic mouse sequence, annotation and variation resource: an aid for investigating type 1 diabetes. <b>2013</b> , 2013, bat032	15
1287	PNUTS/PP1 regulates RNAPII-mediated gene expression and is necessary for developmental growth. <b>2013</b> , 9, e1003885	29
1286	A KH-domain RNA-binding protein interacts with FIERY2/CTD phosphatase-like 1 and splicing factors and is important for pre-mRNA splicing in Arabidopsis. <b>2013</b> , 9, e1003875	62
1285	Analysis of the RelA:CBP/p300 interaction reveals its involvement in NF- <b>B</b> -driven transcription. <b>2013</b> , 11, e1001647	81
1284	Comparative motif discovery combined with comparative transcriptomics yields accurate targetome and enhancer predictions. <b>2013</b> , 23, 74-88	23
1283	Translational profiling of clock cells reveals circadianly synchronized protein synthesis. <b>2013</b> , 11, e1001703	59
1282	Linking transcriptional changes over time in stimulated dendritic cells to identify gene networks activated during the innate immune response. <b>2013</b> , 9, e1003323	21
1281	A conserved upstream motif orchestrates autonomous, germline-enriched expression of Caenorhabditis elegans piRNAs. <b>2013</b> , 9, e1003392	33
1280	DeepSAGE reveals genetic variants associated with alternative polyadenylation and expression of coding and non-coding transcripts. <b>2013</b> , 9, e1003594	32
1279	The genome and development-dependent transcriptomes of Pyronema confluens: a window into fungal evolution. <b>2013</b> , 9, e1003820	65

1278	Hsp70-Hsp40 chaperone complex functions in controlling polarized growth by repressing Hsf1-driven heat stress-associated transcription. <b>2013</b> , 9, e1003886	30
1277	Genomic identification of founding haplotypes reveals the history of the selfing species Capsella rubella. <b>2013</b> , 9, e1003754	72
1276	Evidence for independent evolution of functional progesterone withdrawal in primates and guinea pigs. <b>2013</b> , 2013, 273-88	14
1275	The developmental transcriptome of the mosquito Aedes aegypti, an invasive species and major arbovirus vector. <b>2013</b> , 3, 1493-509	122
1274	Detecting and comparing non-coding RNAs in the high-throughput era. <b>2013</b> , 14, 15423-58	16
1273	Differences in gastric carcinoma microenvironment stratify according to EBV infection intensity: implications for possible immune adjuvant therapy. <b>2013</b> , 9, e1003341	108
1272	Disruption of aryl hydrocarbon receptor homeostatic levels during embryonic stem cell differentiation alters expression of homeobox transcription factors that control cardiomyogenesis. <b>2013</b> , 121, 1334-43	37
1271	Transcriptome profiling of Giardia intestinalis using strand-specific RNA-seq. <b>2013</b> , 9, e1003000	45
1270	Extensive divergence of transcription factor binding in Drosophila embryos with highly conserved gene expression. <b>2013</b> , 9, e1003748	70
1269	Silicon era of carbon-based life: application of genomics and bioinformatics in crop stress research. <b>2013</b> , 14, 11444-83	7
1268	Dystrophin-deficient pigs provide new insights into the hierarchy of physiological derangements of dystrophic muscle. <b>2013</b> , 22, 4368-82	94
1267	Different CHD chromatin remodelers are required for expression of distinct gene sets and specific stages during development of Dictyostelium discoideum. <b>2013</b> , 140, 4926-36	7
1266	H3.3-H4 tetramer splitting events feature cell-type specific enhancers. <b>2013</b> , 9, e1003558	51
1265	Systematically differentiating functions for alternatively spliced isoforms through integrating RNA-seq data. <b>2013</b> , 9, e1003314	58
1264	Gene expression signature of non-involved lung tissue associated with survival in lung adenocarcinoma patients. <b>2013</b> , 34, 2767-73	29
1263	TIGAR: transcript isoform abundance estimation method with gapped alignment of RNA-Seq data by variational Bayesian inference. <i>Bioinformatics</i> , <b>2013</b> , 29, 2292-9	29
1262	Identification of cilia genes that affect cell-cycle progression using whole-genome transcriptome analysis in Chlamydomonas reinhardtti. <b>2013</b> , 3, 979-91	42
1261	Sumoylation at chromatin governs coordinated repression of a transcriptional program essential for cell growth and proliferation. <b>2013</b> , 23, 1563-79	86

1260	Accurate detection of differential RNA processing. <b>2013</b> , 41, 5189-98	30
1259	Analysis of allele-specific expression in mouse liver by RNA-Seq: a comparison with Cis-eQTL identified using genetic linkage. <b>2013</b> , 195, 1157-66	34
1258	The yeast Snt2 protein coordinates the transcriptional response to hydrogen peroxide-mediated oxidative stress. <b>2013</b> , 33, 3735-48	26
1257	RNA-Seq analysis discloses early senescence and nucleolar dysfunction triggered by Tdp1H depletion in Medicago truncatula. <b>2013</b> , 64, 1941-51	27
1256	Identifying key regulatory genes in the whole blood of septic patients to monitor underlying immune dysfunctions. <b>2013</b> , 40, 166-74	59
1255	Coordinated regulation of synthesis and stability of RNA during the acute TNF-induced proinflammatory response. <b>2013</b> , 110, 2240-5	79
1254	Emiliania huxleyi increases calcification but not expression of calcification-related genes in long-term exposure to elevated temperature and pCO2. <b>2013</b> , 368, 20130049	55
1253	A TAF4 coactivator function for E proteins that involves enhanced TFIID binding. <b>2013</b> , 27, 1596-609	26
1252	Complex tissue-specific patterns and distribution of multiple RAGE splice variants in different mammals. <b>2013</b> , 5, 2420-35	29
1251	Characterization of the human ESC transcriptome by hybrid sequencing. <b>2013</b> , 110, E4821-30	222
	Characterization of the human ESC transcriptome by hybrid sequencing. <b>2013</b> , 110, E4821-30  A Prader-Willi locus lncRNA cloud modulates diurnal genes and energy expenditure. <b>2013</b> , 22, 4318-28	112
1250		
1250	A Prader-Willi locus lncRNA cloud modulates diurnal genes and energy expenditure. <b>2013</b> , 22, 4318-28  Bimodal quantitative relationships between histone modifications for X-linked and autosomal loci.	112
1250 1249	A Prader-Willi locus lncRNA cloud modulates diurnal genes and energy expenditure. <b>2013</b> , 22, 4318-28  Bimodal quantitative relationships between histone modifications for X-linked and autosomal loci. <b>2013</b> , 110, 6949-54  Transcriptome profiling of Nasonia vitripennis testis reveals novel transcripts expressed from the	112
1250 1249 1248	A Prader-Willi locus lncRNA cloud modulates diurnal genes and energy expenditure. 2013, 22, 4318-28  Bimodal quantitative relationships between histone modifications for X-linked and autosomal loci. 2013, 110, 6949-54  Transcriptome profiling of Nasonia vitripennis testis reveals novel transcripts expressed from the selfish B chromosome, paternal sex ratio. 2013, 3, 1597-605  Insights from a chimpanzee adipose stromal cell population: opportunities for adult stem cells to	112 8 35
1250 1249 1248	A Prader-Willi locus lncRNA cloud modulates diurnal genes and energy expenditure. 2013, 22, 4318-28  Bimodal quantitative relationships between histone modifications for X-linked and autosomal loci. 2013, 110, 6949-54  Transcriptome profiling of Nasonia vitripennis testis reveals novel transcripts expressed from the selfish B chromosome, paternal sex ratio. 2013, 3, 1597-605  Insights from a chimpanzee adipose stromal cell population: opportunities for adult stem cells to expand primate functional genomics. 2013, 5, 1995-2005  CUL3 and NRF2 mutations confer an NRF2 activation phenotype in a sporadic form of papillary	112 8 35 2
1250 1249 1248 1247	A Prader-Willi locus lncRNA cloud modulates diurnal genes and energy expenditure. 2013, 22, 4318-28  Bimodal quantitative relationships between histone modifications for X-linked and autosomal loci. 2013, 110, 6949-54  Transcriptome profiling of Nasonia vitripennis testis reveals novel transcripts expressed from the selfish B chromosome, paternal sex ratio. 2013, 3, 1597-605  Insights from a chimpanzee adipose stromal cell population: opportunities for adult stem cells to expand primate functional genomics. 2013, 5, 1995-2005  CUL3 and NRF2 mutations confer an NRF2 activation phenotype in a sporadic form of papillary renal cell carcinoma. 2013, 73, 2044-51	112 8 35 2 119

1242	In vitro-differentiated neural cell cultures progress towards donor-identical brain tissue. <b>2013</b> , 22, 3534-46	16
1241	The transcriptome of the baculovirus Autographa californica multiple nucleopolyhedrovirus in Trichoplusia ni cells. <b>2013</b> , 87, 6391-405	129
1240	A discrete ubiquitin-mediated network regulates the strength of NOD2 signaling. <b>2013</b> , 33, 146-58	21
1239	Structure-function studies of STAR family Quaking proteins bound to their in vivo RNA target sites. <b>2013</b> , 27, 928-40	67
1238	Antisense transcripts enhanced by camptothecin at divergent CpG-island promoters associated with bursts of topoisomerase I-DNA cleavage complex and R-loop formation. <b>2013</b> , 41, 10110-23	46
1237	MITIE: Simultaneous RNA-Seq-based transcript identification and quantification in multiple samples. <i>Bioinformatics</i> , <b>2013</b> , 29, 2529-38	40
1236	Epigenetic and genetic influences on DNA methylation variation in maize populations. 2013, 25, 2783-97	174
1235	The Subread aligner: fast, accurate and scalable read mapping by seed-and-vote. <b>2013</b> , 41, e108	1489
1234	Sequential activation of genetic programs in mouse mammary epithelium during pregnancy depends on STAT5A/B concentration. <b>2013</b> , 41, 1622-36	59
1233	ERISdb: a database of plant splice sites and splicing signals. <b>2013</b> , 54, e10	27
1232	Differential splicing across immune system lineages. <b>2013</b> , 110, 14324-9	41
1231	Overview of high throughput sequencing technologies to elucidate molecular pathways in cardiovascular diseases. <b>2013</b> , 112, 1613-23	77
1230	Histone methyltransferase SETD2 coordinates FACT recruitment with nucleosome dynamics during transcription. <b>2013</b> , 41, 2881-93	109
1229	The differential transcription network between embryo and endosperm in the early developing maize seed. <b>2013</b> , 162, 440-55	66
1228	Mosaic genome structure of the barley powdery mildew pathogen and conservation of transcriptional programs in divergent hosts. <b>2013</b> , 110, E2219-28	112
1227	TrueSight: a new algorithm for splice junction detection using RNA-seq. <b>2013</b> , 41, e51	28
1226	Extensive transcript diversity and novel upstream open reading frame regulation in yeast. 2013, 3, 343-52	44
1225	Comprehensive genome- and transcriptome-wide analyses of mutations associated with microsatellite instability in Korean gastric cancers. <b>2013</b> , 23, 1109-17	49

1224	Outlier kinase expression by RNA sequencing as targets for precision therapy. <b>2013</b> , 3, 280-93	33
1223	Program specificity for Ptf1a in pancreas versus neural tube development correlates with distinct collaborating cofactors and chromatin accessibility. <b>2013</b> , 33, 3166-79	23
1222	The maize methylome influences mRNA splice sites and reveals widespread paramutation-like switches guided by small RNA. <b>2013</b> , 23, 1651-62	199
1221	The intronic long noncoding RNA ANRASSF1 recruits PRC2 to the RASSF1A promoter, reducing the expression of RASSF1A and increasing cell proliferation. <b>2013</b> , 9, e1003705	138
1220	Selecting one of several mating types through gene segment joining and deletion in Tetrahymena thermophila. <b>2013</b> , 11, e1001518	64
1219	Gene expression signatures of coronary heart disease. <b>2013</b> , 33, 1418-26	80
1218	RhesusBase: a knowledgebase for the monkey research community. <b>2013</b> , 41, D892-905	23
1217	Cloud Computing with iPlant Atmosphere. <b>2013</b> , 43, 9.15.1-9.15.20	2
1216	IQdb: an intelligence quotient score-associated gene resource for human intelligence. <b>2013</b> , 2013, bat063	13
1215	Role of fat body lipogenesis in protection against the effects of caloric overload in Drosophila. <b>2013</b> , 288, 8028-8042	74
1214	Differential DNA methylation with age displays both common and dynamic features across human tissues that are influenced by CpG landscape. <b>2013</b> , 14, R102	239
1213	Developmental arrest of Drosophila survival motor neuron (Smn) mutants accounts for differences in expression of minor intron-containing genes. <b>2013</b> , 19, 1510-6	41
1212	TriageTools: tools for partitioning and prioritizing analysis of high-throughput sequencing data. <b>2013</b> , 41, e86	5
1211	RIPSeeker: a statistical package for identifying protein-associated transcripts from RIP-seq experiments. <b>2013</b> , 41, e94	31
<b>121</b> 0	Heterochromatinization induced by GAA-repeat hyperexpansion in Friedreich's ataxia can be reduced upon HDAC inhibition by vitamin B3. <b>2013</b> , 22, 2662-75	57
1209	Genomic architecture of adaptive color pattern divergence and convergence in Heliconius butterflies. <b>2013</b> , 23, 1248-57	57
1208	Comparative analysis of mammalian Y chromosomes illuminates ancestral structure and lineage-specific evolution. <b>2013</b> , 23, 1486-95	77
1207	Endogenous gammaretrovirus acquisition in Mus musculus subspecies carrying functional variants of the XPR1 virus receptor. <b>2013</b> , 87, 9845-55	13

1206	mutant lung cancer cell lines identifies spectrum of DNA changes associated with drug resistance. <b>2013</b> , 23, 1434-45		41	
1205	Genome-wide SNP Database for Marker-assisted Background Selection in Tomato. <b>2013</b> , 45, 232-239		7	
1204	SND1 transcription factor-directed quantitative functional hierarchical genetic regulatory network in wood formation in Populus trichocarpa. <b>2013</b> , 25, 4324-41		78	
1203	Rescue of dysfunctional autophagy attenuates hyperinflammatory responses from cystic fibrosis cells. <b>2013</b> , 190, 1227-38		59	
1202	Folate polyglutamylation is involved in chromatin silencing by maintaining global DNA methylation and histone H3K9 dimethylation in Arabidopsis. <b>2013</b> , 25, 2545-59		49	
1201	GeneScissors: a comprehensive approach to detecting and correcting spurious transcriptome inference owing to RNA-seq reads misalignment. <i>Bioinformatics</i> , <b>2013</b> , 29, i291-9	7.2	9	
1200	Probabilistic error correction for RNA sequencing. <b>2013</b> , 41, e109		55	
1199	Dysregulation of synaptogenesis genes antecedes motor neuron pathology in spinal muscular atrophy. <b>2013</b> , 110, 19348-53		134	
1198	Long intergenic non-coding RNA detection benefited from integrative modeling of (Epi)genomic data. <b>2013</b> ,			
1197	Global gene expression response of a population exposed to benzene: a pilot study exploring the use of RNA-sequencing technology. <b>2013</b> , 54, 566-73		9	
1196	Estrogen and progesterone together expand murine endometrial epithelial progenitor cells. <b>2013</b> , 31, 808-22		36	
1195	Differential urinary specific gravity as a molecular phenotype of the bladder cancer genetic association in the urea transporter gene, SLC14A1. <b>2013</b> , 133, 3008-13		22	
1194	Trim24-repressed VL30 retrotransposons regulate gene expression by producing noncoding RNA. <b>2013</b> , 20, 339-46		52	
1193	Exome-based analysis for RNA epigenome sequencing data. <i>Bioinformatics</i> , <b>2013</b> , 29, 1565-7	7.2	83	
1192	Differential gene expression analysis using coexpression and RNA-Seq data. <i>Bioinformatics</i> , <b>2013</b> , 29, 2153-61	7.2	19	
1191	Identification of novel point mutations in splicing sites integrating whole-exome and RNA-seq data in myeloproliferative diseases. <b>2013</b> , 1, 246-59		12	
1190	High-throughput technologies for gene expression analyses: what we have learned for noise-induced cochlear degeneration?. <b>2013</b> , 8, 25-31		2	
1189	Investigating the genetics of Bti resistance using mRNA tag sequencing: application on laboratory strains and natural populations of the dengue vector Aedes aegypti. <b>2013</b> , 6, 1012-27		8	

1188	Protective role of IL-6 in vascular remodeling in Schistosoma pulmonary hypertension. <b>2013</b> , 49, 951-9	38
1187	Discovering high-resolution patterns of differential DNA methylation that correlate with gene expression changes. <b>2013</b> , 41, 6816-27	73
1186	A meta-analysis of the genomic and transcriptomic composition of complex life. <b>2013</b> , 12, 2061-72	102
1185	Chronic ethanol exposure increases cytochrome P-450 and decreases activated in blocked unfolded protein response gene family transcripts in caenorhabditis elegans. <b>2013</b> , 27, 219-28	12
1184	Calculating sample size estimates for RNA sequencing data. <b>2013</b> , 20, 970-8	167
1183	Perturbations of Plasmodium Puf2 expression and RNA-seq of Puf2-deficient sporozoites reveal a critical role in maintaining RNA homeostasis and parasite transmissibility. <b>2013</b> , 15, 1266-83	56
1182	Transcriptome-wide analysis of vernalization reveals conserved and species-specific mechanisms in Brachypodium. <b>2013</b> , 55, 696-709	15
1181	Rice Annotation Project Database (RAP-DB): an integrative and interactive database for rice genomics. <b>2013</b> , 54, e6	409
1180	Intragenic DNA methylation modulates alternative splicing by recruiting MeCP2 to promote exon recognition. <b>2013</b> , 23, 1256-69	405
1179	Building localized bioinformatics platform based on Galaxy and high performance computing cluster. <b>2013</b> ,	1
1178	An RNA recognition motif-containing protein is required for plastid RNA editing in Arabidopsis and maize. <b>2013</b> , 110, E1169-78	103
1177	High mobility group protein N5 (HMGN5) and lamina-associated polypeptide 2⊞LAP2∄interact and reciprocally affect their genome-wide chromatin organization. <b>2013</b> , 288, 18104-9	16
1176	Loss of Arp2/3 induces an NF-B-dependent, nonautonomous effect on chemotactic signaling. <b>2013</b> , 203, 907-16	28
1175	The corepressor CTBP2 is a coactivator of retinoic acid receptor/retinoid X receptor in retinoic acid signaling. <b>2013</b> , 33, 3343-53	21
1174	The shared genomic architecture of human nucleolar organizer regions. <b>2013</b> , 23, 2003-12	75
1173	A quantitative genetic basis for leaf morphology in a set of precisely defined tomato introgression lines. <b>2013</b> , 25, 2465-81	115
1172	Draft genome of the kiwifruit Actinidia chinensis. <b>2013</b> , 4, 2640	316
1171	Utilizing sequence intrinsic composition to classify protein-coding and long non-coding transcripts. <b>2013</b> , 41, e166	879

1170	DiffSplice: the genome-wide detection of differential splicing events with RNA-seq. 2013, 41, e39	100
1169	EBSeq: an empirical Bayes hierarchical model for inference in RNA-seq experiments. <i>Bioinformatics</i> , <b>2013</b> , 29, 1035-43	805
1168	Genome-wide identification of translationally inhibited and degraded miR-155 targets using RNA-interacting protein-IP. <b>2013</b> , 10, 1018-29	29
1167	High-Performance Computing In High-Throughput Sequencing. <b>2013</b> , 981-1002	1
1166	Gene expression profiling by mRNA sequencing reveals increased expression of immune/inflammation-related genes in the hippocampus of individuals with schizophrenia. <b>2013</b> , 3, e321	116
1165	Comparison of normalization methods for differential gene expression analysis in RNA-Seq experiments: A matter of relative size of studied transcriptomes. <b>2013</b> , 6, e25849	52
1164	The non-human primate reference transcriptome resource (NHPRTR) for comparative functional genomics. <b>2013</b> , 41, D906-14	57
1163	Inversion-mediated gene fusions involving NAB2-STAT6 in an unusual malignant meningioma. <b>2013</b> , 109, 1051-5	8
1162	Novel BRD4-NUT fusion isoforms increase the pathogenic complexity in NUT midline carcinoma. <b>2013</b> , 32, 4664-74	32
1161	Long-term cultured mesenchymal stem cells frequently develop genomic mutations but do not undergo malignant transformation. <b>2013</b> , 4, e950	111
1160	Frac-seq reveals isoform-specific recruitment to polyribosomes. <b>2013</b> , 23, 1615-23	71
1159	Harnessing virtual machines to simplify next-generation DNA sequencing analysis. <i>Bioinformatics</i> , <b>2013</b> , 29, 2075-83	21
1158	Genetic associations with hypertension: meta-analyses of six candidate genetic variants. <b>2013</b> , 17, 736-42	14
1157	Modulation of gene expression via overlapping binding sites exerted by ZNF143, Notch1 and THAP11. <b>2013</b> , 41, 4000-14	43
1156	Coevolution and life cycle specialization of plant cell wall degrading enzymes in a hemibiotrophic pathogen. <b>2013</b> , 30, 1337-47	68
1155	Regulation of microRNA expression by rifampin in human hepatocytes. <b>2013</b> , 41, 1763-8	30
1154	Extensive changes in DNA methylation are associated with expression of mutant huntingtin. <b>2013</b> , 110, 2354-9	121
1153	E3-ubiquitin ligase Nedd4 determines the fate of AID-associated RNA polymerase II in B cells. <b>2013</b> , 27, 1821-33	25

1152	The draft genome and transcriptome of Panagrellus redivivus are shaped by the harsh demands of a free-living lifestyle. <b>2013</b> , 193, 1279-95	41
1151	RNA-seq identified a super-long intergenic transcript functioning in adipogenesis. <b>2013</b> , 10, 991-1001	25
1150	Epigenome-wide inheritance of cytosine methylation variants in a recombinant inbred population. <b>2013</b> , 23, 1663-74	189
1149	Canonical Wnt signaling induces a primitive endoderm metastable state in mouse embryonic stem cells. <b>2013</b> , 31, 752-64	30
1148	Comprehensive whole-genome sequencing of an early-stage primary myelofibrosis patient defines low mutational burden and non-recurrent candidate genes. <b>2013</b> , 98, 1689-96	9
1147	Identification of a novel gene fusion RNF213-SLC26A11 in chronic myeloid leukemia by RNA-Seq. <b>2013</b> , 7, 591-7	13
1146	CUX1 is a haploinsufficient tumor suppressor gene on chromosome 7 frequently inactivated in acute myeloid leukemia. <b>2013</b> , 121, 975-83	111
1145	CBFA2T3-GLIS2 fusion transcript is a novel common feature in pediatric, cytogenetically normal AML, not restricted to FAB M7 subtype. <b>2013</b> , 121, 3469-72	88
1144	The long non-coding RNA ERIC is regulated by E2F and modulates the cellular response to DNA damage. <b>2013</b> , 12, 131	61
1143	Transcriptome and proteome quantification of a tumor model provides novel insights into post-transcriptional gene regulation. <b>2013</b> , 14, r133	37
1142	The draft genome of a socially polymorphic halictid bee, Lasioglossum albipes. <b>2013</b> , 14, R142	58
1141	Genetic and genomic analyses of musculoskeletal differences between BEH and BEL strains. <b>2013</b> , 45, 940-7	12
1140	Genome-wide analysis of condensin binding in Caenorhabditis elegans. <b>2013</b> , 14, R112	58
1139	Genome-wide methylated CpG island profiles of melanoma cells reveal a melanoma coregulation network. <b>2013</b> , 3, 2962	15
1138	FusionQ: a novel approach for gene fusion detection and quantification from paired-end RNA-Seq. <b>2013</b> , 14, 193	25
1137	Host-Mycobacterium avium subsp. paratuberculosis interactome reveals a novel iron assimilation mechanism linked to nitric oxide stress during early infection. <b>2013</b> , 14, 694	28
1136	Probing functional polymorphisms in the dengue vector, Aedes aegypti. <b>2013</b> , 14, 739	9
1135	A genome-wide survey of maternal and embryonic transcripts during Xenopus tropicalis development. <b>2013</b> , 14, 762	47

1134	Data compression for sequencing data. <b>2013</b> , 8, 25	60
1133	Mechanisms of small RNA generation from cis-NATs in response to environmental and developmental cues. <b>2013</b> , 6, 704-15	40
1132	PIN6 is required for nectary auxin response and short stamen development. <b>2013</b> , 74, 893-904	62
1131	Patterns of chromatin-modifications discriminate different genomic features in Arabidopsis. <b>2013</b> , 18, 431-440	
1130	Neurospora and the dead-end hypothesis: genomic consequences of selfing in the model genus. <b>2013</b> , 67, 3600-16	24
1129	Pbx and Prdm1a transcription factors differentially regulate subsets of the fast skeletal muscle program in zebrafish. <b>2013</b> , 2, 546-55	20
1128	Global regulation of alternative splicing by adenosine deaminase acting on RNA (ADAR). 2013, 19, 591-604	76
1127	A dynamic pipeline for RNA sequencing on multicore processors. <b>2013</b> ,	5
1126	RNA-seq analysis of transcriptomes in thrombin-treated and control human pulmonary microvascular endothelial cells. <b>2013</b> ,	8
1125	Improved use of a public good selects for the evolution of undifferentiated multicellularity. <b>2013</b> , 2, e00367	82
1124	Multiple knockout mouse models reveal lincRNAs are required for life and brain development. <b>2013</b> , 2, e01749	516
1123	Transposable elements become active and mobile in the genomes of aging mammalian somatic tissues. <b>2013</b> , 5, 867-83	205
1122	Dual functions of TAF7L in adipocyte differentiation. <b>2013</b> , 2, e00170	29
1121	Functional Genomics. 2013, 125-141	1
1120	Coordinate regulation of DNA methylation and H3K27me3 in mouse embryonic stem cells. <b>2013</b> , 8, e53880	74
1119	Expression profile of ectopic olfactory receptors determined by deep sequencing. 2013, 8, e55368	181
1118	The baboon kidney transcriptome: analysis of transcript sequence, splice variants, and abundance. <b>2013</b> , 8, e57563	9
1117	WNT5A inhibits metastasis and alters splicing of Cd44 in breast cancer cells. <b>2013</b> , 8, e58329	39

1116	Contradiction between plastid gene transcription and function due to complex posttranscriptional splicing: an exemplary study of ycf15 function and evolution in angiosperms. <b>2013</b> , 8, e59620	38
1115	Functional impacts of NRXN1 knockdown on neurodevelopment in stem cell models. <b>2013</b> , 8, e59685	44
1114	Maize gene atlas developed by RNA sequencing and comparative evaluation of transcriptomes based on RNA sequencing and microarrays. <b>2013</b> , 8, e61005	125
1113	RNA-Seq profiling reveals novel hepatic gene expression pattern in aflatoxin B1 treated rats. <b>2013</b> , 8, e61768	45
1112	Simultaneous transcriptome analysis of Sorghum and Bipolaris sorghicola by using RNA-seq in combination with de novo transcriptome assembly. <b>2013</b> , 8, e62460	68
1111	Characterization of gonadal transcriptomes from Nile tilapia (Oreochromis niloticus) reveals differentially expressed genes. <b>2013</b> , 8, e63604	146
1110	Genome-wide analysis of the salmonella Fis regulon and its regulatory mechanism on pathogenicity islands. <b>2013</b> , 8, e64688	23
1109	The ligand binding domain of GCNF is not required for repression of pluripotency genes in mouse fetal ovarian germ cells. <b>2013</b> , 8, e66062	7
1108	A novel strategy to increase the proliferative potential of adult human I-cells while maintaining their differentiated phenotype. <b>2013</b> , 8, e66131	28
1107	Evaluating the impact of sequencing depth on transcriptome profiling in human adipose. 2013, 8, e66883	44
1106	ANOVA-like differential expression (ALDEx) analysis for mixed population RNA-Seq. 2013, 8, e67019	270
1105	High-throughput miRNA and mRNA sequencing of paired colorectal normal, tumor and metastasis tissues and bioinformatic modeling of miRNA-1 therapeutic applications. <b>2013</b> , 8, e67461	47
1104	RNA sequencing of the human milk fat layer transcriptome reveals distinct gene expression profiles at three stages of lactation. <b>2013</b> , 8, e67531	129
1103	Detecting splicing variants in idiopathic pulmonary fibrosis from non-differentially expressed genes. <b>2013</b> , 8, e68352	23
1102	The LuWD40-1 gene encoding WD repeat protein regulates growth and pollen viability in flax (Linum Usitatissimum L.). <b>2013</b> , 8, e69124	17
1101	Knockdown of CDKN1C (p57(kip2)) and PHLDA2 results in developmental changes in bovine pre-implantation embryos. <b>2013</b> , 8, e69490	19
1100	Global transcriptional responses of the toxic cyanobacterium, Microcystis aeruginosa, to nitrogen stress, phosphorus stress, and growth on organic matter. <b>2013</b> , 8, e69834	107
1099	Comprehensive characterization of 10,571 mouse large intergenic noncoding RNAs from whole transcriptome sequencing. <b>2013</b> , 8, e70835	46

1098	Identification and characterization of long non-coding RNAs related to mouse embryonic brain development from available transcriptomic data. <b>2013</b> , 8, e71152	38
1097	Transcriptome profile at different physiological stages reveals potential mode for curly fleece in Chinese tan sheep. <b>2013</b> , 8, e71763	37
1096	Sequencing mRNA from cryo-sliced Drosophila embryos to determine genome-wide spatial patterns of gene expression. <b>2013</b> , 8, e71820	50
1095	ARLTS1 and prostate cancer riskanalysis of expression and regulation. <b>2013</b> , 8, e72040	8
1094	RNA-seq characterization of spinal cord injury transcriptome in acute/subacute phases: a resource for understanding the pathology at the systems level. <b>2013</b> , 8, e72567	48
1093	Characterization and comparative analyses of muscle transcriptomes in Dorper and small-tailed Han sheep using RNA-Seq technique. <b>2013</b> , 8, e72686	42
1092	De novo assembly of the sea cucumber Apostichopus japonicus hemocytes transcriptome to identify miRNA targets associated with skin ulceration syndrome. <b>2013</b> , 8, e73506	58
1091	High-throughput RNA sequencing of pseudomonas-infected Arabidopsis reveals hidden transcriptome complexity and novel splice variants. <b>2013</b> , 8, e74183	49
1090	Next-generation sequence analysis of cancer xenograft models. <b>2013</b> , 8, e74432	23
1089	Gaucher disease: transcriptome analyses using microarray or mRNA sequencing in a Gba1 mutant mouse model treated with velaglucerase alfa or imiglucerase. <b>2013</b> , 8, e74912	11
1088	Comparative genomics reveals insight into virulence strategies of plant pathogenic oomycetes. <b>2013</b> , 8, e75072	100
1087	RNA-Seq reveals differential gene expression in Staphylococcus aureus with single-nucleotide resolution. <b>2013</b> , 8, e76572	12
1086	Transcription factors OVOL1 and OVOL2 induce the mesenchymal to epithelial transition in human cancer. <b>2013</b> , 8, e76773	163
1085	F11R is a novel monocyte prognostic biomarker for malignant glioma. <b>2013</b> , 8, e77571	32
1084	Optimal scaling of digital transcriptomes. <b>2013</b> , 8, e77885	20
1083	Identification of differentially expressed transcripts and pathways in blood one week and six months following implant of left ventricular assist devices. <b>2013</b> , 8, e77951	6
1082	Unique transcriptome patterns of the white and grey matter corroborate structural and functional heterogeneity in the human frontal lobe. <b>2013</b> , 8, e78480	35
1081	Inferring polymorphism-induced regulatory gene networks active in human lymphocyte cell lines by weighted linear mixed model analysis of multiple RNA-Seq datasets. <b>2013</b> , 8, e78868	4

1080	Neuropsychological deficits in mice depleted of the schizophrenia susceptibility gene CSMD1. <b>2013</b> , 8, e79501	50
1079	Phenotypic and transcriptional fidelity of patient-derived colon cancer xenografts in immune-deficient mice. <b>2013</b> , 8, e79874	28
1078	Comprehensive analysis of long non-coding RNAs in ovarian cancer reveals global patterns and targeted DNA amplification. <b>2013</b> , 8, e80306	63
1077	Simultaneous transcriptional profiling of bacteria and their host cells. <b>2013</b> , 8, e80597	85
1076	Genome-wide survey of cold stress regulated alternative splicing in Arabidopsis thaliana with tiling microarray. <b>2013</b> , 8, e66511	47
1075	Changes in RNA Splicing in Developing Soybean (Glycine max) Embryos. <b>2013</b> , 2, 1311-37	14
1074	Metabolic and Transcriptional Reprogramming in Developing Soybean (Glycine max) Embryos. <b>2013</b> , 3, 347-72	40
1073	Epigenetic conservation at gene regulatory elements revealed by non-methylated DNA profiling in seven vertebrates. <b>2013</b> , 2, e00348	148
1072	Minor introns are embedded molecular switches regulated by highly unstable U6atac snRNA. <b>2013</b> , 2, e00780	54
1071	Overcoming mutation-based resistance to antiandrogens with rational drug design. <b>2013</b> , 2, e00499	289
1070	Deep sequencing of the transcriptome reveals inflammatory features of porcine visceral adipose tissue. <b>2013</b> , 9, 550-6	25
1069	Statistical Analysis of Mapped Reads from mRNA-Seq Data. 77-104	
1068	Variation in DNA Methylation Patterns is More Common among Maize Inbreds than among Tissues. <b>2013</b> , 6, plantgenome2012.06.0009	24
1067	Pigtailed macaques as a model to study long-term safety of lentivirus vector-mediated gene therapy for hemoglobinopathies. <b>2014</b> , 1, 14055	9
1066	Genome-wide transcriptome analysis reveals that cadmium stress signaling controls the expression of genes in drought stress signal pathways in rice. <b>2014</b> , 9, e96946	83
1065	Whole transcriptome profiling of maize during early somatic embryogenesis reveals altered expression of stress factors and embryogenesis-related genes. <b>2014</b> , 9, e111407	62
1064	Investigation of key genes associated with prostate cancer using RNA-seq data. <b>2014</b> , 29, e86-92	1
1063	A comparative study of techniques for differential expression analysis on RNA-Seq data. <b>2014</b> , 9, e103207	152

1062	Intestinal subepithelial myofibroblasts support the growth of intestinal epithelial stem cells. <b>2014</b> , 9, e84651	75
1061	Deep sequencing-based transcriptome profiling reveals comprehensive insights into the responses of Nicotiana benthamiana to beet necrotic yellow vein virus infections containing or lacking RNA4. <b>2014</b> , 9, e85284	19
1060	Construction of a public CHO cell line transcript database using versatile bioinformatics analysis pipelines. <b>2014</b> , 9, e85568	52
1059	Protection genes in nucleus accumbens shell affect vulnerability to nicotine self-administration across isogenic strains of adolescent rat. <b>2014</b> , 9, e86214	8
1058	Whole genome analyses of a well-differentiated liposarcoma reveals novel SYT1 and DDR2 rearrangements. <b>2014</b> , 9, e87113	13
1057	A pan-cancer analysis of transcriptome changes associated with somatic mutations in U2AF1 reveals commonly altered splicing events. <b>2014</b> , 9, e87361	112
1056	Normalization of RNA-sequencing data from samples with varying mRNA levels. <b>2014</b> , 9, e89158	35
1055	Microarray meta-analysis of RNA-binding protein functions in alternative polyadenylation. <b>2014</b> , 9, e90774	6
1054	Global analysis of Chlorella variabilis NC64A mRNA profiles during the early phase of Paramecium bursaria chlorella virus-1 infection. <b>2014</b> , 9, e90988	12
1053	Natural antisense transcripts and long non-coding RNA in Neurospora crassa. <b>2014</b> , 9, e91353	35
1052	Transcriptome profiling of a multiple recurrent muscle-invasive urothelial carcinoma of the bladder by deep sequencing. <b>2014</b> , 9, e91466	24
1051	Sequencing degraded RNA addressed by 3' tag counting. <b>2014</b> , 9, e91851	60
1050	Characterization of human pseudogene-derived non-coding RNAs for functional potential. <b>2014</b> , 9, e93972	42
1049	Improved annotation of 3' untranslated regions and complex loci by combination of strand-specific direct RNA sequencing, RNA-Seq and ESTs. <b>2014</b> , 9, e94270	21
1048	Dicer regulates differentiation and viability during mouse pancreatic cancer initiation. <b>2014</b> , 9, e95486	20
1047	The DNA methylome and transcriptome of different brain regions in schizophrenia and bipolar disorder. <b>2014</b> , 9, e95875	64
1046	Dissection of estrogen receptor alpha signaling pathways in osteoblasts using RNA-sequencing. <b>2014</b> , 9, e95987	20
1045	Sequence and ionomic analysis of divergent strains of maize inbred line B73 with an altered growth phenotype. <b>2014</b> , 9, e96782	8

1044	The reference transcriptome of the adult female biting midge (Culicoides sonorensis) and differential gene expression profiling during teneral, blood, and sucrose feeding conditions. <b>2014</b> , 9, e98123	15
1043	Fed state prior to hemorrhagic shock and polytrauma in a porcine model results in altered liver transcriptomic response. <b>2014</b> , 9, e100088	6
1042	A systems biology approach to the analysis of subset-specific responses to lipopolysaccharide in dendritic cells. <b>2014</b> , 9, e100613	5
1041	Nom1 mediates pancreas development by regulating ribosome biogenesis in zebrafish. <b>2014</b> , 9, e100796	12
1040	Transcriptome analysis reveals signature of adaptation to landscape fragmentation. <b>2014</b> , 9, e101467	20
1039	JAGuaR: junction alignments to genome for RNA-seq reads. <b>2014</b> , 9, e102398	37
1038	Drug target mining and analysis of the Chinese tree shrew for pharmacological testing. <b>2014</b> , 9, e104191	16
1037	A set of structural features defines the cis-regulatory modules of antenna-expressed genes in Drosophila melanogaster. <b>2014</b> , 9, e104342	2
1036	Pharmacogenomic approach to identify drug sensitivity in small-cell lung cancer. <b>2014</b> , 9, e106784	14
1035	Transcriptome profiling of spinal muscular atrophy motor neurons derived from mouse embryonic stem cells. <b>2014</b> , 9, e106818	26
1034	Systemic suppression of the shoot metabolism upon rice root nematode infection. <b>2014</b> , 9, e106858	11
1033	RNA-Seq gene profilinga systematic empirical comparison. <b>2014</b> , 9, e107026	61
1032	Comparative transcriptome analysis of climacteric fruit of Chinese pear (Pyrus ussuriensis) reveals new insights into fruit ripening. <b>2014</b> , 9, e107562	36
1031	Specific gene expression responses to parasite genotypes reveal redundancy of innate immunity in vertebrates. <b>2014</b> , 9, e108001	21
1030	Genome-wide identification and tissue-specific expression analysis of UDP-glycosyltransferases genes confirm their abundance in Cicer arietinum (Chickpea) genome. <b>2014</b> , 9, e109715	27
1029	Gene expression differences among three Neurospora species reveal genes required for sexual reproduction in Neurospora crassa. <b>2014</b> , 9, e110398	25
1028	Distinct strains of Toxoplasma gondii feature divergent transcriptomes regardless of developmental stage. <b>2014</b> , 9, e111297	24
1027	DNA methylation and transcription in a distal region upstream from the bovine AlphaS1 casein gene after once or twice daily milking. <b>2014</b> , 9, e111556	14

1026	Long term storage of dry versus frozen RNA for next generation molecular studies. <b>2014</b> , 9, e111827	23
1025	Detection theory in identification of RNA-DNA sequence differences using RNA-sequencing. <b>2014</b> , 9, e112040	6
1024	HIV-1 infection causes a down-regulation of genes involved in ribosome biogenesis. <b>2014</b> , 9, e113908	15
1023	The human pancreas proteome defined by transcriptomics and antibody-based profiling. <b>2014</b> , 9, e115421	25
1022	Allele Workbench: transcriptome pipeline and interactive graphics for allele-specific expression. <b>2014</b> , 9, e115740	8
1021	The kidney transcriptome and proteome defined by transcriptomics and antibody-based profiling. <b>2014</b> , 9, e116125	37
1020	Pharmacological inhibition of cystine-glutamate exchange induces endoplasmic reticulum stress and ferroptosis. <b>2014</b> , 3, e02523	723
1019	The transcription factor Pou3f1 promotes neural fate commitment via activation of neural lineage genes and inhibition of external signaling pathways. <b>2014</b> , 3,	85
1018	High-Performance Integrated Virtual Environment (HIVE) Tools and Applications for Big Data Analysis. <b>2014</b> , 5, 957-81	44
1017	Next-generation sequencing of genomic DNA fragments bound to a transcription factor in vitro reveals its regulatory potential. <b>2014</b> , 5, 1115-31	18
1016	Alternative splicing during Arabidopsis flower development results in constitutive and stage-regulated isoforms. <b>2014</b> , 5, 25	32
1015	Brain-expressed 3'UTR extensions strengthen miRNA cross-talk between ion channel/transporter encoding mRNAs. <b>2014</b> , 5, 41	11
1014	On best practices in the development of bioinformatics software. <b>2014</b> , 5, 199	34
1013	Transcriptional responses of the Bdtf1-deletion mutant to the phytoalexin brassinin in the necrotrophic fungus Alternaria brassicicola. <b>2014</b> , 19, 10717-32	8
1012	Electro-acupuncture at Neiguan pretreatment alters genome-wide gene expressions and protects rat myocardium against ischemia-reperfusion. <b>2014</b> , 19, 16158-78	36
1011	Transcriptional Profiles of Mart-1(27-35) Epitope Specific TCReng Human CD8+ and CD4+ T Cells upon Epitope Encounter as Elucidated by RNASeq. <b>2014</b> , 01,	O
1010	Microbial Profile of the Stomach: Comparison between Normal Mucosa and Cancer Tissue in the Same Patient. <b>2014</b> , 44, 162	13
1009	TAF7L modulates brown adipose tissue formation. <b>2014</b> , 3,	20

1008	Mapping Splicing Quantitative Trait Loci in RNA-Seq. <b>2014</b> , 13, 35-43	6
1007	Prediction of Gene Activity in Early B Cell Development Based on an Integrative Multi-Omics Analysis. <b>2014</b> , 7,	11
1006	Molecular mechanism of formation of cortical opacity in CRYAAN101D transgenic mice. <b>2014</b> , 55, 6398-408	6
1005	Spud DB: A Resource for Mining Sequences, Genotypes, and Phenotypes to Accelerate Potato Breeding. <b>2014</b> , 7, plantgenome2013.12.0042	66
1004	Mapping the molecular determinants of BRAF oncogene dependence in human lung cancer. <b>2014</b> , 111, E748-57	76
1003	Phenotypic and Transcriptional Analysis of Divergently Selected Maize Populations Reveals the Role of Developmental Timing in Seed Size Determination. <b>2014</b> , 165, 658-669	33
1002	TRPV4 inhibition counteracts edema and inflammation and improves pulmonary function and oxygen saturation in chemically induced acute lung injury. <b>2014</b> , 307, L158-72	137
1001	Data set for the genome-wide transcriptome analysis of human epidermal melanocytes. <b>2014</b> , 1, 70-2	3
1000	Deep sequencing of HIV-infected cells: insights into nascent transcription and host-directed therapy. <b>2014</b> , 88, 8768-82	31
999	Compact variant-rich customized sequence database and a fast and sensitive database search for efficient proteogenomic analyses. <b>2014</b> , 14, 2742-9	19
998	Transcriptomics in Health and Disease. <b>2014</b> ,	О
997	Isoform Expression Analysis Based on RNA-seq Data. <b>2014</b> , 247-259	
996	A comprehensive survey of non-canonical splice sites in the human transcriptome. <b>2014</b> , 42, 10564-78	72
995	Independent stratum formation on the avian sex chromosomes reveals inter-chromosomal gene conversion and predominance of purifying selection on the W chromosome. <b>2014</b> , 68, 3281-95	45
994	Domestication of the dog from the wolf was promoted by enhanced excitatory synaptic plasticity: a hypothesis. <b>2014</b> , 6, 3115-21	23
993	Mudskipper genomes provide insights into the terrestrial adaptation of amphibious fishes. <b>2014</b> , 5, 5594	89
992	Molecular evolution of the Yap/Yorkie proto-oncogene and elucidation of its core transcriptional program. <b>2014</b> , 31, 1375-90	34
991	Fungal Genomics. <b>2014</b> , 1-52	15

990	Exploring the Transcriptome of Mycorrhizal Interactions. <b>2014</b> , 70, 53-78	6
989	Parallel ionoregulatory adjustments underlie phenotypic plasticity and evolution of Drosophila cold tolerance. <b>2015</b> , 218, 423-32	51
988	The Arabidopsis U11/U12-65K is an indispensible component of minor spliceosome and plays a crucial role in U12 intron splicing and plant development. <b>2014</b> , 78, 799-810	19
987	Altered promoter nucleosome positioning is an early event in gene silencing. <b>2014</b> , 9, 1422-30	20
986	Vascular endothelial growth factor coordinates islet innervation via vascular scaffolding. <b>2014</b> , 141, 1480-91	57
985	Breed-specific transcriptome response of spleen from six to eight week old piglet after infection with Streptococcus suis type 2. <b>2014</b> , 41, 7865-73	10
984	TNFB ignalling primes chromatin for NF-B binding and induces rapid and widespread nucleosome repositioning. <b>2014</b> , 15, 536	22
983	Adaptive genomic structural variation in the grape powdery mildew pathogen, Erysiphe necator. <b>2014</b> , 15, 1081	95
982	New gene models and alternative splicing in the maize pathogen Colletotrichum graminicola revealed by RNA-Seq analysis. <b>2014</b> , 15, 842	24
981	The genome sequence of the Antarctic bullhead notothen reveals evolutionary adaptations to a cold environment. <b>2014</b> , 15, 468	56
980	Genomic signatures of near-extinction and rebirth of the crested ibis and other endangered bird species. <b>2014</b> , 15, 557	56
979	Transcriptome-wide modulation of splicing by the exon junction complex. <b>2014</b> , 15, 551	58
978	The genome of Eimeria falciformisreduction and specialization in a single host apicomplexan parasite. <b>2014</b> , 15, 696	34
977	Flavonoid supplementation affects the expression of genes involved in cell wall formation and lignification metabolism and increases sugar content and saccharification in the fast-growing eucalyptus hybrid E. urophylla x E. grandis. <b>2014</b> , 14, 301	6
976	The parasite Trichomonas Paginalis expresses thousands of pseudogenes and long non-coding RNAs independently from functional neighbouring genes. <b>2014</b> , 15, 906	27
975	Transposable elements modulate human RNA abundance and splicing via specific RNA-protein interactions. <b>2014</b> , 15, 537	64
974	Improved structural annotation of protein-coding genes in the Meloidogyne hapla genome using RNA-Seq. <b>2014</b> , 3, e29158	6
973	Temporal genomic evolution of bird sex chromosomes. <b>2014</b> , 14, 250	31

972	Concurrent transcriptional profiling of Dirofilaria immitis and its Wolbachia endosymbiont throughout the nematode life cycle reveals coordinated gene expression. <b>2014</b> , 15, 1041	29
971	Integrated genomic study of quadruple-WT GIST (KIT/PDGFRA/SDH/RAS pathway wild-type GIST). <b>2014</b> , 14, 685	61
970	Large-scale transcriptional response to hypoxia in Aspergillus fumigatus observed using RNAseq identifies a novel hypoxia regulated ncRNA. <b>2014</b> , 178, 331-9	21
969	Effect of RNA integrity on uniquely mapped reads in RNA-Seq. <b>2014</b> , 7, 753	22
968	Olive fly transcriptomics analysis implicates energy metabolism genes in spinosad resistance. <b>2014</b> , 15, 714	20
967	Gene expression patterns and sequence polymorphisms associated with mosquito resistance to Bacillus thuringiensis israelensis toxins. <b>2014</b> , 15, 926	25
966	Evolutionary history of Methyltransferase 1 genes in hexaploid wheat. <b>2014</b> , 15, 922	8
965	Methylome, transcriptome, and PPAR(I) cistrome analyses reveal two epigenetic transitions in fat cells. <b>2014</b> , 9, 1195-206	8
964	Heterochromatin-mediated gene silencing facilitates the diversification of olfactory neurons. <b>2014</b> , 9, 884-92	48
963	Differential gene expression and alternative splicing in insect immune specificity. <b>2014</b> , 15, 1031	28
962	Fundamental diversity of human CpG islands at multiple biological levels. <b>2014</b> , 9, 483-91	24
961	SpliceVista, a tool for splice variant identification and visualization in shotgun proteomics data. <b>2014</b> , 13, 1552-62	23
960	The bHLH transcription factor HBI1 mediates the trade-off between growth and pathogen-associated molecular pattern-triggered immunity in Arabidopsis. <b>2014</b> , 26, 828-41	132
959	Map of open and closed chromatin domains in Drosophila genome. <b>2014</b> , 15, 988	16
958	Highly expressed captured genes and cross-kingdom domains present in Helitrons create novel diversity in Pleurotus ostreatus and other fungi. <b>2014</b> , 15, 1071	13
957	Transposable element-assisted evolution and adaptation to host plant within the Leptosphaeria maculans-Leptosphaeria biglobosa species complex of fungal pathogens. <b>2014</b> , 15, 891	111
956	Piecing the puzzle together: a revisit to transcript reconstruction problem in RNA-seq. <b>2014</b> , 15 Suppl 9, S3	1
955	Discovery of novel transcripts and gametophytic functions via RNA-seq analysis of maize gametophytic transcriptomes. <b>2014</b> , 15, 414	58

954	Heterogeneity in the inter-tumor transcriptome of high risk prostate cancer. <b>2014</b> , 15, 426	57
953	Increased expression of mitochondria-localized carbonic anhydrase activity resulted in an increased biomass accumulation in Arabidopsis thaliana. <b>2014</b> , 57, 366-374	20
952	Conservation and functional influence of alternative splicing in wood formation of Populus and Eucalyptus. <b>2014</b> , 15, 780	23
951	Genome analysis of a major urban malaria vector mosquito, Anopheles stephensi. <b>2014</b> , 15, 459	80
950	Genomes of the rice pest brown planthopper and its endosymbionts reveal complex complementary contributions for host adaptation. <b>2014</b> , 15, 521	271
949	DNA copy number evolution in Drosophila cell lines. <b>2014</b> , 15, R70	66
948	Integrative analysis of young genes, positively selected genes and lncRNAs in the development of Drosophila melanogaster. <b>2014</b> , 14, 241	8
947	Comparative transcriptome sequencing of tolerant rice introgression line and its parents in response to drought stress. <b>2014</b> , 15, 1026	80
946	Transcriptome-wide investigation of genomic imprinting in chicken. <b>2014</b> , 42, 3768-82	51
945	Genomic characterization of the LEEDPEEDs, a gene family unique to the medicago lineage. <b>2014</b> , 4, 2003-12	10
944	Discovery of functional genomic motifs in viruses with ViReMa-a Virus Recombination Mapper-for analysis of next-generation sequencing data. <b>2014</b> , 42, e11	47
943	Alternative splicing at GYNNGY 5' splice sites: more noise, less regulation. <b>2014</b> , 42, 13969-80	15
942	Genomic organization, transcriptomic analysis, and functional characterization of avian ∃and ☐keratins in diverse feather forms. <b>2014</b> , 6, 2258-73	44
941	Genome-wide expression analysis in a dwarf soybean mutant. <b>2014</b> , 12, S70-S73	3
940	Using normalization to resolve RNA-Seq biases caused by amplification from minimal input. <b>2014</b> , 46, 808-20	11
939	FTO-dependent demethylation of N6-methyladenosine regulates mRNA splicing and is required for adipogenesis. <b>2014</b> , 24, 1403-19	612
938	Liver Med23 ablation improves glucose and lipid metabolism through modulating FOXO1 activity. <b>2014</b> , 24, 1250-65	36
937	Type I interferon signaling genes in recurrent major depression: increased expression detected by whole-blood RNA sequencing. <b>2014</b> , 19, 1267-74	120

936	Genome-wide distribution of Auts2 binding localizes with active neurodevelopmental genes. <b>2014</b> , 4, e431	35
935	Whole-genome sequence of a flatfish provides insights into ZW sex chromosome evolution and adaptation to a benthic lifestyle. <b>2014</b> , 46, 253-60	509
934	Methods to study splicing from high-throughput RNA sequencing data. <b>2014</b> , 1126, 357-97	58
933	Genome-wide comparative analysis of flowering genes between Arabidopsis and mungbean. <b>2014</b> , 36, 799-808	11
932	Transcriptome sequencing reveals differences between anagen and telogen secondary hair follicle-derived dermal papilla cells of the Cashmere goat (Capra hircus). <b>2014</b> , 46, 104-11	10
931	Key regulators control distinct transcriptional programmes in blood progenitor and mast cells. <b>2014</b> , 33, 1212-26	46
930	Mammalian WTAP is a regulatory subunit of the RNA N6-methyladenosine methyltransferase. <b>2014</b> , 24, 177-89	1061
929	A synthetic lethal screen identifies the Vitamin D receptor as a novel gemcitabine sensitizer in pancreatic cancer cells. <b>2014</b> , 13, 3839-56	23
928	Pachytene piRNAs instruct massive mRNA elimination during late spermiogenesis. <b>2014</b> , 24, 680-700	238
927	Sex- and tissue-specific functions of Drosophila doublesex transcription factor target genes. <b>2014</b> , 31, 761-73	83
926	Identification of mutant genes with high-frequency, high-risk, and high-expression in lung adenocarcinoma. <b>2014</b> , 5, 211-8	10
925	SNAI2 controls the undifferentiated state of human epidermal progenitor cells. <b>2014</b> , 32, 3209-18	47
924	The genetic basis for individual differences in mRNA splicing and APOBEC1 editing activity in murine macrophages. <b>2014</b> , 24, 377-89	12
923	Computational evidence of NAGNAG alternative splicing in human large intergenic noncoding RNA. <b>2014</b> , 2014, 736798	3
922	Biased, non-equivalent gene-proximal and -distal binding motifs of orphan nuclear receptor TR4 in primary human erythroid cells. <b>2014</b> , 10, e1004339	6
921	A novel multi-alignment pipeline for high-throughput sequencing data. <b>2014</b> , 2014,	22
920	Inflammatory monocytes orchestrate innate antifungal immunity in the lung. 2014, 10, e1003940	117
919	iRegulon: from a gene list to a gene regulatory network using large motif and track collections. <b>2014</b> , 10, e1003731	463

918	Transcriptome sequencing from diverse human populations reveals differentiated regulatory architecture. <b>2014</b> , 10, e1004549		35
917	Perturbations in small molecule synthesis uncovers an iron-responsive secondary metabolite network in Aspergillus fumigatus. <b>2014</b> , 5, 530		36
916	Bioinformatic Dissecting of TP53 Regulation Pathway Underlying Butyrate-induced Histone Modification in Epigenetic Regulation. <b>2014</b> , 6, 1-7		5
915	Spatial regulation dominates gene function in the ganglia chain. <i>Bioinformatics</i> , <b>2014</b> , 30, 310-6	7.2	5
914	The secreted protein ANGPTL2 promotes metastasis of osteosarcoma cells through integrin <b>5</b> 01, p38 MAPK, and matrix metalloproteinases. <b>2014</b> , 7, ra7		75
913	Genetic background drives transcriptional variation in human induced pluripotent stem cells. <b>2014</b> , 10, e1004432		190
912	Annotation of a hybrid partial genome of the coffee rust (Hemileia vastatrix) contributes to the gene repertoire catalog of the Pucciniales. <b>2014</b> , 5, 594		24
911	Transcript abundance on its own cannot be used to infer fluxes in central metabolism. <b>2014</b> , 5, 668		35
910	Regulation of mRNA abundance by polypyrimidine tract-binding protein-controlled alternate 5' splice site choice. <b>2014</b> , 10, e1004771		11
909	Metabolic respiration induces AMPK- and Ire1p-dependent activation of the p38-Type HOG MAPK pathway. <b>2014</b> , 10, e1004734		29
908	MicroRNA regulation of bovine monocyte inflammatory and metabolic networks in an in vivo infection model. <b>2014</b> , 4, 957-71		32
907	Developmental regulation of ecdysone receptor (EcR) and EcR-controlled gene expression during pharate-adult development of honeybees (Apis mellifera). <b>2014</b> , 5, 445		36
906	Genome sequencing and comparative genomics of the broad host-range pathogen Rhizoctonia solani AG8. <b>2014</b> , 10, e1004281		102
905	Reconstruction of the gene regulatory network involved in the sonic hedgehog pathway with a potential role in early development of the mouse brain. <b>2014</b> , 10, e1003884		10
904	Genetic analysis of DEFECTIVE KERNEL1 loop function in three-dimensional body patterning in Physcomitrella patens. <b>2014</b> , 166, 903-19		28
903	Analysis of Deep Sequencing Data. <b>2014</b> , 325-354		
902	Resistance to dual blockade of the kinases PI3K and mTOR in KRAS-mutant colorectal cancer models results in combined sensitivity to inhibition of the receptor tyrosine kinase EGFR. <b>2014</b> , 7, ra107	7	22
901	Next-Generation Sequencing. <b>2014</b> , 125-145		2

900	Rfx6 maintains the functional identity of adult pancreatic [] cells. <b>2014</b> , 9, 2219-32	78
899	Two miRNA clusters, miR-34b/c and miR-449, are essential for normal brain development, motile ciliogenesis, and spermatogenesis. <b>2014</b> , 111, E2851-7	185
898	Renal Gene Expression Database (RGED): a relational database of gene expression profiles in kidney disease. <b>2014</b> , 2014,	14
897	AnaLysis of Expression on human chromosome 21, ALE-HSA21: a pilot integrated web resource. <b>2014</b> , 2014, bau009	11
896	The SET domain proteins SUVH2 and SUVH9 are required for Pol V occupancy at RNA-directed DNA methylation loci. <b>2014</b> , 10, e1003948	118
895	The SPF27 homologue Num1 connects splicing and kinesin 1-dependent cytoplasmic trafficking in Ustilago maydis. <b>2014</b> , 10, e1004046	13
894	A genome-wide association study of the maize hypersensitive defense response identifies genes that cluster in related pathways. <b>2014</b> , 10, e1004562	43
893	Influence of ND10 components on epigenetic determinants of early KSHV latency establishment. <b>2014</b> , 10, e1004274	44
892	Systematic analysis of Zn2Cys6 transcription factors required for development and pathogenicity by high-throughput gene knockout in the rice blast fungus. <b>2014</b> , 10, e1004432	99
891	Insights into the epigenomic landscape of the human malaria vector Anopheles gambiae. <b>2014</b> , 5, 277	15
890	Genome-wide tissue-specific gene expression, co-expression and regulation of co-expressed genes in adult nematode Ascaris suum. <b>2014</b> , 8, e2678	38
889	RAN-binding protein 9 is involved in alternative splicing and is critical for male germ cell development and male fertility. <b>2014</b> , 10, e1004825	31
888	A scalable and accurate targeted gene assembly tool (SAT-Assembler) for next-generation sequencing data. <b>2014</b> , 10, e1003737	21
887	The Hmr and Lhr hybrid incompatibility genes suppress a broad range of heterochromatic repeats. <b>2014</b> , 10, e1004240	60
886	Phosphoinositide metabolism links cGMP-dependent protein kinase G to essential Call+ signals at key decision points in the life cycle of malaria parasites. <b>2014</b> , 12, e1001806	136
885	Long non-coding RNA and alternative splicing modulations in Parkinson's leukocytes identified by RNA sequencing. <b>2014</b> , 10, e1003517	133
884	Histone modifications are associated with transcript isoform diversity in normal and cancer cells. <b>2014</b> , 10, e1003611	18
883	Comparison of REST cistromes across human cell types reveals common and context-specific functions. <b>2014</b> , 10, e1003671	27

882	The genomic architecture of population divergence between subspecies of the European rabbit. <b>2014</b> , 10, e1003519	69
881	Zinc finger transcription factors displaced SREBP proteins as the major Sterol regulators during Saccharomycotina evolution. <b>2014</b> , 10, e1004076	42
880	Sex-specific embryonic gene expression in species with newly evolved sex chromosomes. <b>2014</b> , 10, e1004159	15
879	Allelic expression of deleterious protein-coding variants across human tissues. <b>2014</b> , 10, e1004304	43
878	SHP2 regulates chondrocyte terminal differentiation, growth plate architecture and skeletal cell fates. <b>2014</b> , 10, e1004364	43
877	The Groucho co-repressor is primarily recruited to local target sites in active chromatin to attenuate transcription. <b>2014</b> , 10, e1004595	20
876	Microevolution of Candida albicans in macrophages restores filamentation in a nonfilamentous mutant. <b>2014</b> , 10, e1004824	49
875	Dual RNA-seq of parasite and host reveals gene expression dynamics during filarial worm-mosquito interactions. <b>2014</b> , 8, e2905	46
874	RNA-seq analysis of host and viral gene expression highlights interaction between varicella zoster virus and keratinocyte differentiation. <b>2014</b> , 10, e1003896	46
873	A locus encompassing the Epstein-Barr virus bglf4 kinase regulates expression of genes encoding viral structural proteins. <b>2014</b> , 10, e1004307	27
872	Genome-wide SNP calling using next generation sequencing data in tomato. <b>2014</b> , 37, 36-42	60
871	Comparative transcriptome analysis to reveal genes involved in wheat hybrid necrosis. <b>2014</b> , 15, 23332-44	7
870	MicroRNAs located in the Hox gene clusters are implicated in huntington's disease pathogenesis. <b>2014</b> , 10, e1004188	73
869	"Out of pollen" hypothesis for origin of new genes in flowering plants: study from Arabidopsis thaliana. <b>2014</b> , 6, 2822-9	24
868	Evolutionary interrogation of human biology in well-annotated genomic framework of rhesus macaque. <b>2014</b> , 31, 1309-24	30
867	The master regulator of the cellular stress response (HSF1) is critical for orthopoxvirus infection. <b>2014</b> , 10, e1003904	26
866	The Glanville fritillary genome retains an ancient karyotype and reveals selective chromosomal fusions in Lepidoptera. <b>2014</b> , 5, 4737	151
865	Efficient RNA isoform identification and quantification from RNA-Seq data with network flows.  Bioinformatics, <b>2014</b> , 30, 2447-55	48

864	Drosophila melanogaster show a threshold effect in response to radiation. 2014, 12, 551-81	10
863	Protein-protein interaction and gene co-expression maps of ARFs and Aux/IAAs in Arabidopsis. <b>2014</b> , 5, 744	106
862	Evidence for widespread positive and negative selection in coding and conserved noncoding regions of Capsella grandiflora. <b>2014</b> , 10, e1004622	83
861	KSHV 2.0: a comprehensive annotation of the Kaposi's sarcoma-associated herpesvirus genome using next-generation sequencing reveals novel genomic and functional features. <b>2014</b> , 10, e1003847	195
860	Transcriptomic profiling of rat liver samples in a comprehensive study design by RNA-Seq. <b>2014</b> , 1, 140021	21
859	Expanding and Vetting Sorghum bicolor Gene Annotations through Transcriptome and Methylome Sequencing. <b>2014</b> , 7, plantgenome2013.08.0025	22
858	Analysis of the genome and transcriptome of Cryptococcus neoformans var. grubii reveals complex RNA expression and microevolution leading to virulence attenuation. <b>2014</b> , 10, e1004261	260
857	COE loss-of-function analysis reveals a genetic program underlying maintenance and regeneration of the nervous system in planarians. <b>2014</b> , 10, e1004746	29
856	Forty-four novel protein-coding loci discovered using a proteomics informed by transcriptomics (PIT) approach in rat male germ cells. <b>2014</b> , 91, 123	18
855	Bionimbus: a cloud for managing, analyzing and sharing large genomics datasets. <b>2014</b> , 21, 969-75	56
854	A Drosophila immune response against Ras-induced overgrowth. <b>2014</b> , 3, 250-60	31
853	Insight into insulin secretion from transcriptome and genetic analysis of insulin-producing cells of Drosophila. <b>2014</b> , 197, 175-92	22
852	RNA-Seq alignment to individualized genomes improves transcript abundance estimates in multiparent populations. <b>2014</b> , 198, 59-73	55
851	Translational control of the oogenic program by components of OMA ribonucleoprotein particles in Caenorhabditis elegans. <b>2014</b> , 198, 1513-33	32
850	A pathway switch directs BAFF signaling to distinct NFB transcription factors in maturing and proliferating B cells. <b>2014</b> , 9, 2098-111	27
849	Microprocessor activity controls differential miRNA biogenesis In Vivo. <b>2014</b> , 9, 542-54	57
848	High-resolution profiling of novel transcribed regions during rat spermatogenesis. 2014, 91, 5	40
847	Tissue- and stage-dependent dosage compensation on the neo-X chromosome in Drosophila pseudoobscura. <b>2014</b> , 31, 614-24	21

## (2014-2014)

846	RNA-seq gene and transcript expression analysis using the BioExtract server and iPlant collaborative. <b>2014</b> ,		1
845	Improved variational Bayes inference for transcript expression estimation. <b>2014</b> , 13, 203-16		8
844	Improving reliability and absolute quantification of human brain microarray data by filtering and scaling probes using RNA-Seq. <b>2014</b> , 15, 154		36
843	Transcriptomic analysis of differentially expressed genes in the Ras1(CA)-overexpressed and wildtype posterior silk glands. <b>2014</b> , 15, 182		12
842	Identification of genes regulating growth and fatness traits in pig through hypothalamic transcriptome analysis. <b>2014</b> , 46, 195-206		19
841	Dynamic shifts in occupancy by TAL1 are guided by GATA factors and drive large-scale reprogramming of gene expression during hematopoiesis. <b>2014</b> , 24, 1945-62		51
840	Population and single-cell genomics reveal the Aire dependency, relief from Polycomb silencing, and distribution of self-antigen expression in thymic epithelia. <b>2014</b> , 24, 1918-31		197
839	Linking system-wide impacts of RNA polymerase mutations to the fitness cost of rifampin resistance in Pseudomonas aeruginosa. <b>2014</b> , 5, e01562		35
838	ORMAN: optimal resolution of ambiguous RNA-Seq multimappings in the presence of novel isoforms. <i>Bioinformatics</i> , <b>2014</b> , 30, 644-51	7.2	12
837	Murine leukemia virus uses NXF1 for nuclear export of spliced and unspliced viral transcripts. <b>2014</b> , 88, 4069-82		27
836	The Cryptococcus neoformans transcriptome at the site of human meningitis. <b>2014</b> , 5, e01087-13		85
835	Protease inhibitor 15, a candidate gene for abdominal aortic internal elastic lamina ruptures in the rat. <b>2014</b> , 46, 418-28		14
834	Small RNA profiling of Xenopus embryos reveals novel miRNAs and a new class of small RNAs derived from intronic transposable elements. <b>2014</b> , 24, 96-106		16
833	Identification of candidate genes involved in coronary artery calcification by transcriptome sequencing of cell lines. <b>2014</b> , 15, 198		8
832	Insights into the maize pan-genome and pan-transcriptome. <b>2014</b> , 26, 121-35		336
831	High-resolution sequencing and modeling identifies distinct dynamic RNA regulatory strategies. <b>2014</b> , 159, 1698-710		136
830	Dynamic transcriptome landscape of maize embryo and endosperm development. <b>2014</b> , 166, 252-64		177
829	Fine-mapping nicotine resistance loci in Drosophila using a multiparent advanced generation inter-cross population. <b>2014</b> , 198, 45-57		37

828	Antigen-specific culture of memory-like CD8 T cells for adoptive immunotherapy. <b>2014</b> , 2, 839-45	4
827	A Sox2 distal enhancer cluster regulates embryonic stem cell differentiation potential. <b>2014</b> , 28, 2699-711	104
826	Low MITF/AXL ratio predicts early resistance to multiple targeted drugs in melanoma. <b>2014</b> , 5, 5712	374
825	Bisulfighter: accurate detection of methylated cytosines and differentially methylated regions. <b>2014</b> , 42, e45	47
824	Genome-wide study of KNOX regulatory network reveals brassinosteroid catabolic genes important for shoot meristem function in rice. <b>2014</b> , 26, 3488-500	77
823	Transcriptional targets of the schizophrenia risk gene MIR137. <b>2014</b> , 4, e404	42
822	Chronic exposure to TGFI1 regulates myeloid cell inflammatory response in an IRF7-dependent manner. <b>2014</b> , 33, 2906-21	73
821	Targeted chromatin profiling reveals novel enhancers in Ig H and Ig L chain Loci. <b>2014</b> , 192, 1064-70	18
820	An SVM-based approach for discovering splicing junctions with RNA-Seq. <b>2014</b> ,	
819	Novel synthetic Medea selfish genetic elements drive population replacement in Drosophila; a theoretical exploration of Medea-dependent population suppression. <b>2014</b> , 3, 915-28	71
818	Maize centromeres expand and adopt a uniform size in the genetic background of oat. <b>2014</b> , 24, 107-16	66
817	Genome-wide patterns of differentiation among house mouse subspecies. <b>2014</b> , 198, 283-97	28
816	Modeling transcriptional networks regulating secondary growth and wood formation in forest trees. <b>2014</b> , 151, 156-63	13
815	Nuclear ARVCF protein binds splicing factors and contributes to the regulation of alternative splicing. <b>2014</b> , 289, 12421-34	6
814	Cis-splicing and translation of the pre-trans-splicing molecule combine with efficiency in spliceosome-mediated RNA trans-splicing. <b>2014</b> , 22, 1176-1187	26
813	Lariat intronic RNAs in the cytoplasm of Xenopus tropicalis oocytes. <b>2014</b> , 20, 1476-87	90
812	Aldehyde dehydrogenase activity enriches for proximal airway basal stem cells and promotes their proliferation. <b>2014</b> , 23, 664-75	23
811	The dicer-like1 homolog fuzzy tassel is required for the regulation of meristem determinacy in the inflorescence and vegetative growth in maize. <b>2014</b> , 26, 4702-17	22

# (2020-2014)

810	Gene expression profiling of replicative and induced senescence. <b>2014</b> , 13, 3927-37	66
809	Digital cell quantification identifies global immune cell dynamics during influenza infection. <b>2014</b> , 10, 720	63
808	Global dissection of alternative splicing in paleopolyploid soybean. <b>2014</b> , 26, 996-1008	178
807	mRNA and Small RNA Transcriptomes Reveal Insights into Dynamic Homoeolog Regulation of Allopolyploid Heterosis in Nascent Hexaploid Wheat. <b>2014</b> , 26, 1878-1900	193
806	Revisiting the identification of canonical splice isoforms through integration of functional genomics and proteomics evidence. <b>2014</b> , 14, 2709-18	28
805	Constructing protein-protein interaction network of hypertension with blood stasis syndrome via digital gene expression sequencing and database mining. <b>2014</b> , 12, 476-82	3
804	Kruppel-like factor-9 (KLF9) inhibits glioblastoma stemness through global transcription repression and integrin <b>8</b> inhibition. <b>2014</b> , 289, 32742-56	44
803	Image_2.TIF. <b>2020</b> ,	
802	lmage_3.TIF. <b>2020</b> ,	
801	Image_4.TIF. <b>2020</b> ,	
800	Image_5.TIF. <b>2020</b> ,	
799	Table_1.docx. <b>2018</b> ,	
798	Image_6.TIF. <b>2020</b> ,	
797	Image_7.TIF. <b>2020</b> ,	
796	Image_8.TIF. <b>2020</b> ,	
795	Image_9.TIF. <b>2020</b> ,	
794	Table_1.XLSX. <b>2020</b> ,	
793	Table_2.XLSX. <b>2020</b> ,	



### (2020-2019)

Image\_13.JPEG. 2019, 774 Image\_14.JPEG. 2019, 773 Image\_2.JPEG. 2019, 772 Image\_3.JPEG. 2019, 771 Image\_4.JPEG. 2019, 770 Image\_5.JPEG. 2019, 769 768 Image\_6.JPEG. 2019, 767 Image\_7.JPEG. 2019, 766 Image\_8.JPEG. 2019, 765 Image\_9.JPEG. 2019, Image\_1.TIF. 2018, 764 Image\_2.TIF. 2018, 763 Table\_1.DOCX. 2018, 762 Data\_Sheet\_1.docx. 2020, 761 760 Data\_Sheet\_2.xlsx. 2020, 759 Image\_1.TIF. **2020**, 758 Image\_2.TIF. 2020, Image\_1.TIFF. 2020, 757



### (2018-2018)

Table\_1.XLSX. 2018, 738 Data\_Sheet\_1.pdf. 2018, 737 Table\_1.pdf. 2018, 736 Table\_1.XLSX. **2020**, 735 Table\_1.xlsx. **2020**, 734 Table\_2.xlsx. **2020**, 733 732 Table\_2.XLS. 2018, 731 Table\_3.XLS. 2018, Table\_4.XLS. 2018, 730 Image\_1.JPEG. 2020, 729 Image\_2.JPEG. 2020, 728 Image\_3.JPEG. 2020, 727 Presentation\_1.pdf. 2020, 726 Image1.TIFF. 2018, 725 Image2.TIFF. 2018, 724 723 Image3.TIFF. **2018**, Image4.TIFF. 2018, 722 721 Image5.TIFF. 2018,



### (2019-2019)





### (2020-2018)





### (2019-2019)

630 Image\_3.pdf. 2019, Image\_4.pdf. **2019**, 629 Image\_5.pdf. 2019, 628 Image\_6.pdf. **2019**, 627 626 Image\_7.pdf. 2019, Table\_1.xlsx. **2019**, 625 624 Table\_2.xlsx. 2019, Table\_3.xlsx. **2019**, 623 Image\_1.JPEG. 2020, 622 621 Image\_2.JPEG. 2020, Table\_1.docx. 2019, 620 Table\_2.docx. 2019, 619 618 Table\_3.docx. **2019**, Data\_Sheet\_1.xls. 2019, 617 Data\_Sheet\_2.xlsx. 2019, 616 615 Data\_Sheet\_3.xls. 2019, Data\_Sheet\_4.xlsx. 2019, 614 Data\_Sheet\_5.pdf. 2019, 613



### (2020-2018)

Table\_4.docx. 2018, 594 Table\_5.docx. 2018, 593 Table\_1.xls. 2020, 592 Table\_2.xlsx. 2020, 591 Table\_3.xls. 2020, 590 589 Table\_4.xls. 2020, 588 Table\_5.xls. 2020, Table\_6.xlsx. **2020**, 587 586 Table\_1.XLS. 2018, 585 Table\_2.XLS. 2018, Table\_3.XLS. 2018, 584 Table\_4.XLSX. 2018, 583 582 Table\_5.XLSX. **2018**, 581 Table\_6.XLS. **2018**, 580 Table\_7.XLSX. 2018, Image\_1.tif. **2020**, 579 578 Table\_1.pdf. 2020, Table\_2.xlsx. **2020**, 577



### (2020-2018)





### (2020-2020)

Table\_2.DOCX. 2020, 522 Data\_Sheet\_1.docx. 2020, 521 Data\_Sheet\_2.docx. 2020, 520 Data\_Sheet\_3.xlsx. 2020, 519 Data\_Sheet\_4.xlsx. 2020, 518 Data\_Sheet\_5.xlsx. 2020, 517 516 Data\_Sheet\_6.xlsx. 2020, Data\_Sheet\_7.docx. 2020, 515 Data\_Sheet\_8.xlsx. 2020, 514 Data\_Sheet\_9.xlsx. 2020, 513 Image\_1.JPEG. 2020, 512 Data\_Sheet\_1.xlsx. 2020, 511 510 Data\_Sheet\_2.docx. 2020, Image\_1.JPEG. 2020, 509 Image\_2.JPEG. 2020, 508 507 Image\_3.JPEG. **2020**, 506 Image\_4.JPEG. 2020, Image\_5.JPEG. 2020, 505



486	Table2.XLSX. <b>2018</b> ,	
485	Table3.XLSX. <b>2018</b> ,	
484	Data_Sheet_1.PDF. <b>2018</b> ,	
483	Data_Sheet_2.PDF. <b>2018</b> ,	
482	IFN-Trytotoxic CD4 T lymphocytes are involved in the pathogenesis of colitis induced by IL-23 and the food colorant Red 40 <b>2022</b> ,	1
481	Transcriptomic analysis of OsRUS1 overexpression rice lines with rapid and dynamic leaf rolling morphology <b>2022</b> , 12, 6736	Ο
480	An overview of technologies for MS-based proteomics-centric multi-omics 2022,	O
479	In vivo temporal resolution of acute promyelocytic leukemia progression reveals a role of in suppressing early leukemic transformation <b>2022</b> ,	O
478	Mrada3 is required for sexual reproduction and secondary metabolite production in industrial fungi Monascus strain <b>2022</b> ,	0
477	Comprehensive transcriptomic analysis of two RIL parents with contrasting salt responsiveness identifies polyadenylated and non-polyadenylated flower lncRNAs in chickpea <b>2022</b> ,	O
476	Comparative transcriptome analysis of experimental cryptorchidism: Of mice and cynomolgus monkeys <b>2022</b> ,	
475	AKIP1 promotes tumor progression by cancer-related pathways and predicts prognosis in tongue squamous cell carcinoma <b>2021</b> , 13, 12338-12351	
474	Identification of Prognostic Biomarkers for Glioblastoma Based on Transcriptome and Proteome Association Analysis <b>2022</b> , 21, 15330338211035270	Ο
473	Bioinformatics-assisted multiomics approaches to improve the agronomic traits in cotton. <b>2022</b> , 233-251	O
472	Heat shock-induced failure of meiosis I to meiosis II transition leads to 2n pollen formation in a woody plant <b>2022</b> ,	1
471	Computational approaches toward single-nucleotide polymorphism discovery and its applications in plant breeding. <b>2022</b> , 513-536	
470	Identification of potential key genes in resveratrol biosynthesis via transcriptional analyses of berry development in grapevine (<i>Vitis</i> spp.) genotypes varying in <i>trans</i>-resveratrol content. <b>2022</b> , 2, 1-11	
469	Release of VAMP5-positive extracellular vesicles from specialized domains of retinal MIler cells in vivo.	

468	The estrogen receptor Eistrome in human endometrium and epithelial organoids.	1
467	Protective Effects of Nuciferine in Middle Cerebral Artery Occlusion Rats Based on Transcriptomics. <b>2022</b> , 12, 572	O
466	Epigenetic regulator UHRF1 suppressively orchestrates pro-inflammatory gene expression in rheumatoid arthritis <b>2022</b> ,	0
465	Gut microbiota-derived metabolites contribute negatively to hindgut barrier function development at the early weaning goat model. <b>2022</b> ,	
464	Gene expression in male and female stickleback from populations with convergent and divergent throat coloration <b>2022</b> , 12, e8860	
463	circMbl functions in cis and in trans to regulate gene expression and physiology in a tissue-specific fashion <b>2022</b> , 39, 110740	2
462	Pathogenic Mechanism of a Highly Virulent Infectious Hematopoietic Necrosis Virus in Head Kidney of Rainbow Trout (Oncorhynchus mykiss) Analyzed by RNA-Seq Transcriptome Profiling. <b>2022</b> , 14, 859	0
461	Reduction in Toxicity of Polystyrene Nanoplastics Combined with Phenanthrene through Binding of Jellyfish Mucin with Nanoplastics <b>2022</b> , 12,	O
460	PredPromoter-MF(2L): A Novel Approach of Promoter Prediction Based on Multi-source Feature Fusion and Deep Forest <b>2022</b> ,	О
459	Thyroid hormone and ALK5 inhibitor improve maturation of human pluripotent stem cell derived hepatocytes.	
458	Expression profile analysis in cells overexpressing DRPLA cDNA to explore the roles of DRPLAp as a transcriptional coregulator.	
457	Whole-Transcriptome Analysis Reveals Long Noncoding RNAs Involved in Female Floral Development of Hickory (Carya cathayensis Sarg.). <b>2022</b> , 13,	O
456	Sex-relevant genes in the embryo stage of Chinese soft-shelled turtles as revealed by RNA-Seq analysis. <b>2022</b> , 1-19	
455	The genome sequencing and comparative analysis of a wild kiwifruit Actinidia eriantha. 2022, 2,	1
454	Genome-Wide Identification and Characterization of Long Noncoding RNAs in Populus Lanescens Roots Treated With Different Nitrogen Fertilizers. <b>2022</b> , 13,	1
453	Identification of functional features underlying heat stress response in Sprague-Dawley rats using mixed linear models <b>2022</b> , 12, 7671	
452	Genome of a giant isopod, Bathynomus jamesi, provides insights into body size evolution and adaptation to deep-sea environment <b>2022</b> , 20, 113	О
451	ETV2 functions as a pioneer factor to regulate and reprogram the endothelial lineage 2022,	2

450	Nicotinamide mononucleotide reduces melanin production in aged melanocytes by inhibiting cAMP/Wnt signaling. <b>2022</b> ,	1
449	Diving, and even diging, into the wild jungle of annotation pathways for non-vertebrate animals.	
448	Transcriptome analysis and identification of genes associated with oil accumulation in upland cotton <b>2022</b> , e13701	0
447	A transferred regulator that contributes to Xanthomonas oryzae pv. oryzicola oxidative stress adaptation and virulence by regulating the expression of cytochrome bd oxidase genes. <b>2022</b> , 21, 1673-1682	O
446	Genomic and transcriptomic somatic alterations of hepatocellular carcinoma in non-cirrhotic livers <b>2022</b> , 264-265, 90-99	1
445	Identification of an Epigenetically Marked Locus within the Sex Determination Region of Channel Catfish. <b>2022</b> , 23, 5471	1
444	The effect of melatonin on the mouse ameloblast-lineage cell line ALCs 2022, 12, 8225	O
443	A model for isoform-level differential expression analysis using RNA-seq data without pre-specifying isoform structure <b>2022</b> , 17, e0266162	
442	Omics sciences. <b>2022</b> , 105-118	
441	Bibliography. <b>2022</b> , 213-236	
441	Bibliography. 2022, 213-236  Heat Shock Protein 70 in Penile Neurovascular Regeneration Requires Cystathionine Gamma-Lyase. 40,	1
	Heat Shock Protein 70 in Penile Neurovascular Regeneration Requires Cystathionine Gamma-Lyase.	1
440	Heat Shock Protein 70 in Penile Neurovascular Regeneration Requires Cystathionine Gamma-Lyase. 40,  Development of transcriptomics-based growth rate indices in two model eukaryotes and relevance	1 0
440	Heat Shock Protein 70 in Penile Neurovascular Regeneration Requires Cystathionine Gamma-Lyase. 40,  Development of transcriptomics-based growth rate indices in two model eukaryotes and relevance to metatranscriptomic datasets.  Chromosome-Scale, Haplotype-Resolved Genome Assembly of Non-Sex-Reversal Females of	
44° 439 438	Heat Shock Protein 70 in Penile Neurovascular Regeneration Requires Cystathionine Gamma-Lyase. 40,  Development of transcriptomics-based growth rate indices in two model eukaryotes and relevance to metatranscriptomic datasets.  Chromosome-Scale, Haplotype-Resolved Genome Assembly of Non-Sex-Reversal Females of Swamp Eel Using High-Fidelity Long Reads and Hi-C Data. 2022, 13,  Characterization of a Deep-Sea Actinobacterium Strain Uncovers Its Prominent Capability of	o
440 439 438 437	Heat Shock Protein 70 in Penile Neurovascular Regeneration Requires Cystathionine Gamma-Lyase. 40,  Development of transcriptomics-based growth rate indices in two model eukaryotes and relevance to metatranscriptomic datasets.  Chromosome-Scale, Haplotype-Resolved Genome Assembly of Non-Sex-Reversal Females of Swamp Eel Using High-Fidelity Long Reads and Hi-C Data. 2022, 13,  Characterization of a Deep-Sea Actinobacterium Strain Uncovers Its Prominent Capability of Utilizing Taurine and Polyvinyl Alcohol. 2022, 13,  Physiological and comparative transcriptome analyses reveal the mechanisms underlying	0
440 439 438 437 436	Heat Shock Protein 70 in Penile Neurovascular Regeneration Requires Cystathionine Gamma-Lyase. 40,  Development of transcriptomics-based growth rate indices in two model eukaryotes and relevance to metatranscriptomic datasets.  Chromosome-Scale, Haplotype-Resolved Genome Assembly of Non-Sex-Reversal Females of Swamp Eel Using High-Fidelity Long Reads and Hi-C Data. 2022, 13,  Characterization of a Deep-Sea Actinobacterium Strain Uncovers Its Prominent Capability of Utilizing Taurine and Polyvinyl Alcohol. 2022, 13,  Physiological and comparative transcriptome analyses reveal the mechanisms underlying waterlogging tolerance in a rapeseed anthocyanin-more mutant. 2022, 15,	0

432	Progesterone Signaling in Endometrial Epithelial Organoids. 2022, 11, 1760	1
431	Transcriptome-wide profiling of acute stress induced changes in ribosome occupancy level using external standards.	
430	Impact of Heat Stress on Expression of Wheat Genes Responsive to Hessian Fly Infestation. <b>2022</b> , 11, 1402	
429	Hematopoietic Prostaglandin D2 Synthase Controls Tfh/Th2 Communication and Limits Tfh Antitumor Effects. OF1-OF17	O
428	Disruption of 🛮 catenin-mediated negative feedback reinforces cAMP-induced neuronal differentiation in glioma stem cells. <b>2022</b> , 13,	O
427	Targeted Inhibition of O-Linked I-N-Acetylglucosamine Transferase as a Promising Therapeutic Strategy to Restore Chemosensitivity and Attenuate Aggressive Tumor Traits in Chemoresistant Urothelial Carcinoma of the Bladder. <b>2022</b> , 10, 1162	1
426	Common gene expression patterns are observed in rice roots during associations with plant growth-promoting bacteria, Herbaspirillum seropedicae and Azospirillum brasilense. <b>2022</b> , 12,	0
425	Histone H3K27 methyltransferase EZH2 interacts with MEG3-lncRNA to directly regulate integrin signaling and endothelial cell function.	
424	Bacterial Infection Induces Ultrastructural and Transcriptional Changes in the King Oyster Mushroom ( Pleurotus eryngii ).	1
423	A homozygous exonic variant leading to exon skipping in ABCC8 as the cause of severe congenital hyperinsulinism.	O
422	How placenta promotes the successful reproduction in high-altitude populations: a transcriptome comparison between adaptation and acclimatization.	2
421	Glutathione S -transferase (GST) genes and their function associated with pyrethroid resistance in the malaria vector Anopheles sinensis.	O
420	Assessing Gene Expression Related to Cisplatin Resistance in Human Oral Squamous Cell Carcinoma Cell Lines. <b>2022</b> , 15, 704	
419	High-throughput analysis of lncRNA in cows with naturally infected Staphylococcus aureus mammary gland. 1-9	
418	A novel kinase subverts Aluminum resistance by boosting Ornithine decarboxylase-dependent putrescine biosynthesis.	O
417	Genomic status of Yellow-breasted Bunting following recent rapid population decline. 2022, 104501	
416	A broadly applicable, stress-mediated bacterial death pathway regulated by the phosphotransferase system (PTS) and the cAMP-Crp cascade. <b>2022</b> , 119,	1
415	Transcriptomic differences in response to Metarhizium anisopliae and Trichoderma harzianum uncovers major regulative genes and pathways for establishment of beneficial relationship in peanut. <b>2022</b> , 104964	O

414	A TRIM66/DAX1/Dux axis suppresses the totipotent 2-cell-like state in murine embryonic stem cells. <b>2022</b> , 29, 948-961.e6	О
413	Liver transcriptome analysis reveals biological pathways and transcription factors in response to high ammonia exposure. 1-11	1
412	Phase separation of Ddx3xb helicase regulates maternal-to-zygotic transition in zebrafish.	2
411	Genome, genetic evolution, and environmental adaptation mechanisms of Schizophyllum commune in deep subseafloor coal-bearing sediments. <b>2022</b> , 25, 104417	1
410	SLAMseq resolves the kinetics of maternal and zygotic gene expression in early zebrafish embryogenesis.	O
409	Comparative transcriptome analysis on candidate genes involved in lipid biosynthesis of developing kernels for three walnut cultivars in Xinjiang. <b>2022</b> , 11, 1201-1214	1
408	Alternative splicing plays key roles in response to stress across different stages of fighting in the fish Betta splendens. <b>2021</b> , 22,	О
407	Chromatin accessibility analysis from fresh and cryopreserved human ovarian follicles. 2022, 28,	O
406	Evolution of sexual systems, sex chromosomes and sex-linked gene transcription in flatworms and roundworms. <b>2022</b> , 13,	O
405	The Antarctic Moss Pohlia nutans Genome Provides Insights Into the Evolution of Bryophytes and the Adaptation to Extreme Terrestrial Habitats. 13,	2
404	Use of a graph neural network to the weighted gene co-expression network analysis of Korean native cattle. <b>2022</b> , 12,	1
403	RNA Sequencing of the Pituitary Gland and Association Analyses Reveal PRKG2 as a Candidate Gene for Growth and Carcass Traits in Chinese Ningdu Yellow Chickens. 9,	
402	A Transcriptomic Response to Lactiplantibacillus plantarum-KCC48 against High-Fat Diet-Induced Fatty Liver Diseases in Mice. <b>2022</b> , 23, 6750	0
401	DNA Methylation Correlates with the Expression of Drought-Responsive Genes and Drought Resistance in Rice. <b>2022</b> , 12, 1445	O
400	Characterization of microRNA and gene expression in the cochlea of an echolocating bat (Rhinolophus affinis). <b>2022</b> , 12,	
399	Aberrant activation of p53/p66Shc-mInsc axis increases asymmetric divisions and attenuates proliferation of aged mammary stem cells.	O
398	Gene network analysis reveals candidate genes related with the hair follicle development in sheep. <b>2022</b> , 23,	О
397	Comparative parallel multi-omics analysis during the induction of pluripotent and trophectoderm states. <b>2022</b> , 13,	O

396	UVB Irradiation-Induced Transcriptional Changes in Lignin- and Flavonoid Biosynthesis and Indole/Tryptophan-Auxin-Responsive Genes in Rice Seedlings. <b>2022</b> , 11, 1618	О
395	Blood brain barrier permeability and immune function of brain in rainbow trout responding to IHNV infection. <b>2022,</b> 104482	O
394	SIRT6 promotes mitochondrial fission and subsequent cellular invasion in ovarian cancer.	1
393	Single B Cell Gene Co-Expression Networks Implicated in Prognosis, Proliferation, and Therapeutic Responses in Non-Small Cell Lung Cancer Bulk Tumors. <b>2022</b> , 14, 3123	O
392	Conservation of Nematocida microsporidia gene expression and host response in Caenorhabditis nematodes.	0
391	Global analyses of mRNA expression in human sensory neurons reveal eIF5A as a conserved target for inflammatory pain. <b>2022</b> , 36,	O
390	Gene fusion as an important mechanism to generate new genes in the genus Oryza. 2022, 23,	О
389	Transgenic Soybeans Expressing Phosphatidylinositol-3-Phosphate-Binding Proteins Show Enhanced Resistance Against the Oomycete Pathogen Phytophthora sojae. 13,	O
388	Nintedanib induces gene expression changes in the lung of induced-rheumatoid arthritis ssociated interstitial lung disease mice. <b>2022</b> , 17, e0270056	О
387	Estimation of tumor cell total mRNA expression in 15 cancer types predicts disease progression.	1
386	The role of endogenous Smad7 in regulating macrophage phenotype following myocardial infarction. <b>2022</b> , 36,	О
385	Prediction and expression analysis of deleterious nonsynonymous SNPs of Arabidopsis ACD11 gene by combining computational algorithms and molecular docking approach. <b>2022</b> , 18, e1009539	
384	Transcriptomic Characterization of Miscanthus sacchariflorus IM. lutarioriparius and Its Implications for Energy Crop Development in the Semiarid Mine Area. <b>2022</b> , 11, 1568	
383	Cardiac fibroblasts regulate the development of heart failure via Htra3-TGF-I-IGFBP7 axis. <b>2022</b> , 13,	1
382	PICLN modulates alternative splicing and ensures adaptation to light and temperature changes in plants.	
381	Shade triggers posttranscriptional PHYTOCHROME- INTERACTING FACTOR-dependent increases in H3K4 trimethylation.	O
380	Saliva and Lung Microbiome Associations with Electronic Cigarette Use and Smoking. OF1-OF11	О
379	Dynamic Genome-Wide Transcription Profiling and Direct Target Genes of CmWC-1 Reveal Hierarchical Light Signal Transduction in Cordyceps militaris. <b>2022</b> , 8, 624	1

378	Genome structure and evolutionary history of frankincense producing Boswellia sacra. 2022, 25, 104574	O
377	Constitutional delay of growth and puberty in female mice is induced by circadian rhythm disruption in utero. <b>2022</b> , 241, 113723	
376	Comprehensive illustration of transcriptomic and proteomic dataset for mitigation of arsenic toxicity in rice (Oryza sativa L.) by microbial consortium. <b>2022</b> , 43, 108377	
375	Exploring Phylogenetic Relationships and Divergence Times of Bioluminescent Species Using Genomic and Transcriptomic Data. <b>2022</b> , 409-423	
374	Bioinformatics Approaches for Determining the Functional Impact of Repetitive Elements on Non-coding RNAs. <b>2022</b> , 315-340	0
373	Molekularpathologische Diagnostik. <b>2022</b> , 1-11	
372	Characterization and Functional Analysis of a New Calcium/Calmodulin-Dependent Protein Kinase (CaMK1) in the Citrus Pathogenic Fungus Penicillium italicum. <b>2022</b> , 8, 667	Ο
371	Somatic structural variations in pediatric brain tumors. <b>2022</b> , 74,	
370	Chloroplast activity provides in vitro regeneration capability in contrasting cultivars.	
369	Pseudomonas phaseolicola preferentially modulates genes encoding leucine-rich repeat and malectin domains in the bean landrace G2333. <b>2022</b> , 256,	
368	Dual role of histone variant H3.3B in spermatogenesis: positive regulation of piRNA transcription and implication in X-chromosome inactivation.	
367	AGO1 and HSP90 buffer different genetic variants in Arabidopsis thaliana.	
366	BcMettl4-Mediated DNA Adenine N6-Methylation Is Critical for Virulence of Botrytis cinerea. 13,	O
365	Machine Learning Identifies Signatures of Macrophage Reactivity and Tolerance that Predict Disease Outcomes.	O
364	Dynamics of the Gut Microbiome and Transcriptome in Korea Native Ricefish (Oryzias latipes) during Chronic Antibiotic Exposure. <b>2022</b> , 13, 1243	0
363	KHSRP combines transcriptional and posttranscriptional mechanisms to regulate monocytic differentiation. Publish Ahead of Print,	
362	Physiological and Transcriptome Analysis on Diploid and Polyploid Populus ussuriensis Kom. under Salt Stress. <b>2022</b> , 23, 7529	1
361	Avian IRF1 and IRF7 Play Overlapping and Distinct Roles in Regulating IFN-Dependent and -Independent Antiviral Responses to Duck Tembusu Virus Infection. <b>2022</b> , 14, 1506	

360	Genome-wide identification and comparative evolutionary analysis of sorbitol metabolism pathway genes in four Rosaceae species and three model plants. <b>2022</b> , 22,	
359	Aminotransferase SsAro8 Regulates Tryptophan Metabolism Essential for Filamentous Growth of Sugarcane Smut Fungus Sporisorium scitamineum.	
358	A chromosome-level genome assembly of the jade perch (Scortum barcoo). <b>2022</b> , 9,	
357	Low Temperature Rather Than Nitrogen Application Mainly Modulates the Floral Initiation of Different Ecotypes of Rapeseed (Brassica napus L.). <b>2022</b> , 12, 1624	1
356	Pectinolytic arsenal of Colletotrichum lindemuthianum and other fungi with different lifestyles.	
355	BysR, a LysR-type Pleiotropic Regulator, Controls Production of Occidiofungin by Activating the LuxR-type transcriptional regulator AmbR1 in Burkholderia sp. JP2-270.	
354	Comparison of gene expression profiles among caste differentiations in the termite Reticulitermes speratus. <b>2022</b> , 12,	О
353	Wun2-mediated integrin recycling promotes apoptotic cell clearance in Drosophila melanogaster.	1
352	Novel cell- and stage-specific transcriptional signatures defining Drosophila neurons, glia and hemocytes.	
351	Transcriptional Analysis on Resistant and Susceptible Kiwifruit Genotypes Activating Different Plant-Immunity Processes against Pseudomonas syringae pv. actinidiae. <b>2022</b> , 23, 7643	O
350	Nuclear receptor HR3 mediates transcriptional regulation of chitin metabolic genes during molting in Tribolium castaneum.	
349	Lagovirus Non-structural Protein p23: A Putative Viroporin That Interacts With Heat Shock Proteins and Uses a Disulfide Bond for Dimerization. 13,	
348	Notch-dependent and -independent functions of transcription factor RBPJ.	Ο
347	Transcriptome Analysis Reveals Molecular Mechanisms under Salt Stress in Leaves of Foxtail Millet (Setaria italica L.). <b>2022</b> , 11, 1864	Ο
346	Multiomic analyses reveal enriched glycolytic processes in I-myosin heavy chain-expressed cardiomyocytes in early cardiac hypertrophy. <b>2022</b> , 1, 100011	
345	Differential effects of Smad2 and Smad3 in regulation of macrophage phenotype and function in the infarcted myocardium. <b>2022</b> , 171, 1-15	1
344	Rearrangement with the nkd2 promoter contributed to allelic diversity of the r1 gene in maize ( Zea mays ).	
343	The AP2/ERF GmERF113 Positively Regulates the Drought Response by Activating GmPR10-1 in Soybean. <b>2022</b> , 23, 8159	2

342	The transcriptional repressors VAL1 and VAL2 mediate genome-wide recruitment of the CHD3 chromatin remodeler PICKLE in Arabidopsis.	0
341	A Detailed Overview About the Single-Cell Analyses of Solid Tumors Focusing on Colorectal Cancer. 28,	О
340	Impact of gestational haloperidol exposure on miR-137-3p and Nr3c1 mRNA expression in the hippocampus of offspring mice.	О
339	Investigation of rumen long noncoding RNA before and after weaning in cattle. 2022, 23,	
338	Ciliogenesis requires sphingolipid-dependent membrane and axoneme interaction. 2022, 119,	О
337	Regulation of alternative polyadenylation by the C2H2-zinc-finger protein Sp1. <b>2022</b> ,	O
336	New Insights into Bacillus-Primed Plant Responses to a Necrotrophic Pathogen Derived from the Tomato-Botrytis Pathosystem. <b>2022</b> , 10, 1547	
335	Dysfunction of histone demethylase IBM1 in Arabidopsis causes autoimmunity and reshapes the root microbiome.	O
334	Expression Plasticity of Peroxisomal Acyl-Coenzyme A Oxidase Genes Implies Their Involvement in Redox Regulation in Scallops Exposed to PST-Producing Alexandrium. <b>2022</b> , 20, 472	
333	TransMeta simultaneously assembles multisample RNA-seq reads. <b>2022</b> , 32, 1398-1407	O
332	The Loss-Function of the Male Sterile Gene ZmMs33/ZmGPAT6 Results in Severely Oxidative Stress and Metabolic Disorder in Maize Anthers. <b>2022</b> , 11, 2318	О
331	RNA-Seq as an Effective Tool for Modern Transcriptomics, A Review-based Study. <b>2022</b> , 3, 236-241	O
330	KSHV infection of endothelial precursor cells with lymphatic characteristics as a novel model for translational Kaposi sarcoma studies.	
329	Agronomical selection on loss-of-function of GIGANTEA simultaneously facilitates soybean salt tolerance and early maturity.	O
328	The genome of the rice planthopper egg parasitoid wasps Anagrus nilaparvatae casts light on the chemo- and mechanosensation in parasitism. <b>2022</b> , 23,	1
328 327		1
	chemo- and mechanosensation in parasitism. <b>2022</b> , 23,	0

324	Effect of benzo[a]pyrene on proliferation and metastasis of oral squamous cell carcinoma cells: A transcriptome analysis based on RNA -seq.	O
323	The DEAD-box helicase Hlc regulates basal transcription and chromatin opening of stress-responsive genes.	O
322	Insights into the complicated networks contribute to adventitious rooting in transgenic MdWOX11 apple microshoots under nitrate treatments.	0
321	Distinct roles of the two SEC scaffold proteins, AFF1 and AFF4, in regulating RNA Pol II transcription elongation.	
320	The genome of a vestimentiferan tubeworm (Ridgeia piscesae) provides insights into its adaptation to a deep-sea environment.	
319	Conceptual framework for the insect metamorphosis from larvae to pupae by transcriptomic profiling, a case study of Helicoverpa armigera (Lepidoptera: Noctuidae). <b>2022</b> , 23,	
318	Characterizing the Mechanisms of Metalaxyl, Bronopol and Copper Sulfate against Saprolegnia parasitica Using Modern Transcriptomics. <b>2022</b> , 13, 1524	
317	Comprehensive molecular analysis of immortalization hallmarks in thyroid cancer reveals new prognostic markers. <b>2022</b> , 12,	1
316	Barley Ror1 encodes a class XI myosin required for mlo -based broad-spectrum resistance to the fungal powdery mildew pathogen.	0
315	Profiling of gene expression in the brain associated with anxiety-related behaviors in the chronic phase following cranial irradiation. <b>2022</b> , 12,	2
314	Elongated nanoporous Au networks improve somatic cell direct conversion into induced dopaminergic neurons for Parkinson's disease therapy. <b>2022</b> ,	
313	Transcriptomic Analysis of the Porcine Gut in Response to Heat Stress and Dietary Soluble Fiber from Beet Pulp. <b>2022</b> , 13, 1456	
312	Genome-wide characterization of laccase gene family in Schizophyllum commune 20R-7-F01, isolated from deep sediment 2 km below the seafloor. 13,	O
311	Pooled resequencing of larvae and adults reveals genomic variations associated with Ostreid herpesvirus 1 resistance in the Pacific oyster Crassostrea gigas. 13,	O
310	POPEYE intercellular localization mediates cell-specific iron deficiency responses.	O
309	Post-transcriptional regulation of 2-acetyl-1-pyrroline (2-AP) biosynthesis pathway, silicon, and heavy metal transporters in response to Zn in fragrant rice. 13,	1
308	A systematic exploration reveals the potential of spermidine for hypopigmentation treatment through the stabilization of melanogenesis-associated proteins. <b>2022</b> , 12,	
307	Biological activity reduction and mitochondrial and lysosomal dysfunction of mesenchymal stem cells aging in vitro. <b>2022</b> , 13,	

306	Lysophosphatidic acid acyltransferase 2 and 5 commonly, but differently, promote seed oil accumulation in Brassica napus. <b>2022</b> , 15,	1
305	METTL3 preferentially enhances non-m6A translation of epigenetic factors and promotes tumourigenesis. <b>2022</b> , 24, 1278-1290	1
304	Reduced calcium levels and accumulation of abnormal insulin granules in stem cell models of HNF1A deficiency. <b>2022</b> , 5,	1
303	Xist exerts gene-specific silencing during XCI maintenance and impacts lineage-specific cell differentiation and proliferation during hematopoiesis. <b>2022</b> , 13,	
302	Infection-induced membrane ruffling initiates danger and immune signaling via the mechanosensor PIEZO1. <b>2022</b> , 40, 111173	0
301	uORF-Mediated Translational Regulation of ATF4 Serves as an Evolutionarily Conserved Mechanism Contributing to Non-Small-Cell Lung Cancer (NSCLC) and Stress Response.	O
300	H 2 S improves salt-stress recovery via organic acid turn-over in apple seedlings.	O
299	Primary specification of blastocyst trophectoderm by scRNA-seq: New insights into embryo implantation. <b>2022</b> , 8,	1
298	Single-cell genomic and transcriptomic landscapes of primary and metastatic colorectal cancer tumors. <b>2022</b> , 14,	O
297	Identification and expression analysis of the lipid phosphate phosphatases gene family reveal their involvement in abiotic stress response in kiwifruit. 13,	
296	Transcriptomics, regulatory syntax, and enhancer identification in mesoderm-induced ESCs at single-cell resolution. <b>2022</b> , 40, 111219	1
295	A lignan from Alnus japonica inhibits glioblastoma tumorspheres by suppression of FOXM1. <b>2022</b> , 12,	О
294	The nearly complete assembly of Cercis chinensis genome and Fabaceae phylogenomic studies provide insights into new gene evolution. <b>2022</b> , 100422	
293	A reference-grade genome assembly for Gossypium bickii and insights into its genome evolution and formation of pigment gland and gossypol. <b>2022</b> , 100421	О
292	Downregulated NPAS4 in multiple brain regions is associated with Major Depressive Disorder.	
291	Hotspots of single-strand DNA BreakomeDare enriched at transcriptional start sites of genes. 9,	O
290	Role of a ZF-HD Transcription Factor in miR157-Mediated Feed-Forward Regulatory Module That Determines Plant Architecture in Arabidopsis. <b>2022</b> , 23, 8665	
289	Molecular profiling of human non-small cell lung cancer by single-cell RNA-seq. <b>2022</b> , 14,	1

288	Nfkb2 deficiency and its impact on plasma cells and immunoglobulin expression in murine small intestinal mucosa.	
287	GDNF Promotes Astrocyte Abnormal Proliferation and Migration Through the GFR#/RET/MAPK/pCREB/LOXL2 Signaling Axis.	
286	Annotation of Siberian Larch (Larix sibirica Ledeb.) Nuclear Genome Dne of the Most Cold-Resistant Tree Species in the Only Deciduous GENUS in Pinaceae. <b>2022</b> , 11, 2062	2
285	A phenotypic rescue approach identifies lineage regionalization defects in a mouse model of DiGeorge syndrome.	
284	Epigenomics of rats' liver and its cross-species functional annotation reveals key regulatory genes underlying short term heat-stress response. <b>2022</b> , 114, 110449	1
283	Nuclear receptor estrogen-related receptor modulates antimicrobial peptide expression for host innate immunity in Tribolium castaneum. <b>2022</b> , 148, 103816	2
282	Hexane Extract of Citrus sphaerocarpa Suppresses the Accumulation of Lipid Droplets in 3T3-L1 Adipocytes. <b>2022</b> , 2, 1507-1516	O
281	MDM2 antagonist improves therapeutic activity of azacitidine in myelodysplastic syndromes and chronic myelomonocytic leukemia. 1-11	O
280	WNT5A-RHOA signaling is a driver of tumorigenesis and represents a therapeutically actionable vulnerability in small cell lung cancer.	О
279	A small proportion of X-linked genes contribute to X chromosome upregulation in early embryos via BRD4-mediated transcriptional activation. <b>2022</b> ,	O
278	Inhibition of ⊞ynuclein aggregation by MT101-5 is neuroprotective in mouse models of Parkinson disease. <b>2022</b> , 154, 113637	O
277	Abnormal overexpression of SoxD enhances melanin synthesis in the Ursa mutant of Bombyx mori. <b>2022</b> , 149, 103832	O
276	Techniques for Analyzing Genome-wide Expression of Non-coding RNA. 2023, 163-184	0
275	Observation of the development of leaf vein and stomata and identification candidate transcription factors related to vein/stoma development in grapevine leaf (Vitis vinifera L.). <b>2023</b> , 307, 111518	O
274	Small RNA-omics: Decoding the regulatory networks associated with horticultural traits. <b>2022</b> , 15-25	О
273	The absence of the queuosine tRNA modification leads to pleiotropic phenotypes revealing perturbations of metal and oxidative stress homeostasis in Escherichia coli K12. <b>2022</b> , 14,	О
272	Computational Tools and Databases for Fusion Transcripts: Therapeutic Targets in Cancer. <b>2022</b> , 115-127	0
271	Release of VAMP5-positive extracellular vesicles by retinal MIler glia in vivo. <b>2022</b> , 11,	O

270	Identification and expression profiling of serine protease-related genes in Tenebrio molitor.	O
269	Runx2 regulates chromatin accessibility to direct the osteoblast program at neonatal stages. <b>2022</b> , 40, 111315	1
268	Induction of Secondary Metabolite Biosynthesis by Deleting the Histone Deacetylase HdaA in the Marine-Derived Fungus Aspergillus terreus RA2905. <b>2022</b> , 8, 1024	1
267	A Botybirnavirus Isolated from Alternaria tenuissima Confers Hypervirulence and Decreased Sensitivity of Its Host Fungus to Difenoconazole. <b>2022</b> , 14, 2093	o
266	Multi-omics provides new insights into the domestication and improvement of dark jute ( Corchorus olitorius ).	0
265	Sensitisation of cancer cells to radiotherapy by serine and glycine starvation.	1
264	Transcriptome Analysis of Berries of Spine Grape (Vitis davidii Fax) Infected by Colletotrichum viniferum during Symptom Development. <b>2022</b> , 8, 843	О
263	Genomic analysis reveals cryptic diversity in aphelids and sheds light on the emergence of Fungi. <b>2022</b> ,	1
262	LATS1/2 control TGFB-directed epithelial-to-mesenchymal transition in the murine dorsal cranial neuroepithelium through YAP regulation. <b>2022</b> , 149,	О
261	Metabolomics-based classification reveals subtypes of hepatocellular carcinoma.	О
260	Convergent evolution of barnacles and molluscs sheds lights in origin and diversification of calcareous shell and sessile lifestyle. <b>2022</b> , 289,	1
259	A Comparative Study of RNA-Seq Aligners Reveals Novoalign Default Setting as an Optimal Setting for the Alignment of HeLa RNA-Seq Reads. <b>2022</b> , 30, 2727-2745	0
258	A high-quality chromosome-level genome assembly of the bivalve mollusk Mactra veneriformis.	1
257	Proteomic, Transcriptomic, Mutational, and Functional Assays Reveal the Involvement of Both THF and PLP Sites at the GmSHMT08 in Resistance to Soybean Cyst Nematode. <b>2022</b> , 23, 11278	О
256	Comparative Transcriptome Analysis Reveals the Molecular Mechanism of UV-B Irradiation in Promoting the Accumulation of Phenolic Compounds in Wounded Carrot. <b>2022</b> , 8, 896	1
255	Re-exploiting multiple RNA-seq data to identify transcript variations in Podospora anserina.	o
254	Identification and Analysis of MADS-box, WRKY, NAC, and SBP-box Transcription Factor Families in Diospyros oleifera Cheng and Their Associations with Sex Differentiation. <b>2022</b> , 12, 2100	0
253	Metabolome and Transcriptome Profiling Reveal Carbon Metabolic Flux Changes in Yarrowia lipolytica Cells to Rapamycin. <b>2022</b> , 8, 939	0

252	Whole Transcriptome Analyses of Apricots and Japanese Plum Fruits after 1-MCP (Ethylene-Inhibitor) and Ethrel (Ethylene-Precursor) Treatments Reveal New Insights into the Physiology of the Ripening Process. <b>2022</b> , 23, 11045	0
251	3-Deazaadenosine alleviates senescence to promote cellular fitness and cell therapy efficiency in mice. <b>2022</b> , 2, 851-866	O
250	Dissecting aneuploidy phenotypes by constructing Sc2.0 chromosome VII and SCRaMbLEing synthetic disomic yeast.	0
249	Molecular Hydrogen Reduces Electromagnetic Pulse-Induced Male Rat Reproductive System Damage in a Rodent Model. <b>2022</b> , 2022, 1-23	0
248	Global identification of quantitative trait loci and candidate genes for cold stress and chilling acclimation in rice through GWAS and RNA-seq. <b>2022</b> , 256,	O
247	Identification of genes controlling compatible and incompatible reactions of pearl millet (Pennisetum glaucum) against blast (Magnaporthe grisea) pathogen through RNA-Seq. 13,	O
246	Drepmel Multi-Omics Melanoma Drug Repurposing Resource for Prioritizing Drug Combinations and Understanding Tumor Microenvironment. <b>2022</b> , 11, 2894	O
245	A chromosome-level genome assembly of the redfin culter (Chanodichthys erythropterus). <b>2022</b> , 9,	O
244	The single Marchantia polymorpha FERONIA homolog reveals an ancestral role in regulating cellular expansion and integrity.	1
243	Analysis of the abomasal transcriptome of LDA affected cattle.	0
242	A chronic signaling TGFb zebrafish reporter identifies immune response in melanoma.	0
241	Hedgehog signaling activates a mammalian heterochronic gene regulatory network controlling differentiation timing across lineages. <b>2022</b> , 57, 2181-2203.e9	O
240	Nuclear Functions of KaeA, a Subunit of the KEOPS Complex in Aspergillus nidulans. <b>2022</b> , 23, 11138	О
239	Transcriptomic analysis of uterine receptivity in Guinea pigs. 2022,	O
238	Platform-Agnostic CellNet (PACNet) enables cross-study meta-analysis of cell fate engineering protocols.	O
237	Determination of Zn Responsive Genes Involved in Zn Fertilization in Peanuts Based on Transcriptome Analysis.	O
236	Favine/CCDC3 deficiency accelerated atherosclerosis and thrombus formation is associated with decreased MEF2C-KLF2 pathway <b>2022</b> , 105252	О
235	Autophagy induction promoted by m6A reader YTHDF3 through translation upregulation of FOXO3 mRNA. <b>2022</b> , 13,	3

234	The draft genome and multi-omics analyses reveal new insights into geo-herbalism properties of Citrus grandis IIomentosa II 2022, 111489	0
233	Comparative genomics of Sarcoptes scabiei provide new insights into adaptation to permanent parasitism and within-host species divergence.	1
232	Chromatin remodeler Znhit1 controls bone morphogenetic protein signaling in embryonic lung tissue branching. <b>2022</b> , 298, 102490	О
231	Bone marrow stromal cell antigen-1 (CD157) regulated by sphingosine kinase 2 mediates kidney fibrosis. 9,	O
230	Decoding the spatial chromatin organization and dynamic epigenetic landscapes of macrophage cells during differentiation and immune activation. <b>2022</b> , 13,	1
229	Pancreatitis-associated PRSS1-PRSS2 haplotype alters T cell receptor beta (TRB) repertoire more strongly than PRSS1 expression <b>2022</b> ,	О
228	Transcriptome analysis identifies TODL as a novel lncRNA associated with proliferation, differentiation, and tumorigenesis in liposarcoma through FOXM1. <b>2022</b> , 185, 106462	О
227	Genome-wide analysis of long non-coding RNAs under diel light exhibits role in floral development and the circadian clock in Arabidopsis thaliana. <b>2022</b> ,	О
226	Integrated transcriptomics and miRNAomics provide insights into the complex multi-tiered regulatory networks associated with coleoptile senescence in rice. 13,	О
225	Ferroptosis induced by the biocontrol agent Pythium oligandrum enhances soybean resistance to Phytophthora sojae.	О
224	Optical Genome and Epigenome Mapping of Clear Cell Renal Cell Carcinoma.	О
223	Role of liquid fructose/sucrose in regulating the hepatic transcriptome in a high-fat Western diet model of NAFLD. <b>2022</b> , 109174	О
222	Transforming growth factor-promotes the postselection thymic development and peripheral function of interferon-producing invariant natural killer T cells.	О
221	Miniature inverted-repeat transposable elements drive rapid microRNA diversification in angiosperms.	1
220	Molecular Biology, Genetics, and Translational Models of Human Cancer. 1-34	O
219	Predictive Network Analysis IdentifiesJMJD6and Other Novel Key Drivers in Alzheimer∄ Disease.	О
218	Karyotype variation, spontaneous genome rearrangements affecting chemical insensitivity, and expression level polymorphisms in the plant pathogen Phytophthora infestans revealed using its first chromosome-scale assembly. <b>2022</b> , 18, e1010869	1
217	Transcriptome Analysis of Early Senescence in the Post-Anthesis Flag Leaf of Wheat (Triticum aestivum L.). <b>2022</b> , 11, 2593	O

216	Genome-wide chromatin accessibility analysis unveils open chromatin convergent evolution during polyploidization in cotton. <b>2022</b> , 119,	1
215	Interleukin-33-activated neuropeptide CGRP-producing memory Th2 cells cooperate with somatosensory neurons to induce conjunctival itch. <b>2022</b> ,	Ο
214	Transcriptome analysis during fruit developmental stages in durian (Durio zibethinus Murr.) var. D24.	O
213	Transcriptomic Dynamics of Active and Inactive States of Rho GTPase MoRho3 in Magnaporthe oryzae. <b>2022</b> , 8, 1060	O
212	Regulation of Parietal Cell Homeostasis by Bone Morphogenetic Protein signaling. 2022,	O
211	Transcriptomics-based network medicine approach identifies metformin as a repurposable drug for atrial fibrillation. <b>2022</b> , 3, 100749	1
<b>2</b> 10	AGO1 and HSP90 buffer different genetic variants in Arabidopsis thaliana.	2
209	Differential regulation of Type 1 and Type 2 mouse eosinophil activation by apoptotic cells. 13,	O
208	Anin vivoavian model of human melanoma to perform rapid and robust preclinical studies.	O
207	Arctic introgression and chromatin regulation facilitated rapid Qinghai-Tibet Plateau colonization by an avian predator. <b>2022</b> , 13,	O
206	Chromosome-level genome assembly ofTorreya grandisprovides insights into the origin and evolution of gymnosperm-specific sciadonic acid biosynthesis.	O
205	Genome-Wide Transcriptome Analysis Reveals That Upregulated Expression of Aux/IAA Genes Is Associated with Defective Leaf Growth of the slf Mutant in Eggplant. <b>2022</b> , 12, 2647	1
204	Multi-omics of Circular RNAs and Their Responses to Hormones in Moso Bamboo (Phyllostachys edulis).	О
203	Recent Advances on Penalized Regression Models for Biological Data. <b>2022</b> , 10, 3695	O
202	Alternative splicing reprogramming in fungal pathogen Sclerotinia sclerotiorum at different infection stages on Brassica napus. 13,	O
201	Biochemical and Molecular Analysis of Field Resistance to Spirodiclofen in Panonychus citri (McGregor). <b>2022</b> , 13, 1011	O
200	An improved, chromosome-level genome of the giant panda (Ailuropoda melanoleuca). <b>2022</b> , 114, 110501	О
199	Human variation in population-wide gene expression data predicts gene perturbation phenotype. <b>2022</b> , 25, 105328	O

198	Inhibition of LIFR Blocks Adiposity-Driven Endometrioid Endometrial Cancer Growth. 2022, 14, 5400	О
197	Whole genome sequencing of the fast-swimming Southern bluefin tuna (Thunnus maccoyii). 13,	O
196	Comparative transcriptome analysis of resistant and susceptible Kentucky bluegrass varieties in response to powdery mildew infection. <b>2022</b> , 22,	O
195	Nuclear stabilization of p53 requires a functional nucleolar surveillance pathway. <b>2022</b> , 41, 111571	4
194	Identification of potential biomarkers associated with meat tenderness in Hanwoo (Korean cattle): an expression quantitative trait loci analysis.	О
193	The allelopathic effect of para-hydroxybenzoic acid on the gene expression of photosynthesis and respiration in Solanum lycopersicum. <b>2022</b> , 32, 100261	O
192	De Novo Transcriptome Analysis in Hevea brasiliensis to Unveil Genes Involved in Low Temperature Stress Response. <b>2023</b> , 92, 559-575	0
191	Ferroptosis contributes to nickel-induced developmental neurotoxicity in zebrafish. 2023, 858, 160078	O
190	Longer Duration of Active Oil Biosynthesis during Seed Development Is Crucial for High Oil Yield Lessons from Genome-Wide In Silico Mining and RNA-Seq Validation in Sesame. <b>2022</b> , 11, 2980	0
189	Whole-genome assembly and annotation for the little yellow croaker (Larimichthys polyactis) provide insights into the evolution of hermaphroditism and gonochorism.	O
188	A high-quality chromosome-level genome assembly of Pelteobagrus vachelli provides insights into its environmental adaptation and population history. 13,	0
187	SRSF10 is essential for progenitor spermatogonia expansion by regulating alternative splicing. 11,	Ο
186	Transcriptomic Analysis Suggests a Coordinated Regulation of Carotenoid Metabolism in Ripening Chili Pepper (Capsicum annuum var. conoides) Fruits. <b>2022</b> , 11, 2245	0
185	A clinician guide to bioinformatics for next-generation sequencing. 2022,	O
184	KRAB family is involved in network shifts in response to osmotic stress in camels. 1-10	0
183	Transcriptome Analysis Revealed the Mechanism of Inhibition of Saprophytic Growth of Sparassis latifolia by Excessive Oxalic Acid. <b>2022</b> , 11, 3636	O
182	Inactivation of Notch4 attenuated pancreatic tumorigenesis in mice.	0
181	Response of gut microbiota and ileal transcriptome to inulin intervention in HFD induced obese mice. <b>2022</b> ,	Ο

180	Genome-wide identification of heat shock transcription factor families in perennial ryegrass highlights the role of LpHSFC2b in heat stress response.	0
179	Prostaglandin E2 receptor Ptger4b regulates female-specific peptidergic neurons and female sexual receptivity in medaka. <b>2022</b> , 5,	1
178	Chromosome-level genome and population genomics reveal evolutionary characteristics and conservation status of Chinese indigenous geese. <b>2022</b> , 5,	1
177	Hematotoxic Effect of Respiratory Exposure to PHMG-p and Its Integrated Genetic Analysis. <b>2022</b> , 10, 694	O
176	Neoepitopes prediction strategies: an integration of cancer genomics and immunoinformatics approaches.	0
175	Dual inhibition of CPT1A and G6PD suppresses glioblastoma tumorspheres.	O
174	Distinct super-enhancer elements differentially control Il2ra gene expression in a cell-type specific fashion.	0
173	Exposure to Morphine and Cocaine Modify the Transcriptomic Landscape in Zebrafish Embryos. <b>2022</b> ,	O
172	Folate inhibits lipid deposition via the autophagy pathway in chicken hepatocytes. <b>2023</b> , 102, 102363	1
171	Genetic analysis of anemone-type and single-type inflorescences in chrysanthemum using genotyping-by-sequencing. <b>2022</b> , 218,	O
170	The Use of Omics Technologies, Random Mutagenesis, and Genetic Transformation Techniques to Improve Algae for Biodiesel Industry. <b>2023</b> , 43-80	0
169	Comparison of CRISPR-Cas9-mediated megabase-scale genome deletion methods in mouse embryonic stem cells.	0
168	Transcriptome Analysis Reveals Potential Mechanism in Storage Protein Trafficking within Developing Grains of Common Wheat. <b>2022</b> , 23, 14851	1
167	Restoring Age-Related Cognitive Decline through Environmental Enrichment: A Transcriptomic Approach. <b>2022</b> , 11, 3864	1
166	Fungal antibiotics control bacterial community diversity in the cheese rind microbiome.	0
165	Endosperm cellularization failure induces a dehydration stress response leading to embryo arrest.	O
164	High-temperature adaptation of an OsNRT2.3 allele is thermoregulated by small RNAs. 2022, 8,	1
163	Expression Analysis of Brassinolide-Metabolism-Related Genes at Different Growth Stages of Pak Choi. <b>2022</b> , 8, 1093	O

162	Identification and Functional Analysis of Long Non-Coding RNA (lncRNA) in Response to Seed Aging in Rice. <b>2022</b> , 11, 3223	O
161	Characterisation of the functional and transcriptomic effects of pro-inflammatory cytokines on human EndoC-IH5 beta cells.	Ο
160	PICLN modulates alternative splicing and light/temperature responses in plants.	0
159	Tyrosine phosphorylation controlled poly(A) polymerase I activity regulates general stress response in bacteria. <b>2023</b> , 6, e202101148	O
158	POU1F1/Pou1f1 c.143-83A & mp;gt; G variant disrupts the branch site in pre-mRNA and leads dwarfism.	1
157	Stress Triggers Expression of Bovine Herpesvirus 1 Infected Cell Protein 4 (bICP4) RNA during Early Stages of Reactivation from Latency in Pharyngeal Tonsil. <b>2022</b> , 96,	2
156	The A-to-I editing of KPC1 promotes intrahepatic cholangiocarcinoma by attenuating proteasomal processing of NF- <b>B</b> 1 p105 to p50. <b>2022</b> , 41,	0
155	Divergence in interspecific and intersubspecific gene expression between two closely related horseshoe bats (Rhinolophus).	Ο
154	Linolenic Acid-Derived Oxylipins Inhibit Aflatoxin Biosynthesis in Aspergillus flavus through Activation of Imizoquin Biosynthesis. <b>2022</b> , 70, 15928-15944	Ο
153	Integrated Transcriptome Profiling Identifies Prognostic Hub genes as Therapeutic Targets of Selenium Deficiency in Chick® Model: Evidenced by Bioinformatic Analysis	O
152	The eINTACT system dissects bacterial exploitation of plant osmosignalling to enhance virulence.	О
151	StripeDiff: Model-based algorithm for differential analysis of chromatin stripe. 2022, 8,	O
150	Conservation of Nematocida microsporidia gene expression and host response in Caenorhabditis nematodes. <b>2022</b> , 17, e0279103	О
149	novoRNABreak: local assembly for novel splice junction and fusion transcript detection from RNA-seq data.	O
148	Arbuscular Mycorrhizal Fungus Alters Alfalfa (Medicago sativa) Defense Enzyme Activities and Volatile Organic Compound Contents in Response to Pea Aphid (Acyrthosiphon pisum) Infestation. <b>2022</b> , 8, 1308	0
147	Abundance of Ruminococcaceae is Associated with Claudin 22 Gene Expression and Body Weight in Mice.	Ο
146	An alternative pathway to plant cold tolerance in the absence of vacuolar invertase activity.	O
145	The structure, binding and function of a Notch transcription complex involving RBPJ and the epigenetic reader protein L3MBTL3.	O

144	The two-component system histidine kinase EnvZ contributes to Avian pathogenic Escherichia coli pathogenicity by regulating biofilm formation and stress responses. <b>2022</b> , 102388	O
143	Lhx2 is a progenitor-intrinsic modulator of Sonic Hedgehog signaling during early retinal neurogenesis. 11,	O
142	Modulation of RNA splicing enhances response to BCL2 inhibition in leukemia. 2022,	O
141	Chemotherapy-induced phlebitis via the GBP5/NLRP3 inflammasome axis and the therapeutic effect of aescin.	O
140	Strobealign: flexible seed size enables ultra-fast and accurate read alignment. 2022, 23,	1
139	Gut microbiota and acylcarnitine connect the beneficial association between estrogen and lipid metabolism disorders in ovariectomized mice.	O
138	Efficacy and transcriptome analysis of golden pompano (Trachinotus ovatus) immunized with a formalin-inactived vaccine against Streptococcus iniae. <b>2022</b> , 108489	O
137	Alternative splicing of POUM2 regulates embryonic cuticular formation and tanning in Bombyx mori.	O
136	Resistance to chicken amyloid arthropathy is associated with a dysfunctional mutation in serum amyloid A. <b>2023</b> , 37,	0
135	Novel Plant Growth Regulator Guvermectin from Plant Growth-Promoting Rhizobacteria Boosts Biomass and Grain Yield in Rice.	O
134	Comparing the infection biology and gene expression differences of Plasmodiophora brassicae primary and secondary zoospores. 13,	O
133	Haploid-resolved and chromosome-scale genome assembly in hexa-autoploid sweetpotato (Ipomoea batatas (L.) Lam).	O
132	Genetic evidence of aberrant striatal synaptic maturation and secretory pathway alteration in a dystonia mouse model. 1,	O
131	The hitchhikers[guide to RNA sequencing and functional analysis.	O
130	A Flexible Automated Pipeline Engine for Transcript-Level Quantification from RNA-seq. <b>2022</b> , 45-54	0
129	Single-cell profiling reveals distinct subsets of CD14+ monocytes drive blood immune signatures of active tuberculosis. 13,	O
128	Statin-mediated reduction in mitochondrial cholesterol primes an anti-inflammatory response in macrophages by upregulating JMJD3.	0
127	Single-cell profiling of lncRNAs in human germ cells and molecular analysis reveals transcriptional regulation of LNC1845 on LHX8. 12,	O

126	High-quality haplotype-resolved genome assembly of cultivated octoploid strawberry.	O
125	Microbe-induced plant drought tolerance by ABA-mediated root morphogenesis and epigenetic reprogramming of gene expression.	O
124	Long-Term Memory Formation in Drosophila Depends on the 3?UTR of CPEB Gene orb2. 2023, 12, 318	O
123	A chemically defined system supports two distinct types of stem cell from a single blastocyst and their self-assembly to generate blastoid.	O
122	DeteX: A highly accurate software for detecting SNV and InDel in single and paired NGS data in cancer research. 13,	O
121	Human SMARCA5 is continuously required to maintain nucleosome spacing. 2023,	O
120	Transcriptome analysis revealed sh2 gene mutation leads reduced zein protein accumulation in maize endosperm.	O
119	Genome-Wide mRNA and Long Non-Coding RNA Analysis of Porcine Trophoblast Cells Infected with Porcine Reproductive and Respiratory Syndrome Virus Associated with Reproductive Failure. <b>2023</b> , 24, 919	O
118	Systems biology's role in leveraging microalgal biomass potential: Current status and future perspectives. <b>2023</b> , 69, 102963	0
117	Genome-wide identification and functional analysis of long non-coding RNAs in Chilo suppressalis reveal their potential roles in chlorantraniliprole resistance. 13,	O
116	Spatio-temporal expression pattern of Raffinose Synthase genes determine the levels of Raffinose Family Oligosaccharides in peanut (Arachis hypogaea L.) seed. <b>2023</b> , 13,	O
115	Summary-data based mendelian randomization identifies gene expression regulatory polymorphisms associated with bovine paratuberculosis by modulation of the nuclear factor Kappa (NF-#mediated inflammatory response.	O
114	Transcriptome analysis and differential expression in Arabidopsis thaliana in response to rohitukine (a chromone alkaloid) treatment. <b>2023</b> , 23,	O
113	Integrative genomic and transcriptomic analyses of a bud sport mutant Ilinzao Wuhelwith the phenotype of large berries in grapevines. 11, e14617	2
112	Increased adipose catecholamine levels and protection from obesity with loss of Allograft Inflammatory Factor-1. <b>2023</b> , 14,	O
111	A computational pipeline to learn gene expression predictive models from epigenetic information at enhancers or promoters. <b>2023</b> , 4, 101948	O
110	Pre-exposure cognitive performance variability is associated with severity of respiratory infection. <b>2022</b> , 12,	O
109	Forces driving transposable element load variation during Arabidopsis range expansion.	O

108	Genome-wide association study reveals the genetic determinism of serum biochemical indicators in ducks. <b>2022</b> , 23,	0
107	Identification of R-Spondin Gene Signature Predictive of Metastatic Progression in BRAFV600E-Positive Papillary Thyroid Cancer. <b>2023</b> , 12, 139	Ο
106	The Jasmine (Jasminum sambac) Genome Provides Insight into the Biosynthesis of Flower Fragrances and Jasmonates. <b>2022</b> ,	1
105	A multi-omics integrative network map of maize. <b>2023</b> , 55, 144-153	1
104	ALS-L1023 from Melissa officinalis Alleviates Liver Fibrosis in a Non-Alcoholic Fatty Liver Disease Model. <b>2023</b> , 13, 100	0
103	New insights into genome annotation in Podospora anserina through re-exploiting multiple RNA-seq data. <b>2022</b> , 23,	O
102	Transcriptome Analysis Identifies Novel Genes Associated with Low-Temperature Seed Germination in Sweet Corn. <b>2023</b> , 12, 159	1
101	Genome-wide association studies demonstrate the genes associated with perimysial thickness in ducks.	Ο
100	Genomic analysis of an ultrasmall freshwater green alga, Medakamo hakoo. 2023, 6,	0
99	The Weimberg pathway: an alternative for Myceliophthora thermophila to utilize d-xylose. <b>2023</b> , 16,	O
98	KSHV infection of endothelial precursor cells with lymphatic characteristics as a novel model for translational Kaposi sarcoma studies. <b>2023</b> , 19, e1010753	0
97	Deletion of Glycogen Synthase Kinase 3 Beta Reprograms NK Cell Metabolism. <b>2023</b> , 15, 705	Ο
96	Identification of a Novel Gene Signature for Neuroblastoma Differentiation using a Boolean Implication Network.	0
95	Genome-wide RNA polymerase stalling shapes the transcriptome during aging.	O
94	ciRS-7-miR7 regulate ischemia induced neuronal death via glutamatergic signaling.	Ο
93	An in⊡ivo avian model of human melanoma to perform rapid and robust preclinical studies.	O
92	Discovery of a gene cluster for the biosynthesis of novel cyclic peptide compound, KK-1, in Curvularia clavata. 3,	0
91	Direct activation of microglia by I-glucosylceramide causes phagocytosis of neurons that exacerbates Gaucher disease. <b>2023</b> ,	Ο

90	What transcriptomics and proteomics can tell us about a high borate perturbed boron tolerant Bacilli strain.	0
89	Transcriptomic Approach for Global Distribution of SNP/Indel and Plant Genotyping. 2023, 147-164	O
88	HERV1-env Induces Unfolded Protein Response Activation in Autoimmune Liver Disease: A Potential Mechanism for Regulatory T Cell Dysfunction. <b>2023</b> , 210, 732-744	O
87	Transcriptional landscape of Burkholderia pseudomallei cultured under environmental and clinical conditions. <b>2023</b> , 9,	O
86	CMTR1 promotes colorectal cancer cell growth and immune evasion by transcriptionally regulating STAT3. <b>2023</b> , 14,	О
85	Estradiol cycling drives female obesogenic adipocyte hyperplasia. <b>2023</b> , 42, 112390	O
84	Conserved hierarchical gene regulatory networks for drought and cold stress response in Myrica rubra. 14,	О
83	Metabolome-Based Genome-Wide Association Study of Duck Meat Leads to Novel Genetic and Biochemical Insights.	O
82	The novel circular RNA CircMef2c is positively associated with muscle growth in Nile tilapia. <b>2023</b> , 115, 110598	0
81	Differences of functionalized graphene materials on inducing chronic aquatic toxicity through the regulation of DNA damage, metabolism and oxidative stress in Daphnia magna. <b>2023</b> , 876, 162735	O
80	Transcriptome and weighted gene co-expression network analysis of jujube (Ziziphus jujuba Mill.) fruit reveal putative genes involved in proanthocyanin biosynthesis and regulation. <b>2023</b> , 12, 1557-1570	O
79	Adverse effects of polystyrene nanoplastics on sea cucumber Apostichopus japonicus and their association with gut microbiota dysbiosis. <b>2023</b> , 330, 138568	O
78	Heterologous expression of SpsLAZY1a in Populus enhanced the sensitiveness of plant architecture. <b>2023</b> , 197, 116572	0
77	Transcriptome analysis during fruit developmental stages in durian (Durio zibethinus Murr.) var. D24. <b>2022</b> , 45,	O
76	Intra-Exon Motif Correlations as a Proxy Measure for Mean Per-Tile Sequence Quality Data in RNA-Seq. <b>2023</b> , 30, 131-148	0
75	Hormesis effects in tomato plant growth and photosynthesis due to acephate exposure based on physiology and transcriptomic analysis.	O
74	The complexity of EGFR exon 19 deletion and L858R mutant cells as assessed by proteomics, transcriptomics, and metabolomics. <b>2023</b> , 424, 113503	O
73	Identification and Functional Prediction of Circular Rnas in Grape Cluster Development.	O

72	Comprehensive Transcriptome Analysis of Arabidopsis thaliana DNA Polymerase Epsilon Catalytic Subunit A and B Mutants.	0
71	A program of successive gene expression in mouse one-cell embryos. <b>2023</b> , 42, 112023	О
70	Histone H2A deubiquitinases in the transcriptional programs of development and hematopoiesis: a consolidated analysis. <b>2023</b> , 157, 106384	О
69	Resetting histone modifications during human prenatal germline development. 2023, 9,	О
68	Differentially expression analyses in fruit of cultivated and wild species of grape and peach. <b>2023</b> , 13,	0
67	TET1 and TDG Suppress Inflammatory Response in Intestinal Tumorigenesis: Implications for Colorectal Tumors With the CpG Island Methylator Phenotype. <b>2023</b> , 164, 921-936.e1	O
66	Genome and haplotype provide insights into the population differentiation and breeding improvement of Gossypium barbadense. <b>2023</b> ,	О
65	The genome of a vestimentiferan tubeworm (Ridgeia piscesae) provides insights into its adaptation to a deep-sea environment. <b>2023</b> , 24,	O
64	Revealing the relationship between nitrogen use efficiency-related QTLs and carbon and nitrogen metabolism regulation in poplar. <b>2023</b> , 15, 575-592	0
63	Blood transcriptome responses to PFOA and GenX treatment in the marsupial biomedical model Monodelphis domestica. 14,	O
62	Multi-omics of Circular RNAs and Their Responses to Hormones in Moso Bamboo (Phyllostachys edulis). <b>2023</b> ,	О
61	The super-enhancer repertoire in porcine liver. <b>2023</b> , 101,	O
60	Transcriptional Profiling Supports the Notochordal Origin of Chordoma and Its Dependence on a TGFB1-TBXT Network. <b>2023</b> , 193, 532-547	О
59	RNA Sequencing Identifies Frequent Mitogen-activated Protein Kinasellssociated Fusion Genes in Intraductal Tubulopapillary Neoplasms of the Pancreas. <b>2023</b> ,	O
58	Mechanobiological Adaptation to Hyperosmolarity Enhances Barrier Function in Human Vascular Microphysiolgical System. 2206384	О
57	High-quality Cymbidium mannii genome and multifaceted regulation of crassulacean acid metabolism in epiphytes. <b>2023</b> , 100564	O
56	Alteration of gene expression profiles in the mutant line of Sorghum bicolor.	0
55	Optogenetic decoding of Akt2-regulated metabolic signaling pathways in skeletal muscle cells using transomics analysis. <b>2023</b> , 16,	O

54	Pro-inflammatory polarization and colorectal cancer modulate alternative and intronic polyadenylation in primary human macrophages.	0
53	Revealing the History and Mystery of RNA-Seq. <b>2023</b> , 45, 1860-1874	O
52	Transcriptomic Analyses of Brains of RBM8A Conditional Knockout Mice at Different Developmental Stages Reveal Conserved Signaling Pathways Contributing to Neurodevelopmental Diseases. <b>2023</b> , 24, 4600	Ο
51	Pangenomic analysis identifies structural variation associated with heat tolerance in pearl millet. <b>2023</b> , 55, 507-518	O
50	Chromosome-level reference genome of Tetrastigma hemsleyanum (Vitaceae) provides insights into genomic evolution and the biosynthesis of phenylpropanoids and flavonoids.	0
49	A gene regulatory network for neural induction. 12,	Ο
48	Olfactory and neuropeptide inputs to appetite neurons in the arcuate nucleus.	O
47	Genome-wide profiling of histone H3 lysine 27 trimethylation and its modification in response to chilling stress in grapevine leaves. <b>2023</b> ,	O
46	Inhibition of Nonsense-Mediated Decay Induces Nociceptive Sensitization through Activation of the Integrated Stress Response. <b>2023</b> , 43, 2921-2933	0
45	Lipid extract derived from newly isolated Rhodotorula toruloides LAB-07 for cosmetic applications. <b>2023</b> , 21, 2009-2017	O
44	Transcriptomic-based analysis to identify candidate genes for blue color rose breeding. <b>2023</b> , 111, 439-454	O
43	Transcriptomes reveal microRNAs and mRNAs in different photoperiods influencing cashmere growth in goat. <b>2023</b> , 18, e0282772	O
42	BysR, a LysR-Type Pleiotropic Regulator, Controls Production of Occidiofungin by Activating the LuxR-Type Transcriptional Regulator AmbR1 in Burkholderia sp. Strain JP2-270. <b>2023</b> , 11,	О
41	11IPHSD1 inhibition does not affect murine tumour angiogenesis but may exert a selective effect on tumour growth by modulating inflammation and fibrosis. <b>2023</b> , 18, e0255709	Ο
40	Elimination of FKBP51 attenuates CCl4-induced liver injury via enhancement of mitochondrial function by increased Parkin activity.	О
39	Distal nucleotides affect the rate of stop codon read-through. <b>2023</b> , 11, 44	Ο
38	Glucocorticoid mediated inhibition of LKB1 mutant non-small cell lung cancers. 13,	0
37	RNA sequencing analysis reveals the role of choline acetyltransferase in regulating development, reproduction, and insecticide susceptibility in Tribolium castaneum (Coleoptera: Tenebrionidae). <b>2023</b> , 53, 106-118	O

36	OverexpressedMalat1Drives Metastasis through Inflammatory Reprogramming of Lung Adenocarcinoma Microenvironment.	0
35	Dissecting the molecular features of bovine-arrested eight-cell embryos using single-cell multi-omics sequencing.	O
34	Genipin Crosslinks the Extracellular Matrix to Rescue Developmental and Degenerative Defects, and Accelerates Regeneration of Peripheral Neurons.	0
33	Duckweed evolution: from land back to water.	O
32	Loss of Fgf9 in mice leads to pancreatic hypoplasia and asplenia. <b>2023</b> , 26, 106500	О
31	An LTR retrotransposon insertion inside CsERECTA for an LRR receptor-like serine/threonine-protein kinase results in compact (cp) plant architecture in cucumber. <b>2023</b> , 136,	O
30	Particulate matter10-induced airway inflammation and fibrosis can be regulated by chitinase-1 suppression. <b>2023</b> , 24,	0
29	The Torreya grandis genome illuminates the origin and evolution of gymnosperm-specific sciadonic acid biosynthesis. <b>2023</b> , 14,	O
28	Beta-adrenergic agonist induces unique transcriptomic signature in inguinal white adipose tissue. <b>2023</b> , 11,	0
27	Physicochemical, Pre-Clinical, and Biological Evaluation of Viscosity Optimized Sodium Iodide-Incorporated Paste. <b>2023</b> , 15, 1072	O
26	Soybean gene co-expression network analysis identifies two co-regulated gene modules associated with nodule formation and development.	О
25	Bta-miR-206 and a Novel lncRNA-lncA2B1 Promote Myogenesis of Skeletal Muscle Satellite Cells via Common Binding Protein HNRNPA2B1. <b>2023</b> , 12, 1028	O
24	Transcriptomic Analysis Reveals Suppression of Photosynthesis and Chlorophyll Synthesis Following Gibberellic Acid Treatment on Oil Palm (Elaies guineensis).	0
23	Muscle cell-type diversification is driven by bHLH transcription factor expansion and extensive effector gene duplications. <b>2023</b> , 14,	O
22	Two haplotype-resolved genomes of highly heterozygous AAB allotriploid bananas provide insights into subgenome asymmetric evolution and banana wilt control.	0
21	Regulatory Networks of lncRNAs, miRNAs, and mRNAs in Response to Heat Stress in Wheat (Triticum Aestivum L.): An Integrated Analysis. <b>2023</b> , 2023, 1-17	O
20	Necrotic cardiac myocytes skew macrophage polarization towards a classically activated phenotype. <b>2023</b> , 18, e0282921	O
19	Transcriptome Profile in Dairy Cows Resistant or Sensitive to Milk Fat Depression. <b>2023</b> , 13, 1199	O

18	Integrated single cell analysis shows chronic alcohol drinking disrupts monocyte differentiation in the bone marrow niche.	O
17	Combined lncRNA and mRNA Expression Profiles Identified the lncRNAthiRNAthRNA Modules Regulating the Cold Stress Response in Ammopiptanthus nanus. <b>2023</b> , 24, 6502	O
16	Circular RNAs in the human brain are tailored to neuron identity and neuropsychiatric disease.	О
15	Exploring body weight-influencing gut microbiota by elucidating the association with diet and host gene expression. <b>2023</b> , 13,	O
14	Super-pangenome analyses highlight genomic diversity and structural variation across wild and cultivated tomato species.	0
13	The ENCODE Uniform Analysis Pipelines.	O
12	Modification of maternally defined H3K4me3 regulates the inviability of interspecific Xenopus hybrids. <b>2023</b> , 9,	О
11	Characterization of the functional and transcriptomic effects of pro-inflammatory cytokines on human EndoC-IH5 beta cells. 14,	O
10	SOX2 downregulation of PML increases HCMV gene expression and growth of glioma cells. <b>2023</b> , 19, e1011316	О
9	Microbiota-derived tryptophan catabolites mediate the chemopreventive effects of statins on colorectal cancer.	O
8	RNA degradome analysis reveals DNE1 endoribonuclease is required for the turnover of diverse mRNA substrates in Arabidopsis.	0
7	Single-cell and spatial transcriptomics identify a macrophage population associated with skeletal muscle fibrosis.	O
6	Cytological, transcriptome and miRNome temporal landscapes decode enhancement of rice grain size. <b>2023</b> , 21,	0
5	Reduced cellular process and developmental process genotoxicity of polystyrene nanoplastics in zebrafish embryogenesis using Aurelia aurita proteins.	O
4	Insight into growth and wood properties based on QTL and eQTL mapping in Populus deltoides <code>Danhong</code> Populus simonii Tongliao102023, 199, 116731	0
3	Transcriptome analysis revealed molecular basis of cold response in Prunus mume. 2023, 43,	O
2	Alternative splicing decouples local from global PRC2 activity.	О
1	FAM46C-mediated tumor heterogeneity predicts extramedullary metastasis and poorer survival in multiple myeloma. <b>2023</b> , 15, 3644-3677	0